

# **Strategies Towards Perovskite Solar Cells with Enhanced Stability: Techniques of stabilizing perovskite solar cells**

*C.A. Georgiou*

*Nanotechnology Processes for Solar Energy Conversion and Environmental Protection, Institute of Nanoscience and Nanotechnology (INN), Department for National Centre for Scientific Research Demokritos (NCSR-D), Department of Chemical Engineering: National Technical University of Athens (NTUA), Athens, Greece*

Corresponding author: *Charalambos (Harry) Andrew Georgiou:*  
[Harry.georgiou40@gmail.com](mailto:Harry.georgiou40@gmail.com)

*72 Southbury Road, Enfield, London, EN1 1YB, UK*

*Keywords: Perovskite; Solar cell; Stability enhancement; Hole transport material*

## **Abstract**

This review discusses how scientists have applied different techniques in order to increase the stability of a new generation of photovoltaics known as perovskite solar cells (PSCs). Research includes changing the ingredients which make up the perovskite crystal, altering the structure of the solar cell itself, using external sealing techniques as well as internally protecting the device from moisture with layers which prevent humidity/atmosphere/light from damaging the vulnerable parts. Other means to overcome this have involved trying to understand hole transport material (HTM) stability. Effort to improve surface/quality of the perovskite layer has also increased resistance that the photoactive layer has against humidity. As well as material degradation, electrical instability known as hysteresis has been a source of investigation. Substrate types and electrodes requirements are described, and the solar cells produced from them must have the endurance during their active use in daily life whatever its use. Stress on solar cells has been correlated to parameters used to measure their performance. High intensity to low intensity illumination on the PSCs has been carried out in different environments to assess their capability of enduring harsh conditions. At present, the most successful PSCs contain lead which is toxic, therefore, alternatives need to be found which produce adequate stability and performance. Commercial barriers need to be overcome, theoretical studies have been undertaken to help improve stability, and testing procedures require implementation. Finally, conceptualised potential software tools need to be developed for future scientists, so they can assess and model stability.

## Abbreviations

Abbreviation	Definition
ALD	atomic layer deposition
AZO	aluminium doped zinc oxide
BIPV	building integrated photovoltaics
C <sub>60</sub>	carbon 60: Buckminsterfullerene
CH <sub>3</sub> NH <sub>3</sub> PbX <sub>3</sub>	methylammonium lead halide (iodide, chloride, bromide)
CH <sub>5</sub> N <sub>2</sub> <sup>+</sup>	formamidinium cation
CH <sub>5</sub> N <sub>2</sub> PbI <sub>3</sub>	formamidinium lead iodide
CuSCN	copper thiocyanate
DMF	dimethylformamide
DSC	dye solar cell (dye sensitized solar cell)
EH44	9-(2-ethylhexyl)-N,N,N,N-tetrakis(4-methoxyphenyl)-9H-carbazole-2,7-diamine
ETM	electron transport material
eV	electron volts
exR <sub>ser</sub>	external series resistance
FF	fill factor
FTO	fluorine doped tin oxide
FZO	fluorine doped zinc oxide
HTM	hole transport material
IEC	International Electrotechnical Commission
IPCE	internal photocurrent conversion efficiency
I <sub>sc</sub>	short circuit current
ITO	indium tin oxide
IZO PET	indium doped zinc oxide coated polyethylene terephthalate substrate
J <sub>sc</sub>	short circuit current density (current/area)
LED	light emitting diode
LiTFSI	lithium bis(trifluoromethanesulfonyl)imide
MMT	Montmorillonite
m-MTDATA	4,4',4"-tris[phenyl( <i>m</i> -tolyl)amino]triphenylamine
M <sub>pp</sub>	maximum power point
mp-TiO <sub>2</sub>	Mesoporous titanium dioxide
P3HT	poly(3-hexylthiophene-2,5-diyl)
PCBM	phenyl-C <sub>61</sub> -butyric acid methyl ester

PCBTDP	poly[ <i>N</i> -9-hepta-decanyl-2,7-carbazole-alt-3,6-bis(thiophen-5-yl)-2,5-dioctyl-2,5-dihydropyrrolo[3,4-]pyrrole-1,4-dione]
PCE	photocurrent conversion efficiency
PDPPDBTE	diketopyrrolopyrrole poly[2,5-bis(2-decyldodecyl)pyrrolo[3,4- <i>c</i> ]pyrrole-1,4(2 <i>H</i> ,5 <i>H</i> )-dione-( <i>E</i> )-1,2-di(2,20-bithiophen-5-yl)ethene]
PEDOT	poly(3,4-ethylenedioxythiophene)
PEDOT:PSS	poly(3,4-ethylenedioxythiophene)-poly(styrenesulfonate)
PEN	poly(ethylene 2,6-naphthalate)
Perovskite	crystal ABO <sub>3</sub> structure discovered by Gustav Rose 1839, named after the Russian count Perovski. Variations to this structure exist which are included in this paper
PSC	perovskite solar cell (perovskite sensitized solar cell)
PTAA	poly[bis(4-phenyl)(2,4,6-trimethylphenyl)amine]
PTPD	poly(tetraphenylbenzidine)
R <sub>s</sub>	series resistance
R <sub>sh</sub>	shunt resistance
RT	room temperature
SMARTS	Simple Model of the Atmospheric Radiative Transfer of Sunshine
Spiro-OMeTAD/Spiro-MeOTAD	<i>N</i> 2, <i>N</i> 2, <i>N</i> 2', <i>N</i> 2', <i>N</i> 7, <i>N</i> 7, <i>N</i> 7', <i>N</i> 7'-octakis(4-methoxyphenyl)-9,9'-spirobi[9 <i>H</i> -fluorene]-2,2',7,7'-tetramine
tBP	<i>tert</i> -butylpyridine
tJ <sub>sc</sub>	true short circuit
UV-Vis	ultraviolet-visible light
V <sub>oc</sub>	open circuit voltage
XRD	X-ray diffraction
Z907	Photosensitizer

# Table of contents

ABSTRACT .....	1
ABBREVIATIONS .....	2
TABLE OF CONTENTS .....	4
1 INTRODUCTION: ENERGY REQUIREMENTS - WHY USE PEROVSKITES?.....	9
1.1 Current situation.....	9
1.2 How does a solar cell work?.....	10
1.3 Where do perovskites come into the picture? .....	11
1.4 Recommended reading of previous review papers at the time of writing.....	12
1.5 The aims of this review .....	12
1.6 What is a perovskite; how was it discovered?.....	12
1.7 Research statistics: .....	14
1.8 Research history on perovskites in photovoltaics .....	16
2 FORMING GREATER INTRINSIC PEROVSKITE STABILITY .....	18
2.1 Understanding the effect of humidity on the perovskite .....	19
2.2 Selection of precursors to increase overall stability .....	19
2.2.1 Mixing different ratios of halides for increased stability.....	19
2.2.2 Understanding the effect of different lead precursors .....	20
2.2.3 Using a pseudohalide: $\text{CH}_3\text{NH}_3\text{Pb}(\text{SCN})_2\text{I}$ .....	21
2.3 How much heat can the perovskites take before breakdown?.....	21
2.3.1 Regular mixed halide perovskite ( $\text{Cl}/\text{I}$ ).....	22
2.3.2 Formamidinium showed greater stability at high temperature for perovskites .....	22
2.4 Alternative perovskites.....	22
2.4.1 Ruddlesdon-Popper perovskite .....	22
2.4.2 Chlorine doping in $\text{CH}_3\text{IN}_2\text{PbI}/\text{Cl}$ .....	23
2.4.3 Tuning both cation and anion for stable tandem applications $((\text{CH}_3\text{IN}_2)_{0.83}\text{Cs}_{0.17})\text{Pb}(\text{Br}_{0.4}\text{l}_{0.6})_3$ .....	24
2.4.4 $\text{CsSnI}_3$ and band gap change .....	24
2.5 Summary of section 2 .....	24

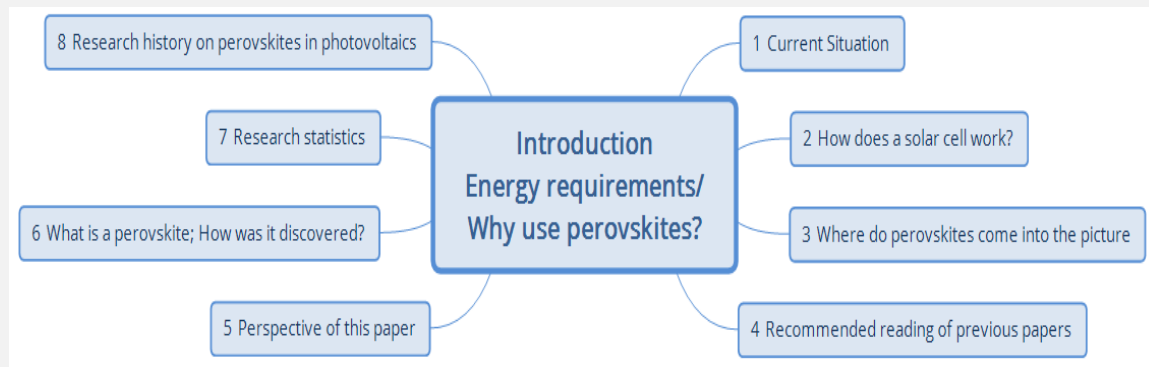
<b>3</b>	<b>VARIOUS WAYS TO PROTECT AGAINST HUMIDITY .....</b>	<b>25</b>
3.1	Altering the solar cell structure.....	26
3.2	Protection from the humidity/atmosphere/temperature via sealing.....	28
3.2.1	Encapsulation .....	28
3.2.2	ZrO <sub>2</sub> /carbon counter electrode .....	30
3.2.3	Buffer layers.....	31
3.2.4	Carbon and hydrophobic HTM .....	31
3.2.5	Al <sub>2</sub> O <sub>3</sub> atomic layer deposition (ALD) protection .....	32
3.3	Summary of section 3 .....	33
<b>4</b>	<b>UNDERSTANDING HTM STABILITY AND PERFORMANCE .....</b>	<b>34</b>
4.1	HTM instability .....	34
4.1.1	Liquid perovskite causing problems .....	34
4.1.2	Replacing the liquid electrolyte and early stability tests .....	34
4.1.3	HTM breakdown in N <sub>2</sub> atmosphere – doped or undoped .....	36
4.2	Spiro-MeOTAD/additive degrades perovskite.....	38
4.2.1	Tin perovskite degraded by spiro-MeOTAD/additives in inert atmosphere .....	38
4.2.2	Alternative to <i>tert</i> -butylpyridine for greater performance .....	38
4.2.3	Storage and fabrication conditions.....	39
4.1	HTM and doping alternatives for greater stability .....	41
4.1.1	Effects of different dopants.....	42
4.1.2	Hydrophobic/hydrophilic HTMs, with/without dopants .....	43
4.1.2.1	P3HT HTM cell stability measurements .....	43
4.1.2.2	Additional HTMs (non-exhaustive) .....	44
4.1.3	An inexpensive spiro-MeOTAD alternative .....	48
4.1.4	Inverted structure and HTM comparison .....	50
4.2	HTM-free solar cells: is the HTM necessary? .....	51
4.2.1	HTM free standard PSC.....	51
4.2.2	Carbon counter electrode.....	51
4.2.3	Mixed halide perovskite .....	51
4.3	Summary of section 4 .....	52
<b>5</b>	<b>SURFACE STRUCTURE/QUALITY (STABILITY AS A RESULT) .....</b>	<b>52</b>
5.1	CH <sub>3</sub> NH <sub>3</sub> Cl addition.....	52
5.2	Two-step → large grain .....	53
5.3	Hot air during spin coating.....	53
5.4	Dipping in C <sub>12</sub> -silane.....	53
5.5	Perovskite layer quality .....	53

5.5.1	HTM hydrophilicity effects .....	54
5.5.2	Other lead precursors.....	54
5.5.3	Fabrication method .....	54
5.5.3.1	Sequential Dipping.....	54
5.5.3.2	Blading method.....	54
5.5.3.3	Perovskite recrystallization .....	55
5.5.3.4	Low-pressure chemical vapour deposition .....	56
<b>5.6</b>	<b>Summary of section 5 .....</b>	<b>56</b>
<b>6</b>	<b>INVESTIGATIONS TO REDUCE HYSTERESIS IN I/V SCANS OF PSCS .....</b>	<b>56</b>
<b>6.1</b>	<b>Doping .....</b>	<b>57</b>
6.1.1	Oxygen P doping.....	57
<b>6.2</b>	<b>Other methods of reducing hysteresis .....</b>	<b>58</b>
6.2.1	Comparison of mesoporous and planar PSC Structures .....	58
6.2.2	HTMs with hydrophilic nature have less hysteresis .....	58
6.2.3	Slower I/V scans are more stable .....	58
6.2.4	Morphology layer interface .....	59
6.2.5	Pacifying trap states using organic/inorganic layers .....	59
6.2.6	Dehydration and recrystallization effects on hysteresis.....	59
<b>6.3</b>	<b>Summary of section 6 .....</b>	<b>60</b>
<b>7</b>	<b>FLEXIBLE/RIGID BEHAVIOUR OF ELECTRODES AND SUBSTRATES .....</b>	<b>60</b>
<b>7.1</b>	<b>Different substrate properties .....</b>	<b>61</b>
7.1.1	Substrate requirements.....	61
7.1.2	Substrate differences.....	62
<b>7.2</b>	<b>Types of substrate .....</b>	<b>62</b>
7.2.1	Mechanical testing and effect on efficiency .....	63
<b>7.3</b>	<b>Electrode response to UV light.....</b>	<b>65</b>
7.3.1	Silver nanowire electrodes .....	65
<b>7.4</b>	<b>Electrode limitations.....</b>	<b>65</b>
7.4.1	Temperature limitations.....	65
7.4.2	Electrode chemical instability.....	65
<b>7.5</b>	<b>Summary of section 7 .....</b>	<b>66</b>
<b>8</b>	<b>THE ROLE OF VARIOUS STRESS TYPES ON SOLAR CELL PARAMETER STABILITY .....</b>	<b>67</b>
<b>8.1</b>	<b><math>J_{sc}</math> reduction from liquid tri-iodide .....</b>	<b>69</b>
<b>8.2</b>	<b>Sealed cell, decay due to <math>V_{oc}</math> reduction: <math>R_{sh}</math> degrades with different illuminations .....</b>	<b>69</b>
<b>8.3</b>	<b>P3HT <math>V_{oc}</math> and FF increase with formamidinium as a cation.....</b>	<b>69</b>

8.4 Reduction of FF and shunt resistance $R_{sh}$ , $R_{sh}$ affects $V_{oc}$ .....	70
8.5 ETL layer affecting $J_{sc}$ and FF .....	70
8.6 Summary of section 8 .....	70
 9 THE EFFECTS OF ILLUMINATION ON CELL STABILITY .....	71
9.1 UV photo induced instability .....	71
9.1.1 Photo related segregation of halide crystal phases.....	71
9.1.2 Preventing UV photocatalysis of perovskite.....	72
9.1.3 Silver nanowire electrode instability .....	73
9.2 Ambient light and inert atmosphere .....	73
9.3 Solar intensity effect.....	73
9.3.1 Degradation as a function of light intensity .....	74
9.4 Raman characterisation breakdown .....	76
9.5 Absorbance spectrum .....	76
9.6 Photodecomposition .....	77
9.6.1 The $\text{CH}_3\text{NH}_3$ cation with $\text{PbX}$ is photosensitive and can decompose.....	77
9.7 Traps states in $\text{TiO}_2$ .....	77
9.7.1 Al doped $\text{TiO}_2$ to reduce deep trap states and the phenomena explained .....	77
9.8 Summary of section 9 .....	78
 10 CHALLENGE TO FIND NON-TOXIC ALTERNATIVES TO LEAD AND OTHER TOXIC PEROVSKITE PRECURSORS .....	79
10.1 Summary of chapter 10 .....	82
 11 COMMERCIAL REQUIREMENTS, THEORETICAL STABILITY MODELLING AND METHODS OF STRESS TESTING FOR ANALYSING AND SIMULATING PSC STABILITY .....	82
11.1 Commercialization .....	83
11.1.1 Requirements .....	83
11.1.2 Problems with focusing only on efficiency .....	83
11.1.3 Considering the region where the technology is to be used and tools towards achieving stability .....	84
11.2 Stability: a theoretical Investigation .....	89
11.2.1 Relative stability in eV of other halides to $\text{CH}_3\text{NH}_3\text{PbI}_3$ and the crystal structures .....	90
11.2.2 What structures are more intrinsically stable .....	90
11.2.3 Lattice defects can also improve stability.....	90
11.2.4 Best method for modelling the interaction between the perovskite and anchoring site ....	90
11.2.5 Prediction on stabilities and mechanisms .....	90

11.2.6	Ionic radius and structure affect properties .....	91
11.2.7	Spectral range of atmosphere depending on earth region .....	91
<b>11.3</b>	<b>Assessment protocol: DSC stability tests initially.....</b>	<b>92</b>
<b>11.4</b>	<b>Protocol must include high and low temperature, dark and continuous illumination at different sun levels .....</b>	<b>95</b>
11.4.1	Tests in the dark .....	95
11.4.2	Tests with illumination .....	95
11.4.3	Changes in humidity .....	96
11.4.4	Reverse bias testing of PSCs .....	96
11.4.5	Open source stability modelling idea .....	96
<b>11.5</b>	<b>Summary of section 11.....</b>	<b>97</b>
<b>12</b>	<b>CONCLUSION .....</b>	<b>98</b>
<b>ACKNOWLEDGEMENTS.....</b>		<b>100</b>
<b>BIBLIOGRAPHY .....</b>		<b>100</b>

# 1 Introduction: energy requirements - why use perovskites?



Scheme 1

## 1.1 Current situation

The world's energy needs are increasing: by 2050 the world's population is predicted to be close to 10 billion [1]. Rather than pollute the environment with fossil fuels, one option is to use renewable sources that are in abundance and easy to utilise without expending fuel or producing waste during its life cycle. One of the means to meet this need is solar power. The reason is because the solar resource is unlimited for as long as the Earth's surface continues to be illuminated by the Sun.

Silicon is the main contending material for solar energy, resulting in a relatively expensive cost of cells at around 0.48 to 0.56 United States Dollars per Watt peak (US \$/W<sub>peak</sub>) although it will come down in price in the long-term future to possibly 0.30 to 35 US \$/W<sub>peak</sub> from efficiency improvements and changes in materials/production methods, etc. [2].

The higher the efficiency the lower the cost of the product over its lifespan [3]. At present though, one of the barriers is the high cost of the technology. Once purchased, the next cost is implementation in the buildings. Following this, maintenance costs and personnel with expertise will need to either train the users or be on hand to address any issues which are also an expense.

How can this be overcome? Potentially lower (at present) manufacturing costs of perovskite solar modules, mainly due to lower substrate costs and fabrication simplicity and high efficiencies may significantly lower their cost barrier [3].

Other technologies have been assessed for their potential commercialization such as organic photovoltaic technology [4] which has a relatively low efficiency of 5% and a limited stability of around 10 years. Dye solar cell (DSC) technology is also an option but stability and low potential are still barriers among others as discussed in two reviews Refs. [5,6].

Roll to roll methods using cheaper flexible substrates with perovskites exist, and perovskites can potentially have comparable costs and make this more economical via tandem combinations with silicon solar cells reducing costs further as investigated by an article and another review Refs. [7,8].

## 1.2 How does a solar cell work?

The most basic solar cell requires three basic components to work:

- A material which absorbs photons from the visible light region and produces excited electrons
- A material which can capture the excited electrons and transfer them to the circuit (grid)
- A material which can return electrons from the grid to the absorber which has lost its electrons.

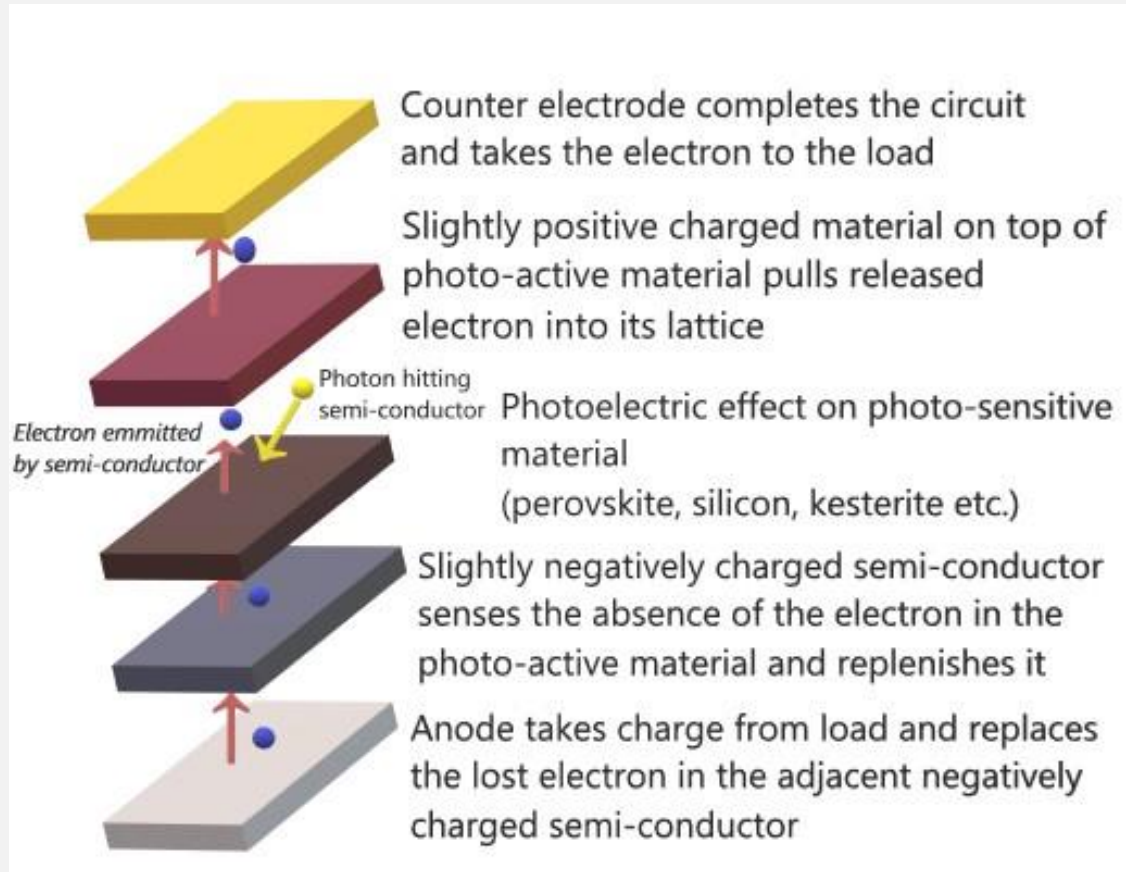


Figure 1. Basic working principle of photovoltaics

DSCs are potentially an alternative to silicon solar cells. They have aesthetic features of being partially transparent and thus can be applied to window facades (see section 4.1 in Ref. [9]) and building integrated photovoltaics (BIPV) [10–12].

They use an electron acceptor in a liquid form comprising a mixture of solvents, electrolytes and a charge transfer chemical known as a redox couple (accepts/donates electrons) (see section 2 of Ref. [5]).

Tri-iodide is a successful redox couple in DSCs. Efficiencies from less than 8% since the patents of DSCs from the 1990s have risen to top efficiencies up to 13% and the latest 14.3% with a cobalt redox couple [13,14]. A good review can be found in Ref. [15]. More detail on how they work can be found in section 15 of Ref. [16].

### **1.3 Where do perovskites come into the picture?**

What was the problem with DSCs? The tri-iodide redox couple in DSCs was corrosive. The liquid electrolyte had problems in temperature stability; high heat with humidity would cause solvent evaporation, freezing of the solvent at sub-zero temperatures, issues with sealing to prevent the evaporation of solvents escaping and leakage through many other mechanisms [17–20]. Thus, the need to find an alternative technology arose to identify alternative solid-state HTMs.

When solid DSCs were made, they had high recombination rates. Currently from 2016, electron recombination has been reduced with promising efficiency of around 8% [21] although this is lower than PSCs in general. DSCs have simpler fabrication procedures. Combining the advantage of having a solid HTM and dye (the dye will later be replaced with a perovskite) would fix the stability issue due to evaporation and high electron recombination. Before solid HTMs were used for this technology, a research group managed to attain 3.8% using perovskite DSCs.[22].

Since then, DSCs have been thoroughly investigated for their stability issues from chemistry and internal mechanisms to the fabrication of the solar cells [17,23] in doctoral theses and review papers alike.

They have undergone tests of up to 90°C with different light intensities, using various combinations of dyes, redox couples and electrodes [24–26]. As of late October 2013, a very good stability standard with less than 10% degradation of the initial efficiency at temperatures in both the dark and light of 1 sun illumination [27] has been achieved though not having efficiencies above 13%.

The companies which are active in the field have solved the main stability issues such as electrolyte leakage, tri-iodide loss, poisoning of the counter electrode, and dye stability, and have proceeded with the production of commercial products with more than 10 years durability. Further to that, a review on their commercial prospects has been written which the author recommends for further information [5].

Parallel to this progress in DSCs, an increase in stability for a 9% efficient solar cell was achieved in 2012 using a mesoporous layer sensitized with a solid perovskite layer and a solid HTM on top [28]. This eliminated the problem of having a liquid electrolyte.

Similarly, through further research of solid-state devices, a breakthrough of 15% efficiency was achieved via vapour deposition of the perovskite mineral as a light sensitizer [29].

What is being brought to the table? The perovskite mineral has semiconducting properties despite being very unstable. As a newcomer to the area of solar technology, PSCs, in comparison to the DSCs, have the added value of being the most efficient solid-state sensitized devices. They absorb in the near infrared spectrum, whilst having the aesthetic feature of optional colours (band gap tuning) and the practicality of transmittance. Thus, perovskites can function as DSCs do in BIPV [11,30].

It is anticipated that when the race for improving efficiency calms down, the more important issue will be addressed; cells working not just efficiently, but under even the harshest conditions, being stable!

## **1.4 Recommended reading of previous review papers at the time of writing.**

There are several different papers including reviews on PSCs, with some focusing on different aspects such as materials and HTMs, general improvements in the technology to acquire higher efficiencies and many more subjects within this field. Reviews have even been published in other languages, for example, Ref. [31].

The papers give different perspectives and discuss various issues on PSCs and DSCs and even their introduction towards undergraduates' perspectives [22,23,31–55] . It is recommended to read these and more recent ones that have since been published depending on the research area one is about to embark upon.

Regarding a list of reviews on general photovoltaics one can check the Photovoltaics literature survey 144 (July 2018) [56].

For those with a chemistry background, a specific paper on the chemical stability of perovskites in solar cells has been published [44]. Also useful is a review on different types of perovskites with various elements, lead/lead-free, their performances and properties for photovoltaics [45], whilst a similar review on research in this field discusses future trends, while ending with a roadmap of this technology [14].

There is also an in-depth review which provides references to stability, although it is more of a review on different aspects of solar cell research on how techniques can improve efficiency, device structure, materials and applications of PSCs and more [46].

## **1.5 The aims of this review**

Like many other reviews, the present paper looks at the different areas of the developments of stability research. Its ultimate aim is to categorize different changes and tests on overcoming the instability issues, without being exhaustive of the current literature available, but enough to present the main directions that various groups are going in.

It is hoped to become a basic text for further research and understanding of later/previous reviews in a more stimulating style. This is intended to make it easier to digest the vast amount of information that this field contains. Hence, while not being state of the art, it is a good base to start with.

Included mind maps help the reader to appreciate the main points of each section in the review.

## **1.6 What is a perovskite; how was it discovered?**

Perovskites in general have the property of crystal structure  $\text{ABO}_3$ . They were originally discovered as being orthorhombic crystals known as calcium titanate ( $\text{CaTiO}_3$ ) mineral by Gustav Rose in 1839 in the Ural mountains of Russia and named after the Russian Count Lev Aleksevich von Perovski [57]

The original documentation on their discovery was written by Gustav Rose in his book, which can be found by searching for the word perowskit in Google: this brings up the account and description of it on page 129 and other sections where this mineral is mentioned in Ref. [58].

Their most basic form consists of a cubic orthorhombic lattice having a metal molecule in the centre which for the untrained reader is a rectangular structure with a different length for each of the axes, e.g.  $x = 2$ ,  $y = 4$  and  $z = 1$ .

Perovskite structures vary, two examples of which are double perovskites where ‘the unit cell is of twice that of the perovskite. It has the same architecture of 12 coordinate A sites and six coordinate B sites, but two cations are ordered on the B site’ [59], and inverse perovskites where the anions and cations are reversed. There are many more types; perovskites have applications in photocatalysis and ferroelectricity [60–63]. In the last nine years, their use in solar energy production has caused a great stir in the photovoltaics research community and is showing great promise although their stability is something that needs to be dealt with in the systems they are used in.

Even more recently, a paper looking at their properties involving PSCs discusses their potential as laser emitters due to their luminescence properties [64].

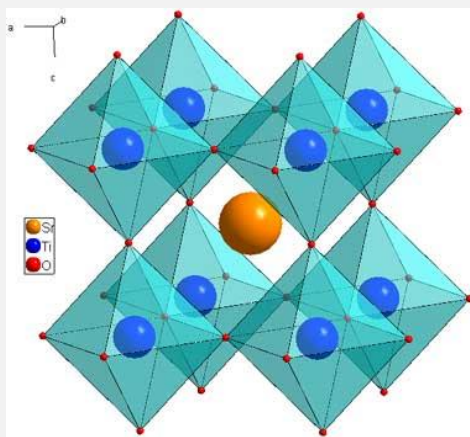
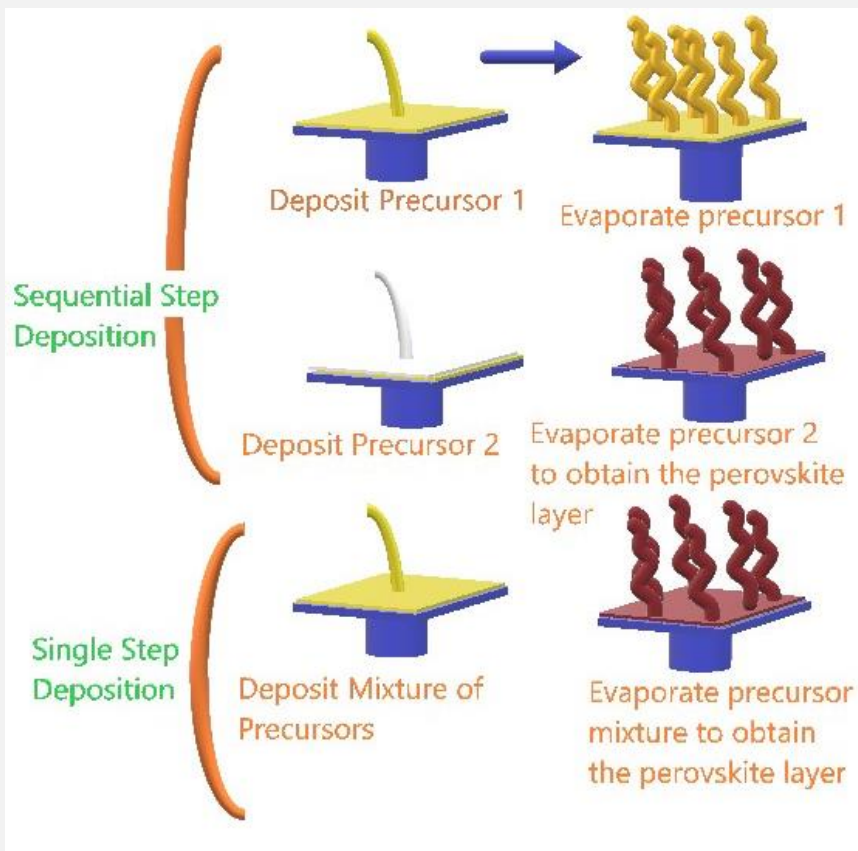


Figure 2: Structure of a cubic perovskite  $\text{SrTiO}_3$  (strontium titanate), sourced from <https://www.princeton.edu/~cavab/tutorials/public/structures/perovskites.html> [59]

In order to form a perovskite layer on a substrate two basic methodologies are used: one is to employ two solutions with separate chemicals, the other being to use a single solution which contains both chemicals.



*Figure 3: Basic outline of single/double-step deposition methods for PSCs*

The two solutions method is carried out using just two chemical ingredients called precursors and a solvent to create the two solutions of these chemicals, which is then applied to the substrate.

Sometimes the two mixtures are deposited separately, with the solvent being evaporated, leaving the chemical spread across a substrate. When the second solution is deposited and the solvent evaporated, the perovskite layer is formed. Most of the fabrication methods in the majority of the perovskite papers are known as single/double-step deposition.

The single-step deposition method uses a single solution with the chemicals which is then deposited on the substrate and has the solvent(s) evaporated usually via heat. The result is a thin perovskite surface on top of a substrate. [65,66].

### **1.7 Research statistics:**

The number of articles on PSCs has risen sharply in the last three years as can be seen in Figure 4. Under half of these papers consider stability as part of the search keyword.

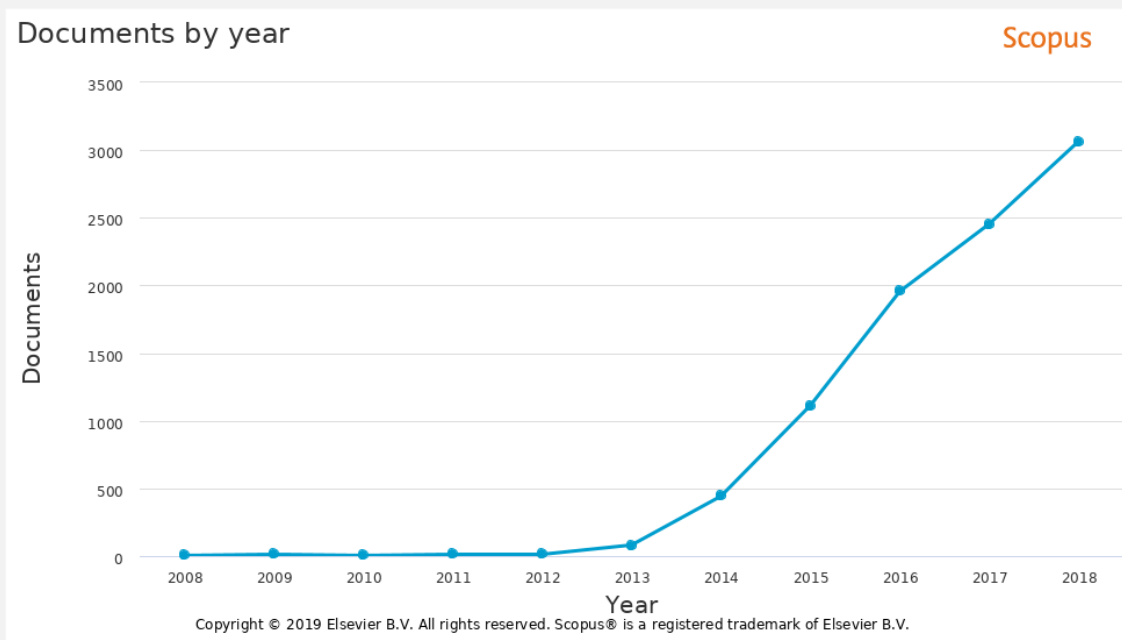


Figure 4: Number of published papers with key words 'perovskite solar cells' in a given year from 2008-2018 from Scopus analysis feature

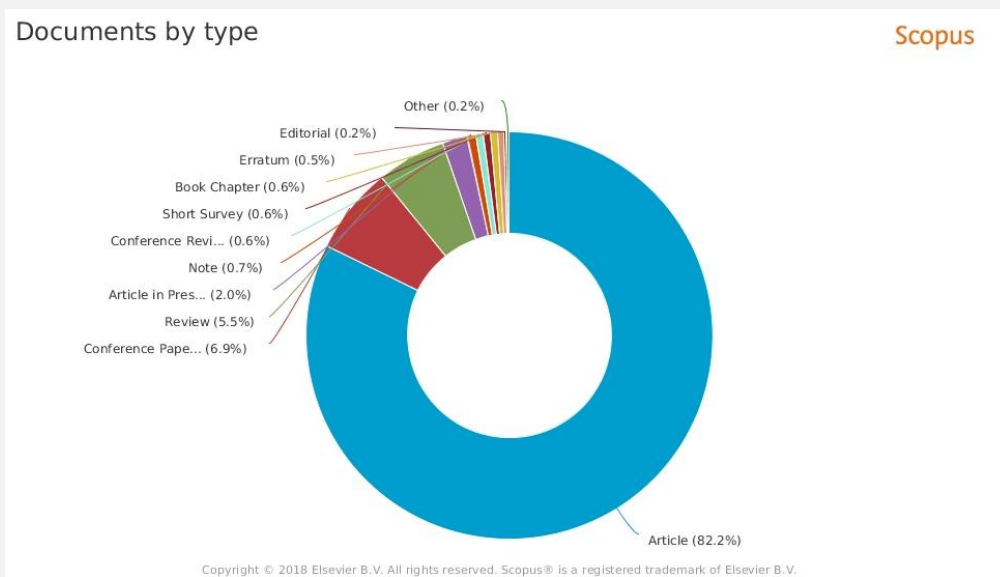


Figure 5: Scopus analysis of document types of perovskite solar cells from 2008-2018

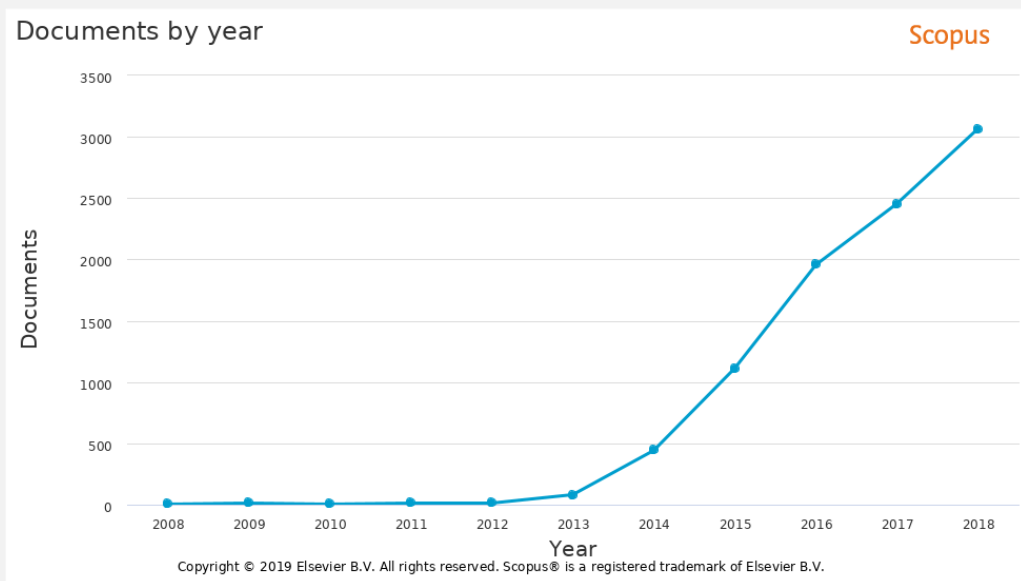


Figure 6: Results of key word search 'perovskite solar cell stability' in a given year from 2009-2018 from Scopus analysis feature

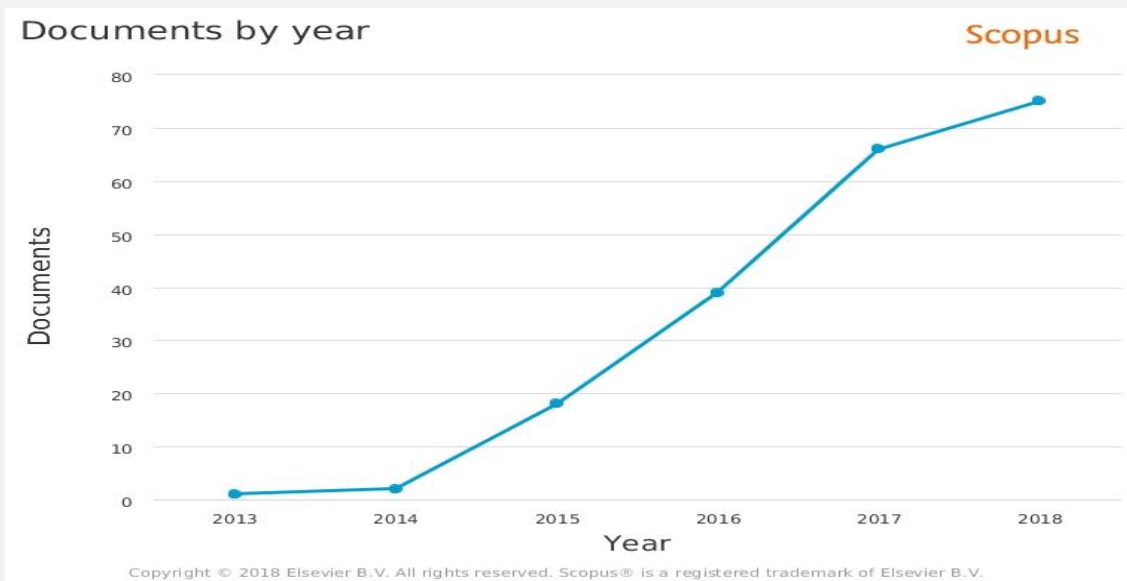


Figure 7: Scopus results of key word search 'perovskite solar cell stability' with the review papers selected in a given year from 2013-2018

## 1.8 Research history on perovskites in photovoltaics

Research using perovskites in solar cells was kick-started when mesoscopic solar cells (solar cell with a layer containing many small holes) were developed using a crystallized methylammonium lead halide  $\text{CH}_3\text{NH}_3\text{PbX}_3$  (where X is I or Br) perovskite as a light absorber [67]. In 2009 this device reached a photoelectrical conversion efficiency (converting photons into electricity) of 3.8% using the perovskite  $\text{CH}_3\text{NH}_3\text{PbI}_3$  as a light absorber giving a photovoltage (voltage from the illumination) of 0.61 V, a fill factor of 57% and short circuit current of  $11 \text{ mA cm}^{-2}$ . When the investigators used bromine instead of iodine ( $\text{CH}_3\text{NH}_3\text{PbBr}_3$ ), a lower efficiency of 3.13% was achieved along with a

much lower photocurrent of  $5.57 \text{ mA cm}^{-2}$  but with a higher photovoltage of  $0.91 \text{ V}$  and slightly higher fill factor of 59%.

Later in 2013, a review paper was published outlining different mesoscopic solar cells [68] where the highest efficiency at the time stated in the paper was over 10.9% using alumina as a scaffold layer and a mixed halide of  $(\text{CH}_3\text{NH}_3\text{PbI}_2\text{Cl})$  [69].

Following that, in the same year, a perovskite layer was modified with alumina protecting it from electrolyte corrosion, thus increasing absorption and hence giving a better photocurrent.

Considering its higher interface resistance: recombination resistance between the  $\text{TiO}_2$  and redox couple being dominant led to an efficiency increase from 3.58-6% [70]. Not long after at the end of 2013, efficiencies increased to 15.7% using zinc as a compact layer and single iodine trihalide [71].

Fast forward towards the end of 2017, the official PSC efficiency hit record efficiencies of 22.7% (see red circles yellow dots; NREL chart, Figure 8).

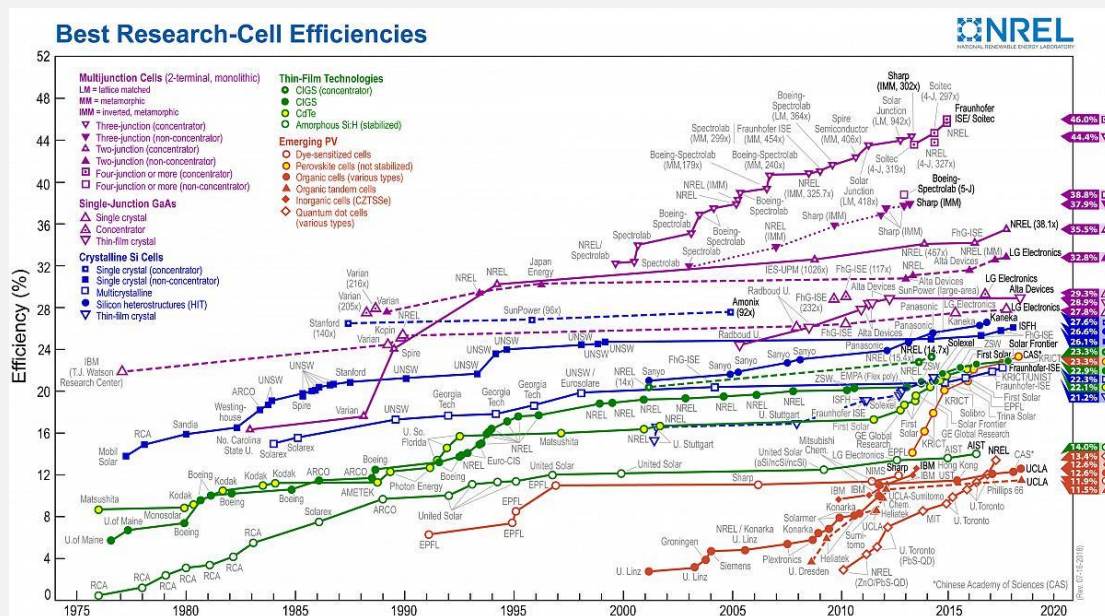


Figure 8: This plot is courtesy of the National Renewable Energy Laboratory, Golden, CO.

Despite this rapid increase in efficiency, the stability of perovskites for use in solar technology is still an issue since they are very sensitive not only to moisture but also to other environmental factors (see Figure 4-8 on how stability as a key word takes time to increase in comparison to papers without stability as a key word). This indicates that researchers were focusing on increasing the efficiencies and took their time to look at stability.

The lack of studies/literature that focused on their stability raised the urgency for research into how to achieve this by improved or new fabrication techniques, for acquiring an understanding into the mechanisms behind photon to electricity conversion, degradation, and stability, etc.

Early on, perovskites in a solar cell were initially used as part of a DSC. Now they are a separate technology. Thus far in photovoltaics, there are two main functions of perovskites: HTMs [68], or sensitizers [72].

One of the HTM perovskites is an inorganic crystal known as  $\text{CsSnI}_3$ . Of the perovskites used in photovoltaics, photosensitizers dominate the vast majority of PSC research due to the simple methods of growth and the high efficiencies attained by the corresponding cells.

Perovskites are hybrid organic/inorganic materials usually containing methylammonium in the cation position. The general formula is  $\text{CH}_3\text{NH}_3\text{PbI}_x$ ,  $\text{CH}_3\text{NH}_3\text{PbA}_{3-x}\text{B}_x$  where A or B are Cl, I, or Br and x is the number of atoms. Other organic molecules such as formamidinium ( $\text{CH}_5\text{N}_2/\text{R}_2\text{N}-\text{CH}=\text{NR}_2^+$ ) and cations like  $\text{Sn}^{4+}/\text{Sn}^{2+}$  have also been used.

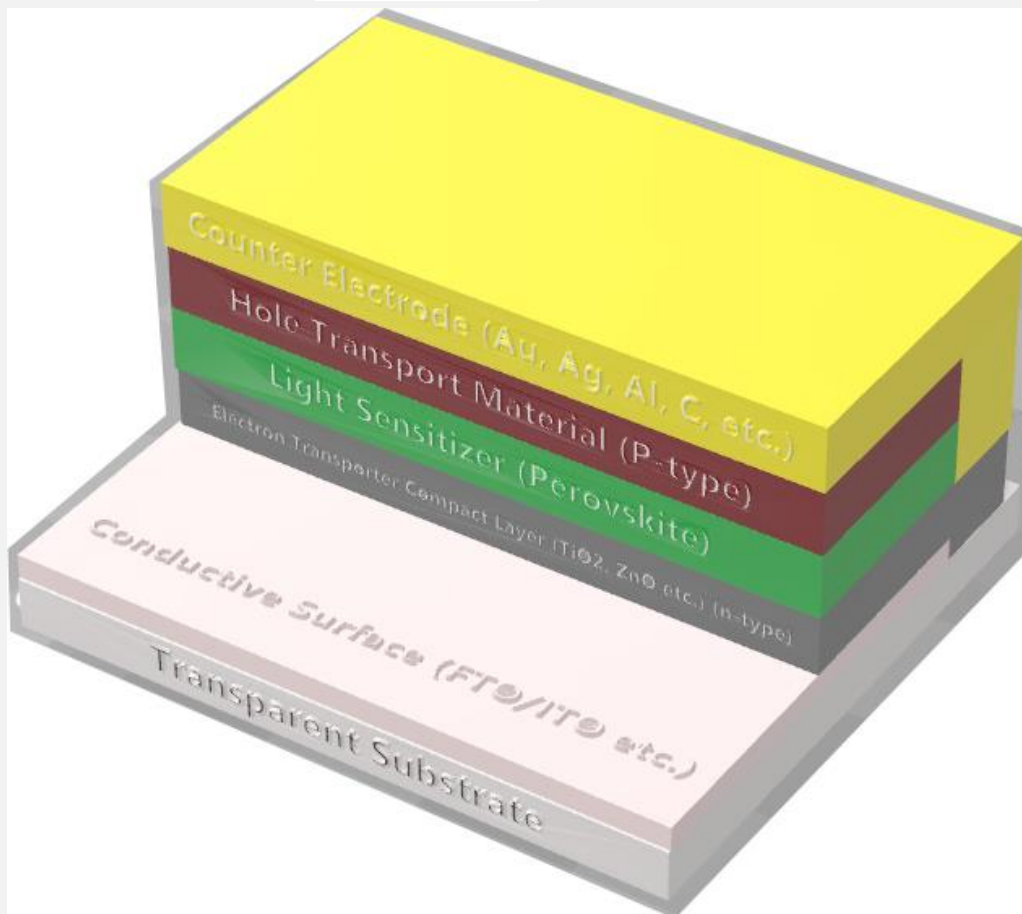
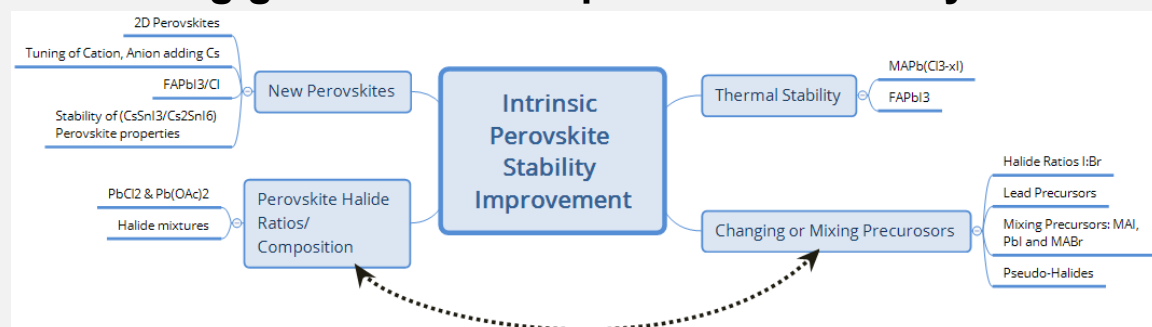


Figure 9: Typical structure of a PSC P-i-N junction

## 2 Forming greater intrinsic perovskite stability



Scheme 2

Stability is affected by the properties of the crystal structure as indicated in previous sections. To synthesise a perovskite crystal which is intrinsically stable will go a long way towards achieving commercialization.

This is at present a problem for the  $\text{CH}_3\text{NH}_3\text{PbI}_3$  perovskite crystal which is sensitive to moisture and oxygen and reacts to form a hydrogenated or oxidized structure which can be insulating and non-photo-absorbing [73,74] (see also sections 2.1, 6.2.6, and 11.2.5 in the present paper).

Crystal structures such as cubic ones and others are more stable, e.g.,  $\text{CH}_3\text{NH}_3\text{PbBr}_3$ , with orthorhombic being the most stable as stated in section 11.2.2 in the present paper regarding a research article using computer modelling [75]. Researchers use mixed halides to change this structure in order to improve the stability and also to increase the photovoltage depending on the band gap the halide atom has in the lattice which as mentioned before impacts stability.

## **2.1 *Understanding the effect of humidity on the perovskite***

Understanding perovskite recrystallization has shown that a new crystal forms under exposure to humidity [73]. The following perovskite reaction pathway was discovered through the test of (30 days, 0%, 25%, 50% and 90% humidity, with and without illumination):  $\text{CH}_3\text{NH}_3\text{PbI}_3 + \text{H}_2\text{O} \rightarrow (\text{CH}_3\text{NH}_3)_4\text{PbI}_6 \cdot 2\text{H}_2\text{O}$  [73]. While in storage, the perovskite was taken out for measurements for absorption spectra. An almost negative exponential decay correlation between humidity and the absorption spectra of photons of 600 nm was found.

## **2.2 *Selection of precursors to increase overall stability***

Various investigations have been undertaken in order to reduce the sensitivity to moisture and atmospheric effects such as changing the number of halide atoms in the perovskite structure, replacing one or having a combination of them changing the overall stability.

### **2.2.1 *Mixing different ratios of halides for increased stability***

The structure of the perovskite crystal with mixed halides for the methylammonium precursors has been shown to improve intrinsic stability due to changes in the band gap and lattice parameters.

This was found through depositing  $\text{CH}_3\text{NH}_3:2\text{CH}_3\text{NH}_3\text{I}$  via sequential dipping and then spin coating  $\text{PbI}_2$ , giving 8.54% efficiency with a stability test (unencapsulated/80 days/no atmosphere or humidity specified/ambient measurement) showing hardly any change [76].

In this investigation, while a bromide halide phase showed the least stability, despite its more stable cubic structure as compared to the plain tetragonal iodide phase, the mixed ratio which is also cubic showed the best stability at the aforementioned ratio ( $\text{CH}_3\text{NH}_3\text{Br}:2\text{CH}_3\text{NH}_3\text{I}$ ).

The present author thinks that possible photocatalytic behaviour could be taking place due to the increased band gap shown in the supporting information, considering it had no HTM. Other effects could have been occurring such as electron recombination, film morphology, crystal sizes being smaller for Br, and the surface interface at the gold

counter electrode and previous layer (see section 5 for ways on handling some of these effects on morphology).

Another procedure for enhancing stability with mixed halides is forming of  $\text{CH}_3\text{NH}_3\text{Pb}(\text{I}_{3-x}\text{Br}_x)_3$  with the optimum stability performance at  $x = 0.2+$  (colour ranges from dark brown to yellow); the lattice parameter reduces and the band gap changes [77]. These cells were using poly(triaryl amine)poly[bis(4-phenyl)(2,4,6-trimethylphenyl)amine] (PTAA) as an HTM.

Test: (Unencapsulated cells/20 days/35% humidity /air/room temperature (RT)) (fourth day/55% humidity); minimal change in an initial efficiency of 9.5% at  $x = 0.2$  and 0.29 whereas at  $x = 0$  and 0.06 a sharp decrease occurred from 10% and 11.5% to <5% and 3% efficiency, respectively.

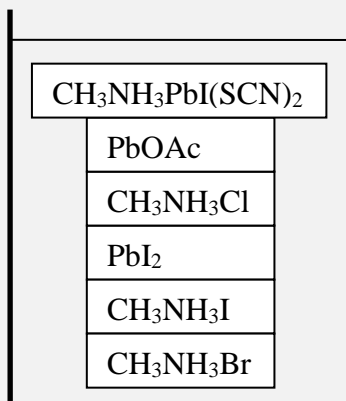


*Figure 10: Solution containing perovskite solution or different precursors; sometimes a solution can contain different combinations and quantities of some or all of them*

The research group achieved an efficiency starting at 13% with chlorine, iodine and no bromine but dropped to 5.5% after 30 days. Bromine demonstrated an inverse relationship to efficiency but proportional relationship to stability except where there is no chlorine involved [78] (see also following section 2.2.2 for more information).

### 2.2.2 Understanding the effect of different lead precursors

In addition to changing halides and having a combination of different ones in a single mixture, one can change the precursor on the metallic ion. An example is the different stability measurements of lead acetate and lead chloride perovskite solutions.

*Table 1: Cell performances of samples stored under conditions C (dark and  $\text{N}_2$  atmosphere) during two months*  
Reproduced ("Adapted" or "in part") from {J. Mater. Chem. A, 2015, 3, 9194-9200 } (or Ref [79]) with permission of The Royal Society of Chemistry.

Entry	Precursor	$J_{sc}$ (mA/cm <sup>2</sup> )	$V_{oc}$ (V)	FF (%)	Efficiency (%)
1	PbCl <sub>2</sub> time zero	15.29	0.831	69.31	8.7
2	PbCl <sub>2</sub> two months	14.12	0.854	69.73	8.4
3	Pb(OAc) <sub>2</sub> time zero	15.02	0.839	62.73	7.9
4	Pb(OAc) <sub>2</sub> two months	11.95	0.865	63.90	6.6

Other properties in this paper included morphology which affected performance [79] (see section 5.5.2 of the current review).

Researchers who investigated this found varying stability in some parameters depending on the precursor used [79]. Comparing the precursors  $\text{PbCl}_2$  or  $\text{Pb}(\text{OAc})_2 + \text{CH}_3\text{NH}_3\text{I} \Rightarrow \text{CH}_3\text{NH}_3\text{PbI}_3$  (with chlorine it is not clear how much goes into the structure): (unencapsulated/15 days/ambient/light) and (unencapsulated/30 days/ambient/dark) showed an equal efficiency loss after 15 days from  $J_{sc}$  reduction;  $\text{Pb}(\text{OAc})_2$  had a slightly better  $J_{sc}$  decay although very similar and better fill factor whereas the  $\text{PbCl}_2$  showed itself to have a more stable  $V_{oc}$ .

When they explored how these mixtures fared without illumination,  $\text{PbCl}_2$  showed slightly better performance in all the parameters. In a non-HTM test (40 days/light), a reduction in the absorbance spectra explained the degradation of the perovskite and thus stability. Table 1 highlights their long-term nitrogen stability test.

### 2.2.3 Using a pseudohalide: $\text{CH}_3\text{NH}_3\text{Pb}(\text{SCN})_2\text{I}$

The perovskite does not necessarily need a halide molecule: another change to the metallic ion precursor is using pseudohalides. Pseudohalides are molecules that behave like the atoms in the halide group; requiring one additional atom for their molecular orbital to be complete.

One such pseudohalide is thiocyanate ( $\text{SCN}$ ), which has shown better stability in (4 h/95% relative humidity/closed chamber/dark) and (open air/ambient laboratory light) tests. High humidity at 95% did not have any effect on the perovskite  $\text{CH}_3\text{NH}_3\text{PbI}(\text{SCN})_2$  after 4 h while the standard  $\text{CH}_3\text{NH}_3\text{PbI}_3$  based perovskite shown by XRD diffraction (XRD) data in the supporting information showed degradation to  $\text{PbI}_2$  within 1.5 h for the  $\text{CH}_3\text{NH}_3\text{PbI}_3$  perovskite. Performance of the perovskite with  $N_2,N_2,N_2',N_2',N_7,N_7,N_7',N_7'$ -octakis(4-methoxyphenyl)-9,9'-spirobi[9H-fluorene]-2,2',7,7'-tetramine (Spiro-MeOTAD) as the HTM showed efficiency of 8.3% while that of  $\text{CH}_3\text{NH}_3\text{PbI}_3$  was 8.8% due to a higher  $J_{sc}$ .

When the same investigators carried out long-term testing (14 days/20-40% humidity), the pseudohalide perovskite showed only 0.9% absolute reduction in efficiency whilst  $\text{CH}_3\text{NH}_3\text{PbI}_3$  demonstrated 1.9% absolute reduction within 7 days with complete failure after 14 days. Other tests in their absorbance spectra show similar stability trends [80].

Suggestions for the causes of the previously reported observations are the strength of the interaction of the lone pair electron in the linear Lewis base structure of  $\text{SCN}$  being greater than that of the spherical Lewis base structure of iodine, thus strengthening and stabilizing the structure (the formation constant of  $\text{SCN}$  and  $\text{Pb}^{2+}$  is 7 and that of  $\text{Pb}^{2+}$  and  $\text{I}_4^-$  is 3.5).

## 2.3 How much heat can the perovskites take before breakdown?

Aside from the chemical stability of the structure in interaction with other materials/substances, different conditions also provide information on the perovskite crystal stability.

### 2.3.1 Regular mixed halide perovskite (Cl/I)

The mixed halide including chlorine was assessed for its performance under duress of different temperatures. Chemical stability measurements of the  $\text{CH}_3\text{NH}_3\text{PbI}_x\text{Cl}_{3-x}$  perovskite in air have shown exothermic peaks at 100°C, meaning minor mass loss as the perovskite forms, implying excess amounts of precursors indicating stability of the structure.

This indicates that cells made with this material could withstand high temperatures. Another peak at 230°C indicates perovskite decomposition via significant mass loss, thus the limit of the perovskite structures' stability [81].

### 2.3.2 Formamidinium showed greater stability at high temperature for perovskites

Comparing cations for perovskites, both bare spin coated substrates of  $\text{CH}_3\text{NH}_3\text{PbI}_3$  and  $\text{CH}_5\text{N}_2\text{PbI}_3$  were compared for degradation in an oven (RT/100 % humidity/15 min): degradation for 15 min was similar but in air at 150°C formamidinium based cells showed no signs of degradation whereas methylammonium based cells were discoloured after approximately 30 min [82].

## 2.4 Alternative perovskites

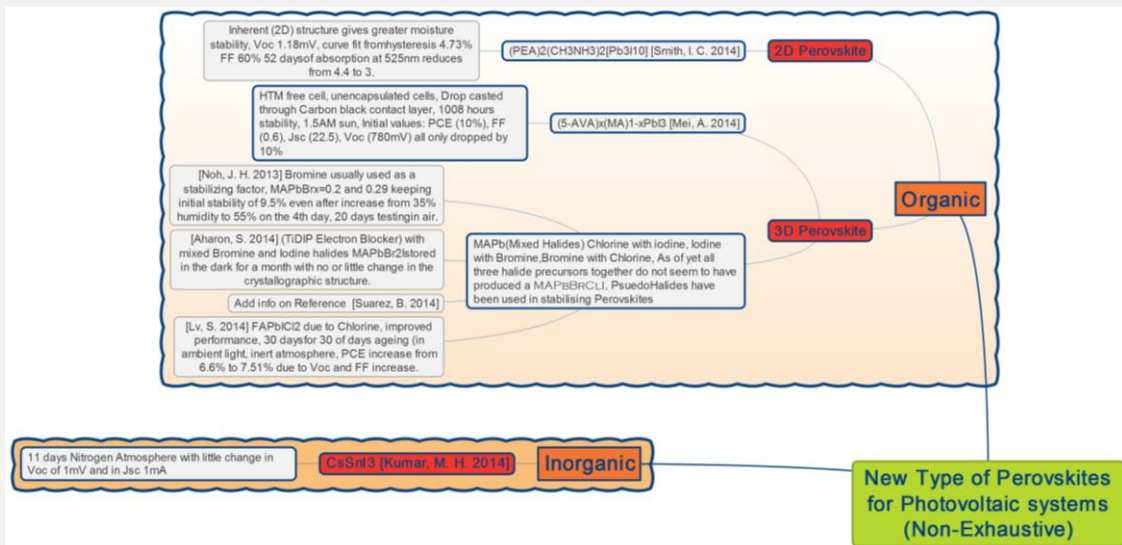


Figure 11: Mind map of alternative type of perovskites

### 2.4.1 Ruddlesdon-Popper perovskite

The family of Ruddlesdon-Popper perovskites is worthy of a review in itself showing potential towards stable perovskite photovoltaics. The first recorded photovoltaic perovskite belonging to this family with very good intrinsic stability consisted of a 2D structure such as  $(\text{PEA})_2(\text{CH}_3\text{NH}_3)_2[\text{Pb}_3\text{I}_{10}]$  (where PEA is). Its advantages are greater moisture stability than the standard 3D perovskite [83]. The performance of the two structure types was compared in the cell architecture of (fluorine doped tin oxide coated (usually glass) (FTO)/TiO<sub>2</sub> mesoporous/perovskite (3D/2D)/Spiro-MeOTAD/Au).

One property of the 2D structure is the ability to have a layered structure, increasing the  $V_{oc}$  and film quality. Scientists found the higher  $V_{oc}$  at 1.18 V was due to a greater band

gap. There was high hysteresis with a top efficiency of 7.02%,  $J_{sc}$  11.53 mA cm<sup>-2</sup> and  $V_{oc}$  1.21 V. A more accurate measurement at a slow scan rate with the voltage point held constant for (70 s) still showed capacitive effects, hence fitting this data gave a fill factor of 60%,  $J_{sc}$  6.72 mA cm<sup>-2</sup>  $V_{oc}$  1.18 V and an efficiency of 4.73%.

When they assessed the crystal's stability, XRD data showed no evidence of decay to PbI<sub>2</sub> (46 days/52% RH/RT/air) whereas CH<sub>3</sub>NH<sub>3</sub>Pb(I/Cl)<sub>3</sub> showed clear evidence of degradation within 5 to 40 days. The absorbance spectrum data in their supporting information shows little change after 47 days from the region 525 nm and lower: above this the absorbance is reduced from 4.4 to 3, but this is far more stable than the 3D CH<sub>3</sub>NH<sub>3</sub>PbX<sub>3</sub> based perovskite where loss occurs along the whole spectrum.

They also observed this in the visual inspection over 20 days. Suggestions to increase stability such as fluorocarbons were also mentioned.

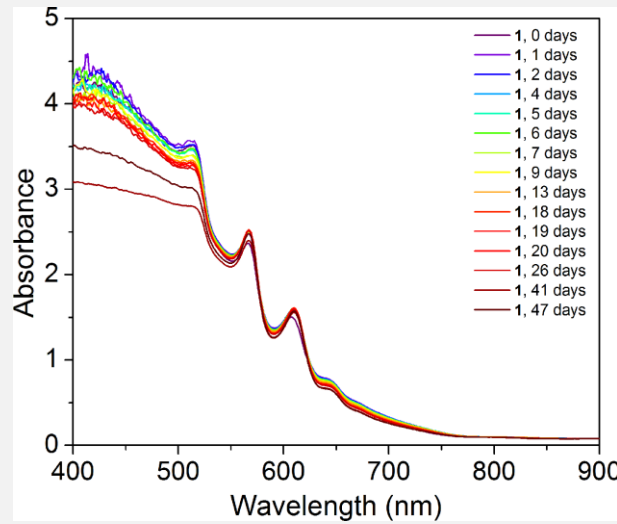


Figure 12: Absorption spectra of film (PEA)<sub>2</sub>(CH<sub>3</sub>NH<sub>3</sub>)<sub>2</sub>[Pb<sub>3</sub>I<sub>10</sub>] upon exposure to 52% relative humidity (reproduced with permission from Ref. [83]) (find out on the way to reference from Wiley)

More recent information on their performance and stability can be found in a short report/review [48] and Refs. [84,85].

#### 2.4.2 Chlorine doping in CH<sub>5</sub>IN<sub>2</sub>PbI/Cl

Other cations and mixtures of halides can affect the performance of solar cells. A single-step solution method to form pure phase formamidinium perovskite film doped with chlorine, which was formed at 140°C, has shown almost double the efficiency of the equivalent CH<sub>5</sub>N<sub>2</sub>PbI<sub>3</sub> cell (3.8%). The researchers found the chlorine based formamidinium perovskite under long term tests (30 days/ambient light, inert atmosphere) with a poly(3-hexylthiophene-2,5-diyl) (P3HT) HTM provided an absolute efficiency increase (0.91%) from 6.6 to 7.51%, mainly due to an increase in the  $V_{oc}$  and FF [86]. Why this occurred is unclear, but the authors felt it was related to the coarsening of the absorber or as a result of ambient light soaking leading to a better HTM layer.

Interestingly, they comment that the 30-day old cell efficiency, made via single-step deposition of a chlorine doped perovskite, is greater than that of the one which is freshly produced, via the two-step dipping process referenced from another article using an only

iodide halide perovskite (7.5%). It was uncertain as to why chlorine enhanced the performance, although it was hypothesised that it produced better film formation.

#### **2.4.3 Tuning both cation and anion for stable tandem applications $((\text{CH}_5\text{IN}_2)_{0.83}\text{Cs}_{0.17})\text{Pb}(\text{Br}_{0.4}\text{I}_{0.6})_3$**

Having an intrinsically stable structure which can produce high efficiencies and match with tandem applications is key for silicon perovskite devices. The PSCs will increase the silicon-based cells' efficiency by a small percentage, thus reducing the overall cost and accelerating commercialization.

Scientists applied this idea towards this goal with the purpose of having high but stable efficiencies. They tuned cations and anions producing  $((\text{CH}_5\text{IN}_2)_{0.83}\text{Cs}_{0.17})\text{Pb}(\text{Br}_{0.4}\text{I}_{0.6})_3$  to match the band gap of silicon of 1.7 eV in a tandem configuration. It gave promise towards the potential that through layer optimization, an efficiency of 30% could be attained [87].

Moreover, the perovskite alone was air stable, remaining black after 6 h: the XRD patterns for this showed only a single phase in the XRD spectrum whereas the formamidinium mixed halide tuning alone produced multiple phases. Photoluminescence spectroscopy showed no redshift, albeit an increase in the intensity of the spectrum after 1 h of illumination.

They achieved high efficiencies using a 0.38 V/s forward bias scan rate and various counter electrodes (Ag 17.1%, indium doped tin oxide (ITO) 15.1%, combined Si and perovskite 19.2%, silicon cell with perovskite incorporating UV filtering of the incoming light 7.3%).

#### **2.4.4 $\text{CsSnI}_3$ and band gap change**

Observing band gap change and structures formed will help in the understanding of stability under different conditions. Recrystallization properties of caesium tin iodide ( $\text{CsSnI}_3$ ) HTM have been studied after being dissolved in different solvents, resulting in cubic and octahedral structures due to the  $\text{Cs}_2\text{SnI}_6$  and  $\text{CsSn}_2\text{I}_5$  formations.

This is useful for applications in HTMs and photoabsorbers. Needle-like structures formed from the 1D double-chain yellow  $\text{CsSnI}_3$  when in ethanol, showing that 3D orthorhombic black-coloured- $\gamma$ - $\text{CsSnI}_3$  was formed [88] and its band gap would change linearly in relation to temperature.

In general, recrystallization of perovskites is not common in the literature and it is useful to study it in order to further understand perovskite stability. Temperatures used to observe the band gap change were from 93 to 473 K (200°C).

### **2.5 Summary of section 2**

Degradation mechanisms of perovskite crystals due to moisture have been documented looking at the inverse relationship of absorbance spectra and humidity. Some means to prevent such decay have involved mixing different quantities of precursors for various methylammonium and halide combinations of  $\text{CH}_3\text{NH}_3\text{I}:2\text{CH}_3\text{NH}_3\text{Br}$  and the  $\text{CH}_3\text{NH}_3\text{PbI}_{2.8}\text{Br}_{0.2}$  perovskite crystal. As a result, when the optimal ratio was formed, the resulting changes in the crystal structure would produce higher stability.

Other attempts at improving the intrinsic stability involved using precursors such as  $\text{PbCl}_2$  and lead acetate  $[\text{Pb}(\text{OAc})_2]$ . These precursors affect the performance and stability differently. Tests showed that under illumination for 15 days  $\text{PbCl}_2$  favours  $V_{\text{oc}}$ , while  $\text{Pb}(\text{OAc})_2$  prefers  $J_{\text{sc}}$ .

Scientists tried using a pseudohalide precursor and discovered a significant change in stability with a pseudohalide, giving a stability enhancement of two weeks with only 0.9% efficiency reduction while stored in humidity. Their assessment of perovskite crystal stability at different temperatures and duration showed results with mixed chlorine and iodine halides, with the first exothermic peak at 100°C while the next one was at 230°C.

In other heat tests, formamidinium based PSCs showed better stability at 150°C in comparison to methylammonium cation perovskites. They also showed good stability when doped with chlorine.

Other types of perovskites such as 2D structures are a recent innovation in producing crystals with greater moisture stability despite the lower efficiency. Mixing chlorine with formamidinium and having P3HT as an HTM also showed promising results of 4.73% efficiency and tests on the crystal after 46 days showed very good stability in comparison to the methylammonium lead halide version.

Adding optimal combinations of different cations and anions of  $((\text{CH}_3\text{IN}_2)_{0.83}\text{Cs}_{0.17})\text{Pb}(\text{Br}_{0.4}\text{I}_{0.6})_3$  in combination with silicon produced a tandem cell where the perovskite would remain in a stable phase with an efficiency of 19.2% which also shows potential for further increase in efficiency when perovskites are commercially used to increase the efficiency of available solar panel technology.

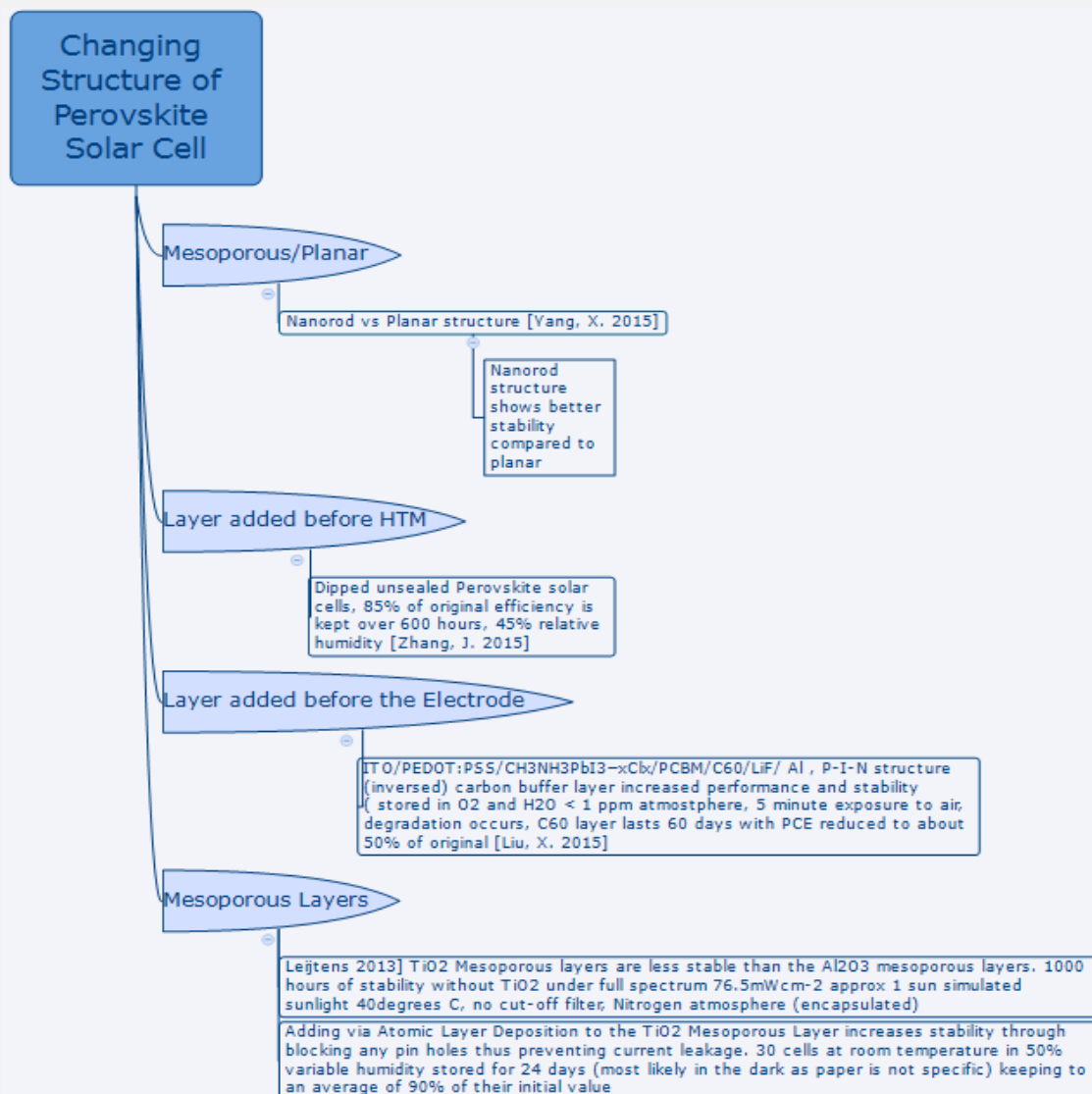
Understanding changes in band gaps at different temperature changes with tin inorganic based perovskites under conditions producing crystallization provided interesting results on the crystal structures produced.

### 3 Various ways to protect against humidity



Scheme 3

### 3.1 Altering the solar cell structure



Scheme 3-1

Initial steps to increase solar cell stability used alumina as the mesoporous layer instead of the standard mesoporous TiO<sub>2</sub>. The ultraviolet visible light spectroscopy (UV-Vis) absorbance spectra from the CH<sub>3</sub>NH<sub>3</sub>PbI<sub>2</sub>Cl perovskite device using alumina remains approximately the same (1000 h, N<sub>2</sub>, sealed between two sheets of glass, simulated 1 sun air mass 1.5 global (1.5 AM G)<sup>\*</sup>) [69] (see section 4.1.1 of the present paper).

\*Two standards are defined for terrestrial use. The AM1.5 Global spectrum is designed for flat plate modules and has an integrated power of 1000 W/m<sup>2</sup> (100 mW/cm<sup>2</sup>). The AM1.5 Direct (+circumsolar) spectrum is defined for solar concentrator work. It includes the direct beam from the Sun plus the circumsolar component in a disk 2.5 degrees around the Sun. The direct plus circumsolar spectrum has an integrated power density of 900 W/m<sup>2</sup>. The SMARTS (Simple Model of the Atmospheric Radiative

Following studies on the structure of the electron transport material (ETM) (planar/mesoporous/nanostructure) as well as the material it is made from (alumina/titanium/zinc oxide/and many more) gave information on how to create a more stabilized device structure. A planar PSC architecture has shown lower stability compared to mesoporous rutile  $\text{TiO}_2$  nanorod structures whether or not treated with  $\text{TiCl}_4$  [89].

The untreated structures were not as efficient as the planar devices but after treatment they were comparable if not better. This was attributed to their increased absorbance. The problem in stability was mainly in the loss of  $J_{sc}$  over a period of 55 days, <35% humidity at RT in the dark in a closed box containing a silica desiccant.  $V_{oc}$  measurements seemed to drop to 80% of the original while the planar configuration dropped to this value a few hours later but at >40 h a reduction to 50% of the original  $V_{oc}$  occurred.

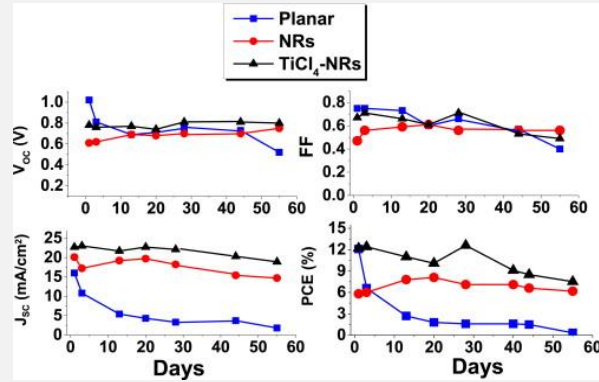


Figure 13: The photovoltaic parameters of the three devices measured for 55 days. The devices were kept at <35% humidity level and at RT during the shell life measurements. Reprinted from Role of morphology and crystallinity of nanorod and planar electron transport layers on the performance and long term durability of perovskite solar cells, 283 /1 June 2015, A. Fakharuddin, F. D. Giacomo, I. Ahmed, Q. Wali, T.M. Brown, R. Jose, Role of morphology and crystallinity of nanorod and planar electron transport layers on the performance and long term durability of perovskite solar cells, Pages 61-67, Copyright (2015), with permission from Elsevier. Ref. [89].

The stability of the aforementioned treated nanorod devices seem very promising as a result of a possible blocking layer being formed which increases recombination resistance. This treatment according to their investigation also reduces trap states and increases carrier lifetimes as well as increasing the interface between the perovskite and the scaffold interface due to the different crystal structure.

One can also use  $\text{ZnO}$  nanorod structures for the ETM

(FTO/ $\text{ZnO}$  nanorods/ $\text{CH}_3\text{NH}_3\text{PbI}_3$ /Spiro-MeOTAD/Ag), producing a long-term stability of 500 h (unencapsulated/stored/RT/air). Light absorbance was proportional to the rod length with the optimum for all the parameters being 1000 nm, 800 nm being recommended to prevent faster electron recombination. Initial efficiency was at 4%, quickly rose to 5%, then after 500 h a gradual decline to about 4.5% [90].

As mentioned previously in section 2, one part of the architecture that can be changed for greater stability is altering the perovskite composition; observation of a mixed halide crystal with a bromine in its constitution provided higher stability over the period of 30

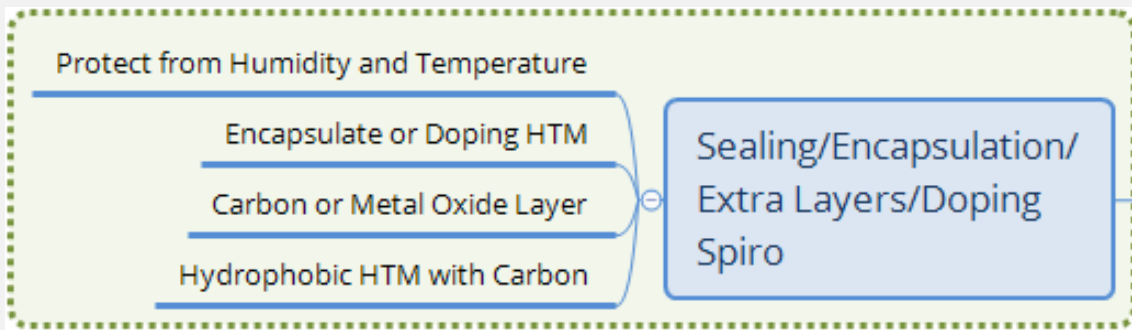
---

Transfer of Sunshine) program is used to generate the standard spectra and can also be used to generate other spectra as required.'[215]

days [78] (for further information on this finding see sub-section 4.2.3 of the current paper).

Another aspect of changing the PSC architecture is having different HTMs, as discussed in sub-section 4.1.2. To remove the negative issues related to HTMs, cells without such a layer have been produced and results showed to have promising stability. Another advantage would be more cost-effective devices (see sub-section 4.2 of the current paper).

### 3.2 ***Protection from the humidity/atmosphere/temperature via sealing***



Scheme 3-2

#### 3.2.1 **Encapsulation**

If one can fully encapsulate cells, this will lead to long term stability for the commercial production of such devices [91]. One example is the tin based perovskite, which was found to be very sensitive; it was sealed with film (DuPont™ Surlyn® film 1702) and stored in a nitrogen atmosphere for up to 24 h [92].

The values of the parameters stayed to within 80% during a 12 h time frame; by 24 h only 36% of the initial performance of each parameter remained.  $J_{sc}$ : 16.34 mA cm<sup>-2</sup> at 0 h, 15.05 mA cm<sup>-2</sup> at 12 h, 8.92 mA cm<sup>-2</sup> after 24 h;  $V_{oc}$ : 0.7 V at 0 h 7 V at 12 h, 0.62 V at 24 h; FF: 47% at 0 h, 40% at 12 h, 35% at 24 h; efficiency: 5.38% at 0 h, 4.21% at 12 h and 1.94% after 24 h (the supplementary information provides further insight on this in Ref. [92]).

There have been very harsh stress tests involving high and low temperatures, combined with high humidity to test the sealing methods on PSCs. Good stability was observed under dry conditions at temperatures below freezing (-20°C) resulting in efficiencies remaining close to the fresh and unstressed values. An increase in humidity by 10% combined with a jump in temperature at 55°C resulted in a photocurrent conversion efficiency (PCE) dropping to approximately one third of the initial value after 120 h; with a higher humidity of 80%, the PCE dropped to 0% after only 20 h (see Figure 15 referring to the stability graph with normalized PCE and 140 h of testing in Ref. [93]).

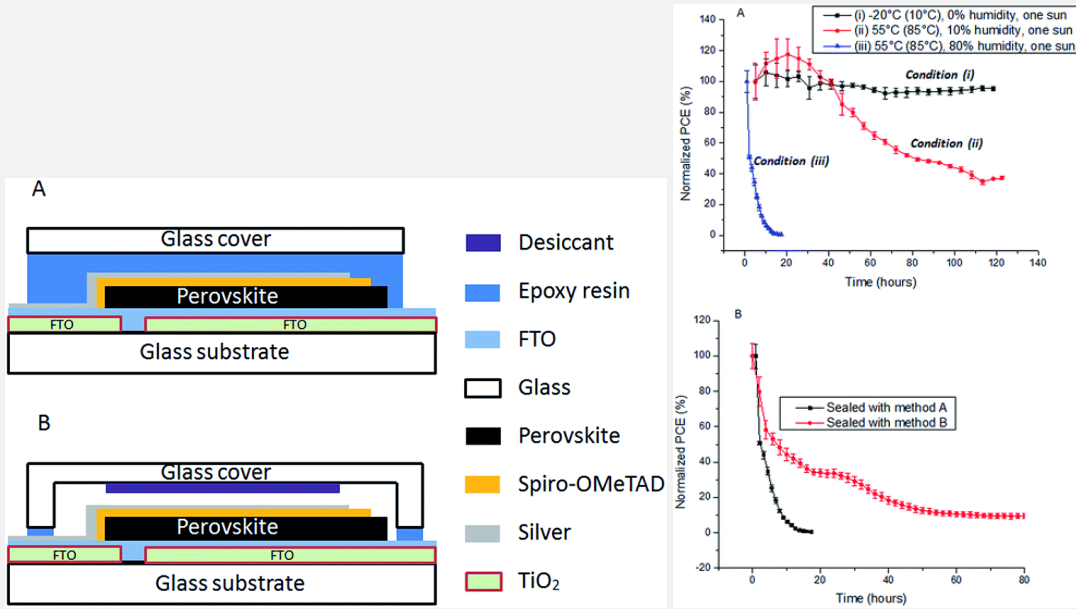
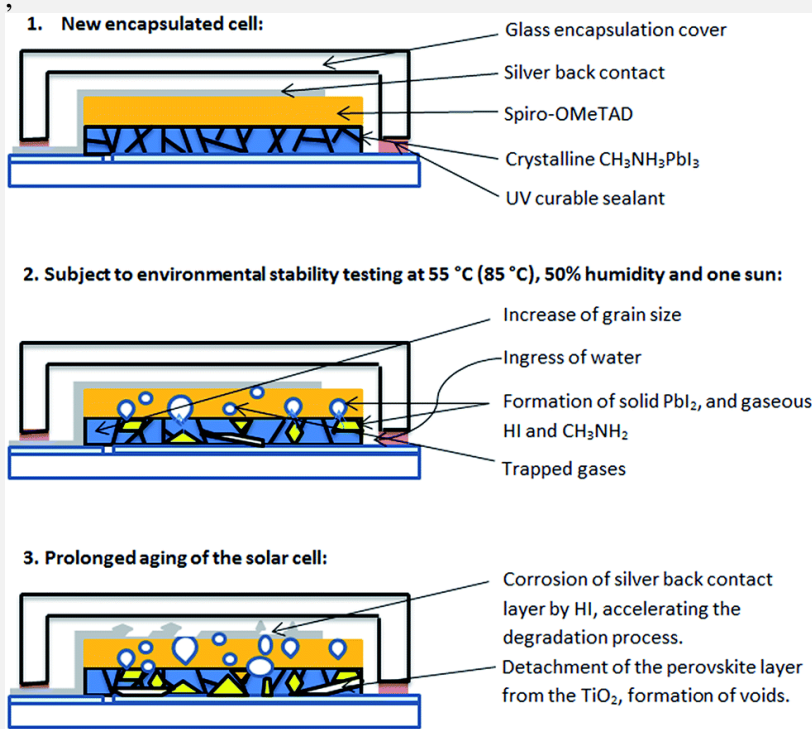


Figure 14: schematic cross-section of perovskite solar cells sealed according to technique A (top) and B (bottom) Ref. [93] Republished with permission of [Royal Society of Chemistry], from [Degradation observations of encapsulated planar  $\text{CH}_3\text{NH}_3\text{PbI}_3$  perovskite solar cells at high temperatures and humidity, H. Yu, M. Steffen, D. Yasmina, W. Karl, P. Jennifer M., B. Udo, S. Leone, C. Yi-Bing, Vol. 3, Issue 15, 2015]; permission conveyed through Copyright Clearance Center, Inc.

Figure 15: Graphs- (A) Stability testing of perovskite solar cells sealed by method A under three different environmental conditions; (B) comparison of the stability of devices sealed by method A and B and tested under environmental condition (iii). The efficiency of the devices before the test was set as 100% and the results were all normalized and plotted against the initial efficiency. Three devices were averaged for each test and the error bars show the standard deviation Ref. [93] Republished with permission of [Royal Society of Chemistry], from [Degradation observations of encapsulated planar  $\text{CH}_3\text{NH}_3\text{PbI}_3$  perovskite solar cells at high temperatures and humidity, H. Yu, M. Steffen, D. Yasmina, W. Karl, P. Jennifer M., B. Udo, S. Leone, C. Yi-Bing, Vol. 3, Issue 15, 2015]; permission conveyed through Copyright Clearance Center, Inc.



*Figure 16: Schematic of the degradation process of encapsulated methylammonium lead iodide perovskite solar cells illuminated at elevated temperatures and high humidity Ref. [93] Republished with permission of [Royal Society of Chemistry], from [Degradation observations of encapsulated planar CH<sub>3</sub>NH<sub>3</sub>PbI<sub>3</sub> perovskite solar cells at high temperatures and humidity, H. Yu, M. Steffen, D. Yasmina, W. Karl, P. Jennifer M., B. Udo, S. Leone, C. Yi-Bing, Vol. 3, Issue. 15, 2015]; permission conveyed through Copyright Clearance Center, Inc.*

### 3.2.2 ZrO<sub>2</sub>/carbon counter electrode

Carbon electrodes have also been employed to increase stability as well as spacer layers for improving the performance. Stability measurements (unencapsulated/dark/RT/dry atmosphere/840 h) were carried out on a carbon nanosphere graphene counter electrode stated as spheroidal graphite in Ref. [94] using zirconium dioxide (ZrO<sub>2</sub>) as a spacer layer after the TiO<sub>2</sub> layer to prevent short circuits. The perovskite solution was dripped over the electrode and due to the porous surface of the carbon it passed through; following this, the cell was annealed and produced an efficiency of 6.64% with the device architecture FTO/TiO<sub>2</sub>/ZrO<sub>2</sub>/CH<sub>3</sub>NH<sub>3</sub>PbI<sub>3</sub>/carbon [94].

Over the period of 840 h/35 d, J<sub>sc</sub> was slightly reduced, V<sub>oc</sub> increased by a small amount and then decreased to near its previous value; FF dropped slightly at first but then increased towards the end. The changes were not significant enough to affect the efficiency which remained above 6.5%.

This is not an uncommon method of fabricating perovskite devices with porous carbon electrodes. An HTM-free unencapsulated cell with a carbon electrode was constructed, in which the perovskite layer was treated with ammoniumvaleric acid ((5-AVA)<sub>x</sub>(CH<sub>3</sub>NH<sub>3</sub>)<sub>1-x</sub>PbI<sub>3</sub>). As stated in the previous paragraph, the perovskite solution was drop casted through the porous carbon back contact layer; this showed significant stability lasting 1008 h in ambient air under an illumination of 1 sun 1.5 air mass (AM) [95].

The carbon printed layer acted as an effective protection against the moisture which normally causes cell degradation. In the initial hour a jump in performance was seen; all the parameters changed <10% of their initial values: efficiency 10%, FF 0.6,  $J_{sc}$  of 22.5 mA cm<sup>-2</sup> and  $V_{oc}$  about 780 mV.

### 3.2.3 Buffer layers

A buffer layer is simply a layer acting to reduce the impact of some effect, e.g., performance degradation. For PSCs their use has been to protect against moisture; in some cases, this has positive or negative effects on efficiency.

For a p-i-n junction PSC containing phenyl-C61-butyric acid methyl ester (PCBM) ETM, with the structure ITO/PEDOT:PSS/CH<sub>3</sub>NH<sub>3</sub>PbI<sub>3-x</sub>Cl<sub>x</sub>/PCBM/C<sub>60</sub>/LiF/Al, including a carbon buffer layer before the cathode was shown to increase performance of the device. The ETM layer increased its stability.

Without the C<sub>60</sub> layer there was mild improvement in efficiency. The stability test (storage, nitrogen glove box: O<sub>2</sub> and H<sub>2</sub>O < 1 ppm, exposure to air for 5 min) caused the cells to begin significantly degrading as the  $J_{sc}$  was markedly affected due to the increase in the resistance caused by the interface between the perovskite and PCBM layer.

The  $V_{oc}$  remained stable in both a double and triple carbon buffer layer and perovskite did not degrade, while efficiency stayed at just over 50% of the original value in the triple cathode after 60 days [96]. The C<sub>60</sub> layer was shown to improve the stability considering that without it the cell lasted 30 d compared to 60 d with the extra layer.

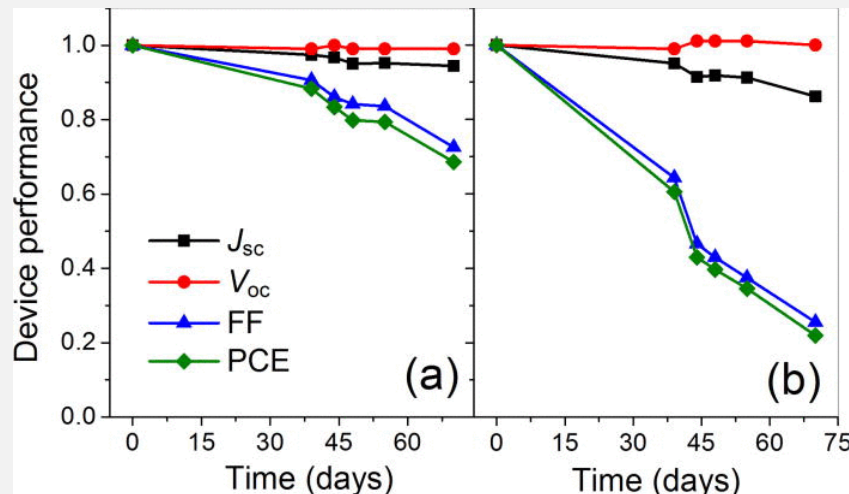


Figure 17: Reprinted (adapted) with permission from (CS Appl. Mater. Interfaces, 2015, 7 (11), pp 6230–6237). Copyright (2015) American Chemical Society Photovoltaic characteristics normalized by their initial values, for the p-i-n PSCs with (a) PCBM/C<sub>60</sub> (15 nm)/LiF (1 nm) and (b) PCBM/LiF (1 nm) carbon buffer layers, as a function of the storage time in the glovebox. Asterisks denote the data points of air exposure for ~5 min. Perovskites without the CH<sub>3</sub>NH<sub>3</sub>PbX<sub>3</sub> Structure (reproduced with permission from Ref. [96]).

### 3.2.4 Carbon and hydrophobic HTM

Using HTMs with hydrophobic properties or carbon positively influences PSC stability (see section 4.1.2 for further information).

As mentioned earlier, cell stability is improved when treated with 5-ammoniumvaleric-acid ((5-AVA)<sub>x</sub>(MA)<sub>1-x</sub>PbI<sub>3</sub>) drop casted through the protective carbon, onto the perovskite (see section 3.2.2).

### 3.2.5 $\text{Al}_2\text{O}_3$ atomic layer deposition (ALD) protection

The initial step of using alumina as one of the layers (see the beginning of section 3.1) has also been employed after the HTM. As a protective layer, alumina ( $\text{Al}_2\text{O}_3$ ) was used as a buffer layer on top of the HTM to reduce possible pinholes between the perovskite layer and electrode which the HTM may not cover. This also protects the PSC from moisture and it was found on average that this increased the overall performance in all areas due to a better fill factor [97]. For an assessment of batches tested for 350 h at 1 solar intensity/ $V_{oc}$  condition/ no UV filter/encapsulated/ $\text{N}_2$ , performances stayed close to 90% of their original values and their most robust cell remained to within 5% of its initial measurement.

A batch of eight cells, four control and four buffered, had a large variation which overlapped with the results of the control, but the average performance parameters were higher.

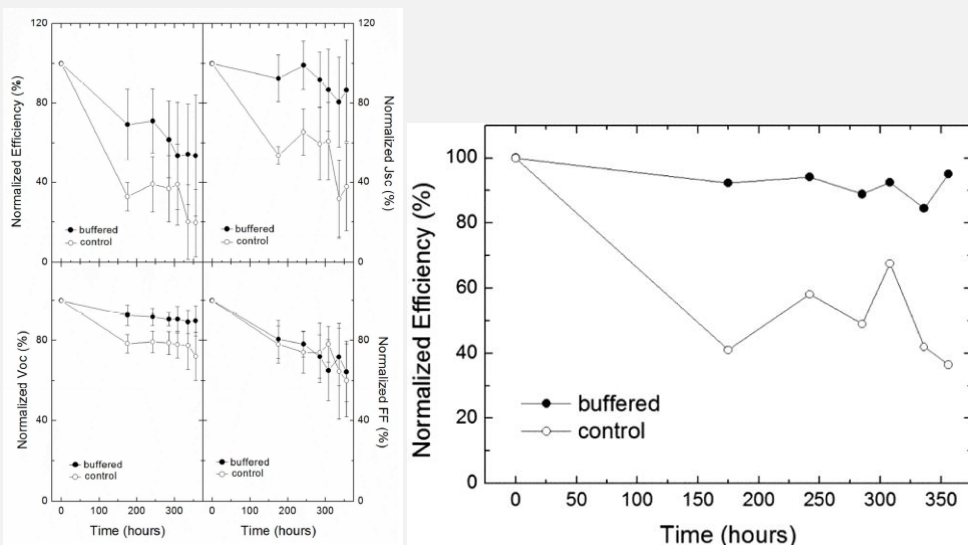


Figure 18: "Reprinted (adapted) with permission from (Chem. Mater., 2013, 25 (22), pp 4613–4618). Copyright (2015) American Chemical Society." Statistics of normalized JV parameters of encapsulated cells with (black dots) and without (white dots) buffer layer, under 1.5 AM G illumination condition (4-cells for each type). The cells were encapsulated and maintained at  $V_{oc}$  condition during the Ageing (reproduced with permission from Ref. [97]).

Other work with buffer layers by another research team involved using atomic layer deposition (ALD). Alumina deposited on top of the HTM with parameters: 70°C, optimum 0.3 nm thick, from a 3 nm x 0.1 nm/cycle increases the stability of a batch of 30 cells (RT/ 50% variable humidity/stored 24 d) to an average of 90% of their initial value [74].

Without this ALD coating, performance is better, but stability was severely compromised; five of these films showed the performance to be reduced substantially and seven demonstrated a very low performance. Electrical impedance analysis measurements of, series, recombination and, hole-transport resistance, all were higher as a result of the layers of alumina.

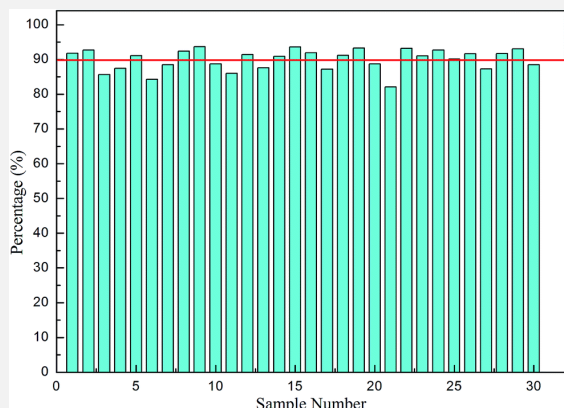


Figure 19: The histogram of the PCE of thirty solar cells after 24 days in air compared with the original efficiency hydration Reproduced ("Adapted" or "in part") from {J. Mater. Chem. A, 2015, 3, 5360-5367} or Ref. [74] with permission of The Royal Society of Chemistry

This method of using ALD for cell fabrication for one of the layers has also been used to provide over 30 days of stability in ambient air for memory based devices [98] but whether this is a manufacturable technique that can be applied for commercialization would require further investigation as it requires expensive equipment and takes a long time.

### 3.3 Summary of section 3

Using different materials in the layers of the solar cell including different morphological properties can help to improve stability. Among the many that are used, in this section, alumina, carbon and zirconia have been listed; probably more recently, groups have found many other types of materials. The materials in this section are non-exhaustive and the idea helps the reader to think about other techniques such as which materials to use, to add stability to the system they are designing/working on. Morphology of nanostructures, e.g., zinc oxide nanorods for ETM layers, was found to be promising and further research can be done in this area to optimise the right shape for each system.

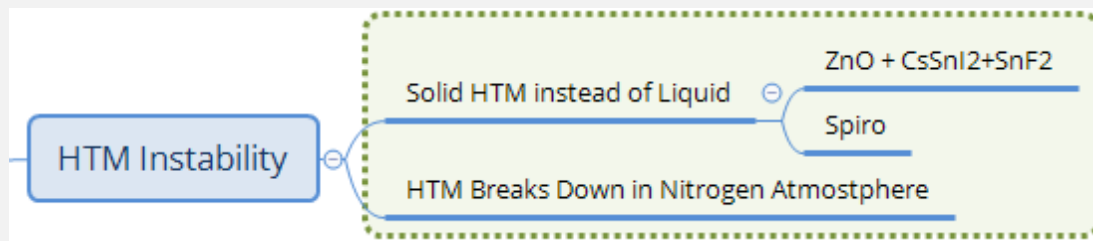
Finding the best way to protect the perovskite layer from the atmosphere through different methods of encapsulation will be important for commercialization when PSCs reach the required standards; adding thin hydrophobic layers like alumina and carbon or hydrophobic HTMs are also useful. Carbon electrodes are generally good barriers against moisture ingress, as well as the ALD technique of alumina layers, although the latter technique's practical use in commercialization would be questionable.

## 4 Understanding HTM stability and performance



Scheme: 4

### 4.1 HTM instability



Scheme 4-1

#### 4.1.1 Liquid perovskite causing problems

In the early stages of PSCs, adding liquid tri-iodide electrolyte to a photosensitive perovskite caused bleaching; the crystal dissolves into the liquid electrolyte. Even though the perovskite was synthesized at a low concentration of 0.08 M LiI, 0.04 M I<sub>2</sub>, 0.05 M 4-*tert*-butylpyridine (tBP), and 0.005 M urea in ethyl acetate, in order to improve the stability the team emphasised the need to produce a solid-state HTM [99].

As a result the perovskite Spiro-MeOTAD was implemented as a solid hole transporter and indicated stabilized absorption with hardly any change under the following conditions: sealed between two sheets of glass/nitrogen/1.5 AM G sunlight 1 sun/1000 h and having an architecture of Al<sub>2</sub>O<sub>3</sub>; CH<sub>3</sub>NH<sub>3</sub>PbI<sub>2</sub>Cl; Spiro-MeOTAD [69] (for further information see section 3.1 of the present paper).

The stability was not measured in this investigation at the time. This paper also was referenced in Ref. [68] reviewing different mesoscopic solar cells. The significant difference was the use of alumina as a scaffold for the perovskite making it higher in efficiency and stability despite being an insulator, implying quantum tunnelling of charges was taking place.

Charge transfer comparison indicated that Al<sub>2</sub>O<sub>3</sub> quantum tunnelling is more efficient than TiO<sub>2</sub> conduction band charge transfer, giving at the time a 10.9% efficiency with a mixed halide of CH<sub>3</sub>NH<sub>3</sub>PbCl<sub>3-x</sub>Cl<sub>x</sub> [69].

#### 4.1.2 Replacing the liquid electrolyte and early stability tests

As mentioned in the previous sub-section, DSCs degrade due to the corrosive tri-iodide redox couple in the electrolyte. The method implemented to overcome this challenge was using solid charge transport layers instead. One means to address this was synthesising the inorganic perovskite CsSnI<sub>3</sub>, which is a solid HTM. The best performance was

achieved with  $\text{CsSnI}_{2.95}\text{F}_{0.05}$  doped with 5%  $\text{SnF}_2$ , cell structure FTO/ $\text{CsSnI}_{2.95}\text{F}_{0.05}$ /N719/TiO<sub>2</sub>/FTO and having ZnO photonic crystals on the top of the counter electrode to increase the amount of light being diffused into the cell which provided optimum performance [68]. They reached an efficiency of 10.2% or with a mask 8.51%, showing no need to have a liquid electrolyte.

Another means to counteract this corrosion when ZnO is used as an electron transport material in one of the layers in DSCs (due to greater electron mobility and electron density) is employing an inorganic perovskite as part of the blocking layer in solid-state DSCs and copper thiocyanate (CuSCN) as a HTM.

This electron transport layer had the morphology of a rod nanostructure. The ZnO nanorods were dissolved slightly by BaFeO<sub>3</sub> (BFO) solution when directly applied due to its very strong acidity pH = 1, so an aminosilane layer solution was deposited first. Following this, BFO was deposited and used as an n-type layer as part of a solid-state solar cell (ZnO/N719/CuSCN spray coated/sputtered Au) system to make the cell architecture ZnO/BFO/N719/CuSCN spray coated/sputtered Au. The BFO perovskite acted as an electron blocker and thus electrons tunnelled through it from the N719 to the ZnO layer. Performance was raised, going from 0.095 to 0.217%. While this had lower efficiency than DSCs, it was a solid-state system using ZnO and aqueous solutions together with a solid-state HTM CuSCN. [100].

Early on in solid-state PSC research, a mesoporous layer filled with  $\text{CH}_3\text{NH}_3\text{PbI}_3$  and a Spiro-MeOTAD HTM in 2012 was reported to reach 9.7% efficiency [28]. It was the first publication where the HTM was implemented with PSCs as an absorber in this structure. The stability under conditions of 500 h/unencapsulated/storage/air with the structure 0.6  $\mu\text{m}$  thick TiO<sub>2</sub> mesoporous layer/Spiro-MeOTAD demonstrated promise and was encouraging to researchers due to an increase in the fill factor which in turn improved the efficiency and thus helped towards significant progress in long term stability testing.

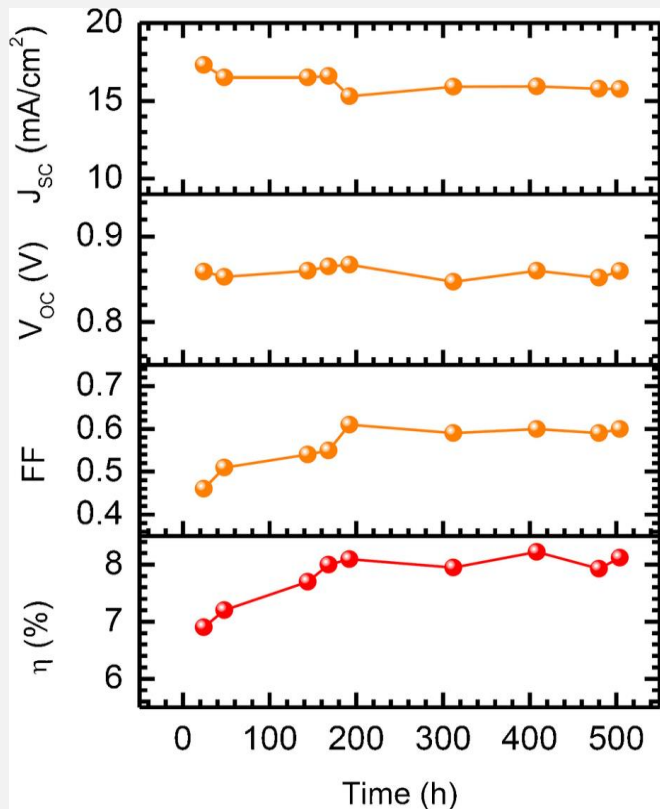


Figure 20: Stability of  $(\text{CH}_3\text{NH}_3)\text{PbI}_3$  sensitized solid-state solar cell stored in air at RT without encapsulation and measured under one sun illumination Reprinted by permission from Macmillan Publishers Ltd: [Nature Scientific Reports] (Ref. [28]), copyright (2012) (awaiting permission)

#### 4.1.3 HTM breakdown in N<sub>2</sub> atmosphere – doped or undoped

HTMs are very important in PSC stability. Measuring the absorbance at 410 nm in harsh humidity tests using HTMs: Spiro-MeOTAD, PTAA and P3HT, resulted with half-lives defined in the paper as ‘normalized absorbance was halfway between its initial (1.00) and final ( $\sim 0.33$ ) values’ for high relative humidity of 98% and 80%, to be approximately 4 and 34 h respectively, while those of lower humidity 50% and 20% demonstrated half-lives of 1000 and 10000 h respectively [101].

Oxygenated air or N<sub>2</sub> affected stability differently; humidity impacted the performance rather than oxygen, oxygen only slightly increasing degradation levels. Undoped P3HT seemed to show the greatest stability among Spiro-MeOTAD, PTAA and P3HT, although undoped PTAA stood out as the best.

The HTM mechanically breaks down as the humidity seeps through and begins to degrade the perovskite, thus reducing the performance of the cell as PbI<sub>2</sub> is formed. Further to this, glancing incident XRD diffraction showed a new crystal of  $(\text{CH}_3\text{NH}_3)_4\text{PbI}_6 \cdot 2\text{H}_2\text{O}$  as a result of contact with moisture, giving the reversible chemical equation:



due to HTM damage.

They suggest that possible further decomposition of the other products will prevent any reversible reaction, thus leaving  $\text{PbI}_2$  as the only by-product.

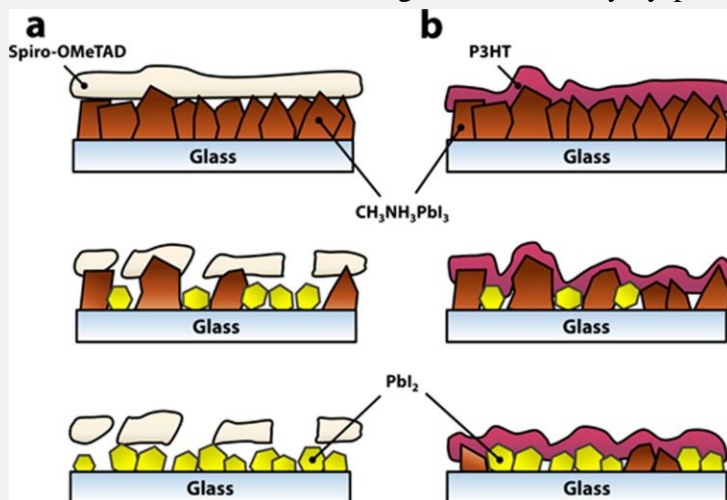


Figure 21: Cartoon depiction of the structural and morphological differences between (a) Spiro-MeOTAD and (b) P3HT HTLs upon exposure to water vapour Ref. [101]. Reprinted with permission from (ACS Nano, 2015, 9 (2), pp 1955–1963). Copyright {2015} American Chemical Society.

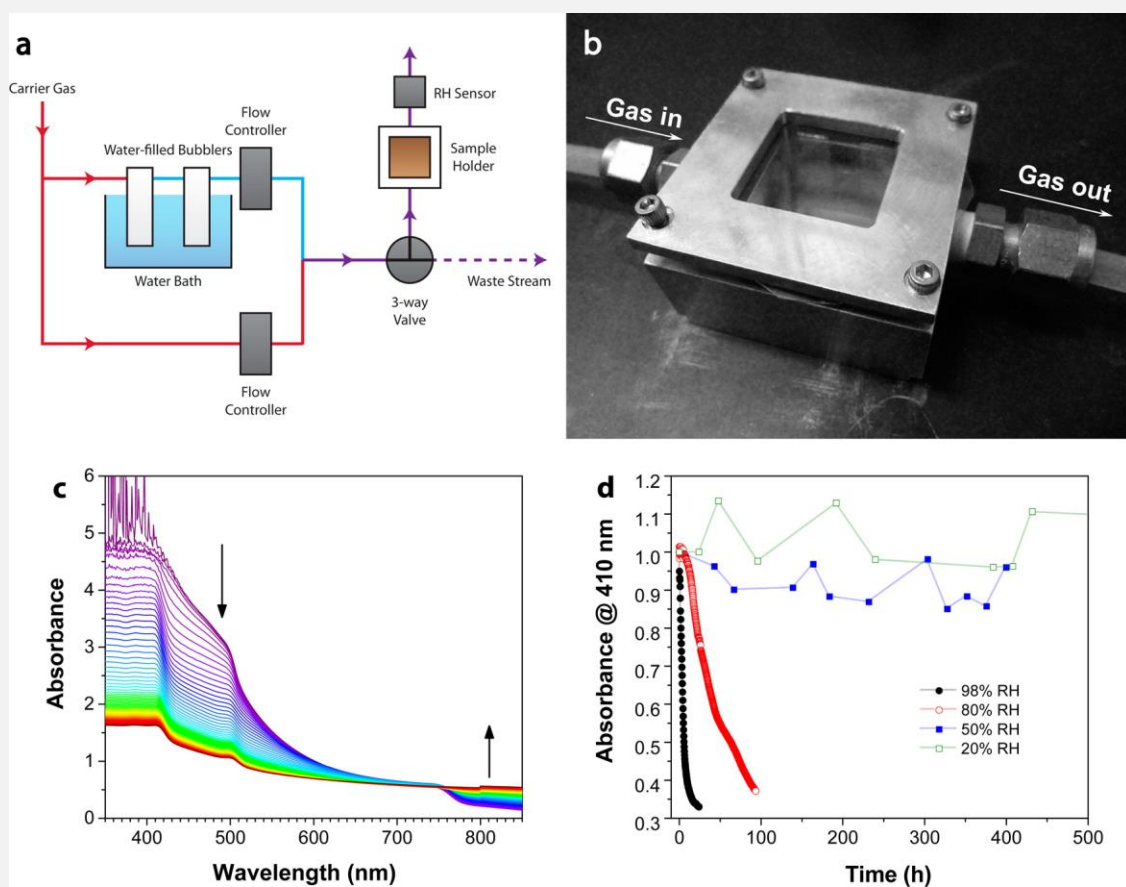
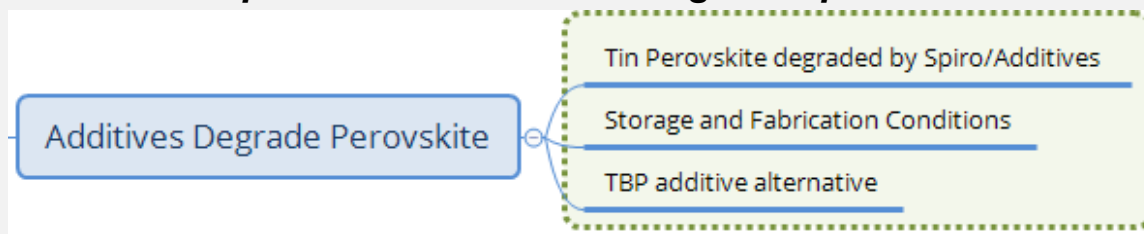


Figure 22: Reprinted with permission from (ACS Nano, 2015, 9 (2), pp 1955–1963). Copyright {2015} American Chemical Society. UV-vis spectra, acquired at 15 min intervals, of a  $\text{CH}_3\text{NH}_3\text{PbI}_3$  film exposed to flowing  $\text{N}_2$  gas with  $\text{RH} = 98 \pm 2\%$ , (d) Normalized absorbance at 410 nm as a function of time for perovskite films exposed to various relative humidities. Data at 50% and 20% RH were acquired once per 24h. The temperature was measured to be  $22.9 \pm 0.5^\circ\text{C}$  for all measurements (reproduced with permission from Ref. [101]).

## 4.2 Spiro-MeOTAD/additive degrades perovskite



Scheme 4-2

### 4.2.1 Tin perovskite degraded by spiro-MeOTAD/additives in inert atmosphere

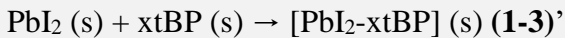
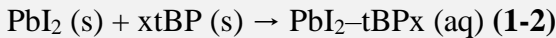
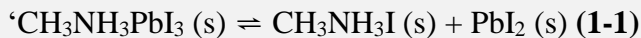
Tin perovskites are very sensitive to the environment and have also been found to break down due to the Spiro-MeOTAD HTM. This may be from the presence of the Spiro-MeOTAD HTM plus its additives. In an inert atmosphere where one would expect stability, degradation still can occur. The perovskite ( $\text{CH}_3\text{NH}_3\text{Pb}_{x-1}\text{Sn}_x\text{I}_3$ ) showed this effect despite being in an inert atmosphere [102].

An alternative to spiro-MeOTAD being used with a tin based PSC would be better for stability; degradation might be due to one, if not more of the required additives.

### 4.2.2 Alternative to *tert*-butylpyridine for greater performance

Another factor affecting some perovskite recipes is the use of tBP in the hole transporter [103].

They find three mechanisms responsible:



The use of Montmorillonite (MMT) in chlorobenzene (0.53 mg ml<sup>-1</sup> diluted 0.00625 times) was used as a buffer layer on top of the perovskite layer to protect it from the Spiro-MeOTAD HTM. IR spectroscopy suggested the interaction of the tBP and MMT is through the hydrogen bonds.

The O-H bonds in MMT significantly reduce in strength due to the nitrogen atoms in tBP, thus creating hydrogen bonds with the hydrogen atoms in the MMT [103]. Electrical impedance spectroscopy showed that despite an increase in the interface layer resistance, recombination resistance increased more, thus improving the cell. Increases were seen in the light harvesting efficiency, absorption of the solar spectrum, photo current conversion, and in the XRD, greater film stability was measured.

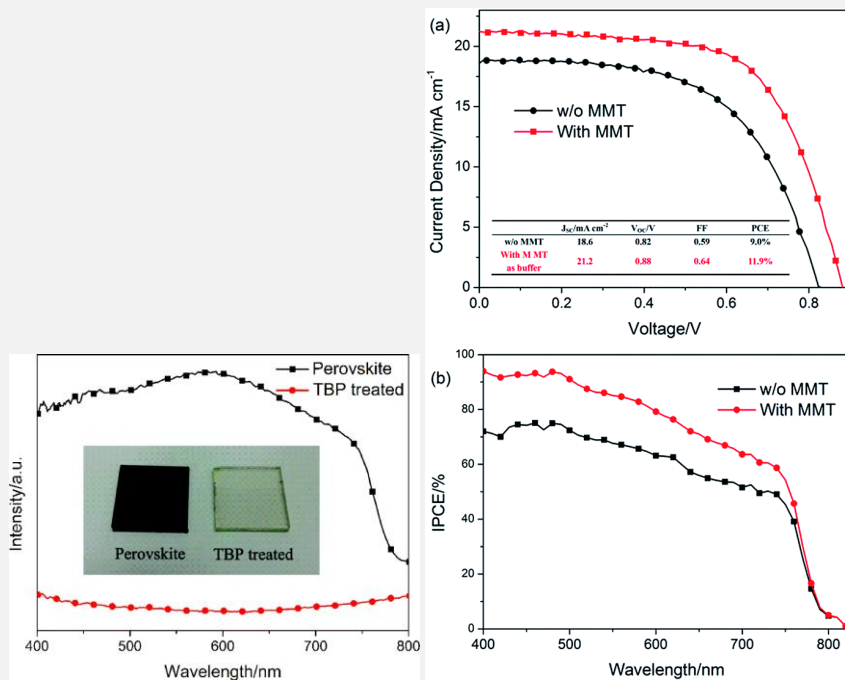


Figure 23: (Left) UV-vis spectra of  $\text{TiO}_2$ /perovskite film and TBP-treated film including the inserted photos, (Right) The J-V characteristics and IPCE of devices (dark) without MMT addition and (red) with MMT addition to the HTL: the inset in the top graph shows the parameters of the cells ,Reproduced ("Adapted" or "in part") from {J. Mater. Chem. A, 2014, 2, 13587-13592} (or Ref. [103]) with permission of The Royal Society of Chemistry.

#### 4.2.3 Storage and fabrication conditions

Storage and fabrication conditions such as the atmosphere in which cells are made can affect the performance and stability of devices. With the HTM Spiro-MeOTAD drying in the dark, efficiencies and stabilities have been shown to be best under the effect of a dry atmosphere, followed by  $\text{N}_2$ , and the lowest performance was when the cells were stored in a vacuum. They found that the drying condition of the HTM was critical for high performance of cells at RT for 12 h in a dry atmosphere as opposed to  $\text{N}_2$  and vacuum conditions, regardless of the storage conditions afterwards. The oxidation of Spiro-MeOTAD increases conductivity through greater carrier density and mobility and thus charge carrier recombination is reduced which lowers series resistance. Without the oxygen in the environment the conduction band was lowered, likely due to the lack of oxygen ions, thus causing lower  $V_{\text{oc}}$ .

Despite greater performance, stability showed similar trends in behaviour (stored 240 h, 60% mean ambient humidity during characterisation measurements, dark, dry) and investigators believe this is due to the Spiro-MeOTAD being affected by residual oxygen in the  $\text{N}_2$  and vacuum environments, although more articles would need to be viewed to confirm this since its time of publishing [104].

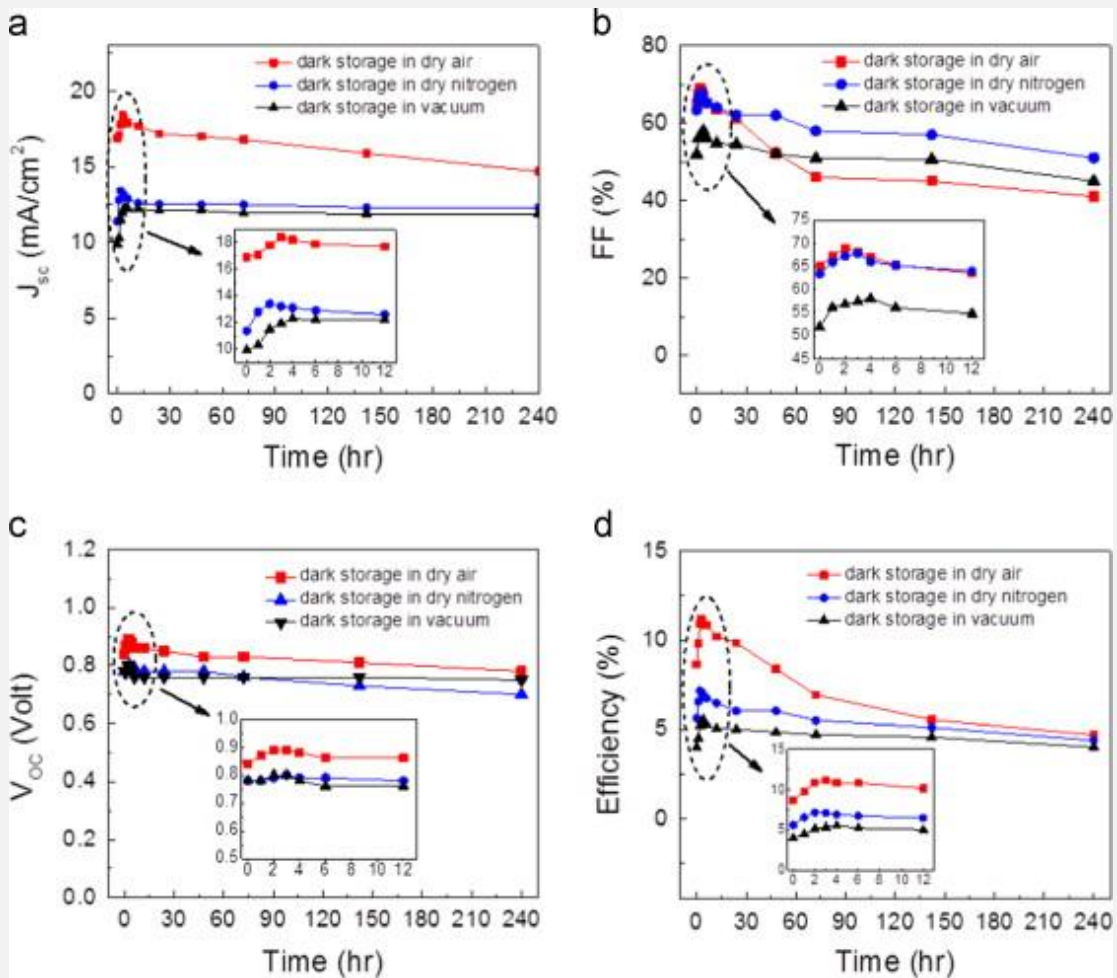
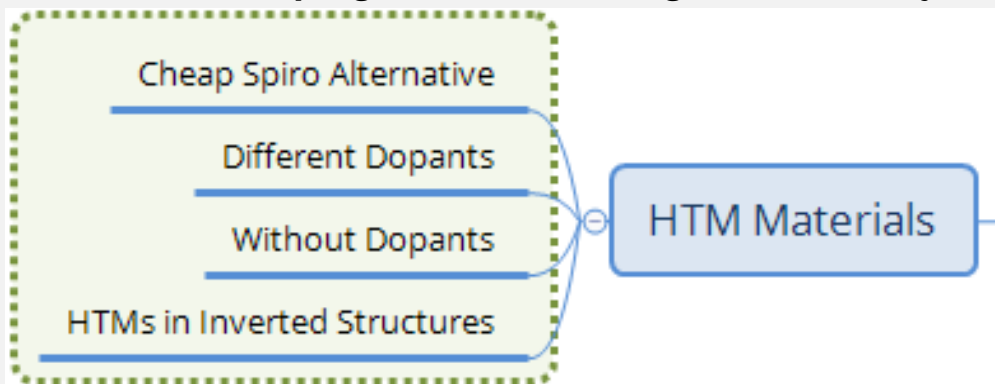


Figure 24: Time-dependent evolutions of (a) short-circuit current density,  $J_{sc}$  (b) fill factor, (c) open-circuit voltage,  $V_{oc}$  and (d) efficiency of the solar cells without encapsulation stored in the dark and under different atmospheric conditions (reproduced with permission from [104]). Reprinted from Atmospheric effects on the photovoltaic performance of hybrid perovskite solar cells, Vol. 137, Sheikh, Arif D., Bera, Ashok, Haque, Md Azimul, Rakhi, Raghavan B., Gobbo, Silvano Del, Alshareef, Husam N., Wu, Tom, Atmospheric effects on the photovoltaic performance of hybrid perovskite solar cells/ Results and discussion, Pages 6-14., Copyright (2015), with permission from Elsevier.

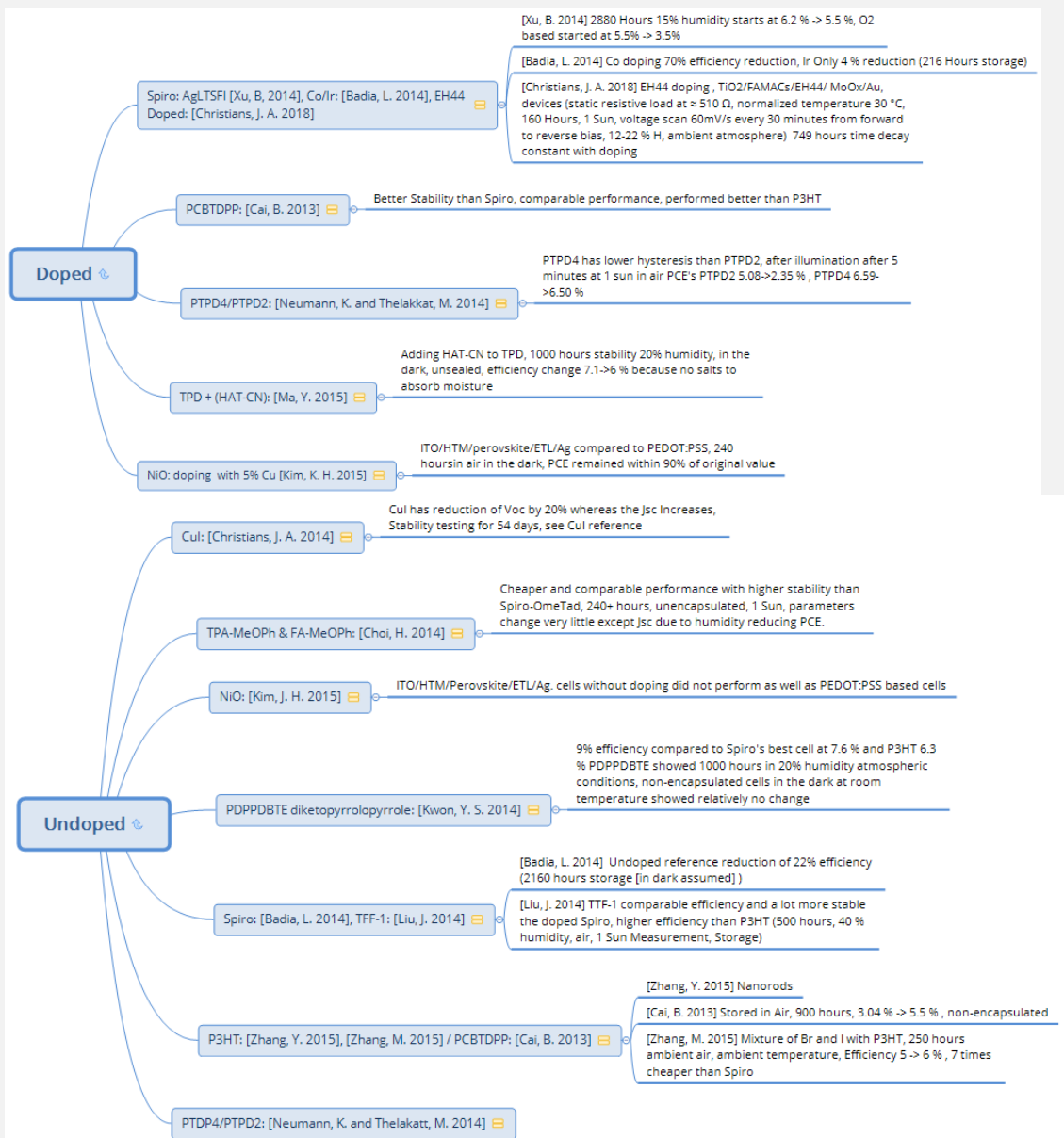
#### 4.1 HTM and doping alternatives for greater stability



Scheme 4-3

Doped HTM: [Authors and Publication year]	Undoped HTM: [Authors and Publication year]
Spiro: AgLTSFI [Xu, B. 2014], Co/Ir: [Badia, L. 2014], EH44 Doped: [Christians, J. A. 2018] PCBTDP: [Cai, B. 2013] ⓘ PTPD4/PTPD2: [Neumann, K. and Thelakkat, M. 2014] ⓘ TPD + (HAT-CN): [Ma, Y. 2015] ⓘ NiO: doping with 5% Cu [Kim, K. H. 2015] ⓘ	CuI: [Christians, J. A. 2014] ⓘ TPA-MeOPh & FA-MeOPh: [Choi, H. 2014] ⓘ NiO: [Kim, J. H. 2015] ⓘ PDPPDBTE diketopyrrolopyrrole: [Kwon, Y. S. 2014] ⓘ Spiro: [Badia, L. 2014], TFF-1: [Liu, J. 2014] ⓘ P3HT: [Zhang, Y. 2015], [Zhang, M. 2015] / PCBTDP: [Cai, B. 2013] ⓘ PTPD4/PTPD2: [Neumann, K. and Thelakkat, M. 2014]

Scheme 4-4



Scheme 4-5

#### 4.1.1 Effects of different dopants

When an additive of lithium bis(trifluoromethanesulfonyl)imide (LiTFSI) salt is added to Spiro-MeOTAD, the PSC performance is higher. The HTM PTAA was compared to Spiro-MeOTAD with and without the same dopant.

Despite LiTFSI improving the charge transport and electron lifetime, without it the stability (150 h/storage/50-60% humidity/unencapsulated) is significantly improved to over 150 h.

The undoped cell's stability had an efficiency decrease of 10.7 to 9.4%, compared to the doped HTM cell's efficiency reducing from 12.3 to 3.6% [105]. It was suggested that one of the reasons for poor performance was due to the lithium's hydroscopicity.

Due to oxygen causing problems for LiTFSI in solid-state solar cells, similar research in the trial of other dopants for Spiro-MeOTAD [silver bis(trifluoromethanesulfonyl)imide (AgTFSI) and oxygen] was assessed.

These same dopants in unencapsulated cells were also reported in another article; the cell architecture was FTO/TiO<sub>2</sub>/mesoporous TiO<sub>2</sub> (mp-TiO<sub>2</sub>)/LEG4 dye/HTM/Ag under test conditions of 120 days/4 months (2880 h)/dark, 15% humidity). With AgTFSI, parameters except the  $V_{oc}$  had better stability than cells with oxygen as a dopant [106]. The main reason for improved performance in the voltage curves was the higher fill factor.

Efficiency started at 6.2%, increasing to 6.5%, followed by reduction to 5.5% with AgLTFSI. With the oxygen doped cells which were left in the dark for a night before the counter electrode was evaporated, 5.5% was the initial value falling to about 3.5%.

Other metals such as Co and Ir are dopants that have also been tested with Spiro-MeOTAD compared to undoped Spiro-MeOTAD [107]. Such cells showed that Co was the least stable, with all parameters being reduced: the efficiency loss was 70%, and the undoped reference cell's efficiency fell by 22% as a result of a lowered FF. The Iridium-based device displayed impressive stability; the HTM doped with Ir only degraded by 4%. They state how this value is less than the experimental error via storage for three months (90 days, 2160 h, storage – likely dark, humidity unspecified).

While Spiro-MeOTAD performs well, it is a very expensive material at 358 € g<sup>-1</sup> from a supplier found online; thus, it is important to discover an alternative, which balances performance and cost.

#### **4.1.2 Hydrophobic/hydrophilic HTMs, with/without dopants**

##### **4.1.2.1 P3HT HTM cell stability measurements**

As mentioned in an earlier section, P3HT is a hydrophobic HTM which has shown promise for PSC photovoltaics.

P3HT cells with rutile TiO<sub>2</sub> nanorods as the ETM layer were found to have greater electron lifetime due to reduced charge recombination and hence higher fill factor and voltage compared to cells without an HTM. The performance in general is shown to be better with this HTM than without due to better conductivity for charge flow [108].

Results have shown that an increase in stability was due to the hydrophobicity; additionally, the rutile TiO<sub>2</sub> nanorods assisted by preventing interaction with the perovskite. Stability test results showed that the P3HT perovskite reduced from 6.06% efficiency to 3.51% mainly due to fill factor reduction and partial decrease in  $V_{oc}$ , and the cell without dopants dropped from 4.92-2.20% due to all three parameters degrading in value (14 days/ambient environment/storage/unencapsulated) [108].

Another undoped hole transporter being a tetrathiafulvalene derivative was developed and shown to be better in terms of stability for 500 h; it had comparable efficiency to doped Spiro-MeOTAD and was more efficient than P3HT (500 h, 40% humidity, ambient temperature, storage) as measured under illumination 1.5 AM G [109].

Starting at just over 2%, the Spiro-MeOTAD based cell jumped to just under 11.5% efficiency after 25 h, followed by relatively constant stability; after 100 h a significant decline to 1% ensued at a rate of 0.0225% per h for the following 400 h. The

tetrathiafulvalene undoped cell started at 10%, at 25 h reached 11%, followed by 225 h of relative stability, leading to a gradual decline to about 8.5% with a gradient of  $0.008\% \text{ h}^{-1}$  for the subsequent 350 h [109].

In other investigations, which compared spun coated  $\text{CH}_3\text{NH}_3\text{PbI}_3$  and  $\text{CH}_3\text{NH}_3\text{PbI}_{3-x}\text{Cl}_x$  on a plain glass substrate, underneath a film of undoped P3HT (undoped was said to have better performance), after they were stored for one month in ambient conditions with  $>50\%$  humidity, UV-Vis spectroscopy showed change with the single halide but the mixed halide remained unchanged (see section 9.5 of this paper). After 6 months, degradation was also observed with the mixed halide due to a change in XRD peaks. 50 cells (FTO/TiO<sub>2</sub>/CH<sub>3</sub>NH<sub>3</sub>PbI<sub>3-x</sub>Cl<sub>x</sub>/P3HT/Ag) ranging from 2-6% efficiency were stored in an air tight container for 50 days with a humidity of  $>50\%$ . The efficiency was degraded to 0.11% which was due to both electrode oxidation and HTM degradation [110].

See section 2.4.2 on investigators employing tests using a similar setup, but using formamidinium as a cation in a lead perovskite where chlorine improved the performance and gave good stability for 30 days of ageing [86].

Looking at the cost of P3HT, one finds that the cost at the time of writing is  $439 \text{ € g}^{-1}$  from a supplier found online. This is still very expensive, and if it is possible to produce an economical P3HT due to it being a polymer HTM, it would be very useful.

One such version of P3HT was implemented in halide mixtures of Br and I in a perovskite device. It proved to be successful in producing stable, efficient, unencapsulated solar cells starting with approximately 5% efficiency, increasing to 6% after 250 h in air at ambient temperature; this combination was also shown to improve the charge carrier lifetime as well as acting as an electron blocker; the other significant point they state was that this was at least seven times less expensive than the Spiro-MeOTAD HTM. It would be very useful if it is still feasible to purchase the HTM at a molecular weight of 54000–75000[111].

#### 4.1.2.2 Additional HTMs (non-exhaustive)

Perovskite stability testing has seen many other new hole transporters, among them one containing poly[2,5-bis(2-decyldodecyl)pyrrolo[3,4-c]pyrrole-1,4(2H,5H)-dione-(E)-1,2-di(2,20 -bithiophen-5-yl) ethene] (PDPPDBTE), also known as diketopyrrolopyrrole; having a hydrophobic nature and used within the cell structure as (FTO/mesoporous TiO<sub>2</sub>/CH<sub>3</sub>NH<sub>3</sub>PbI<sub>3</sub>/HTM/Au) [112]. A brief search for this HTM shows it is not available for purchase which implies it can only be synthesised in the laboratory.

The best PDPPDBTE cell achieved a 9% efficiency, compared to Spiro-MeOTAD's best cell at 7.6% with a 70° hydrophobicity, while P3HT's efficiency was 6.3% and had the same hydrophobicity as PDPPDBTE which was 105°.

Stability testing (1000 h/20% humidity/atmospheric conditions/unencapsulated/dark/RT) showed relatively no change in efficiency except the cell with HTM PDPPDBTE demonstrating a minor increase of almost 1% at 25 h which returned to the initial value by 100 h. The P3HT cell sustained an initial efficiency decrease after 25 h, returning to its initial value, and hovered around 6%. The Spiro-MeOTAD HTM cell showed reduction from 7.6% to about 6.6% in 25 h, then a gradual decline to almost 5% due to the degradation of the short circuit current.

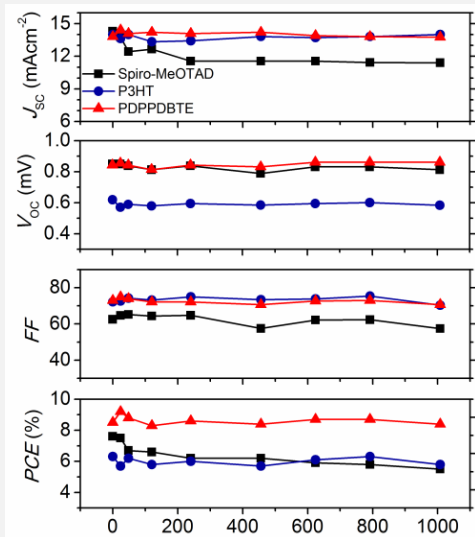


*Figure 25: Evolution of photovoltaic parameters for 3 HTM-based hybrid solar cells with aging time over 1000 hours stored under ca. 20% humidity atmosphere reproduced from with permission from the Royal Society of Chemistry. Reproduced ("Adapted" or "in part") from {Energy Environ. Sci., 2014, 7, 1454-1460} (or Ref. [112]) with permission of The Royal Society of Chemistry.*

Research into other types of hydrophobic systems did not stop there. A hole transporter called poly[N-9-heptadecanyl-2,7-carbazole-alt-3,6-bis-(thiophen-5-yl)-2,5-diethyl-2,5-dihydropyrrolo[3,4-]pyrrole-1,4-dione] (PCBTDP) was synthesised and used in a  $\text{CH}_3\text{NH}_3\text{PbBr}_3$  PSC system which has a band gap of -2 eV where the absorbance of light is only at 540 nm or less. Considering this, the efficiency peak was found with a 0.5 M precursor solution compared to the P3HT at the same concentration achieving 0.76% efficiency. To purchase this material, a quote-form is provided online, which suggests it is expensive.

The valence band of PCBTDP is -5.4 eV, which makes it more appropriate for this system; additionally, it has approximately 70X higher hole-mobility in contrast to P3HT [113].

Stability measurements (dark, air, RT, 900 h) showed great promise with PCBTDP compared to Spiro-MeOTAD HTM based cells in the same test; Spiro-MeOTAD cell's efficiency started at 6.4%, decreased to 5.01% in 30 h but afterwards reduced to 3.34% at the end of 71 h. Comparing this to PCBTDP we see in the first 100 h a quick rise from 3.04-5.3% followed by gentle efficiency increase to 5.5% at 900 h. All parameters tend to rise gradually except for the current which shows initial elevation but a gradual return to the original value [113]; performance was also better than P3HT based cells.

In other alternative HTM stability tests, two star shaped amine centre based HTMs tris{bis(4-methoxyphenylethenyl)-*N*-phenyl}amine (TPA-MeOPh) and tris{bis(4-methoxyphenylethenyl)-*N*-phenyl}amine quinolizino (FA-MeOPh), were produced to be less expensive and have comparable performance to Spiro-MeOTAD. These HTMs would require synthesis in the laboratory

The stability performance of the unencapsulated cells in comparison to Spiro-MeOTAD was greater, enduring >240 h under 1 sun under ambient conditions in air at RT. The majority of the parameters of the cells hardly changed except the short circuit current as a result of the humidity, thus causing the efficiency to decline [114].

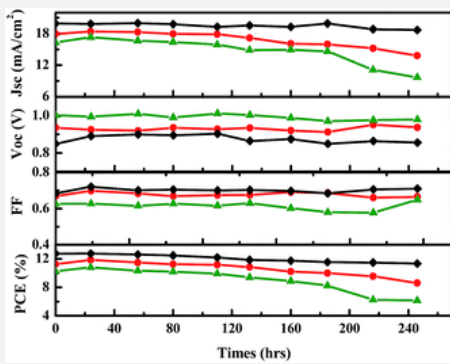


Figure 26: Stability test for devices in ambient air at RT at 1 sun) red = FA-MeOPh, green= TPA-MePh, black= Spiro-MeOTAD) Reproduced ("Adapted" or "in part") from {J. Mater. Chem. A, 2014,2, 19136-19140} (or Ref. [114]) with permission of The Royal Society of Chemistry. .

Further alternative developments by those in the scientific community, synthesised a triphenylamine derivative of *N,N'*-di(3-methylphenyl)-*N,N'*-diphenyl-4,4'-diaminobiphenyl (TPD HTM 1,4,5,8,9,11); to be used with buffer layer hexaazatriphenylenehexacarbonitrile (HAT-CN); a search online for the HTM's CAS number found that this was much cheaper at almost 65 € g<sup>-1</sup>, but the buffer layer was very expensive at 345 € g<sup>-1</sup> depending on the purity required; if low purity is not an issue, then 1 g costs almost 100 €.

The addition of HAT to TPD is promising in that it shows much higher IPCE (10%-20% in all wavelengths, shunt resistance (over 4X), almost half the series resistance and almost 10X the conductivity.

Also, it was found to be quite stable in ambient air/< 20% humidity/RT/unencapsulated/dark/1000 h with the effect of FF and  $J_{sc}$  slightly decreasing, causing efficiency to change from an initial approximate value of 7.1% to just over 6%. This was suggested to be because there were no lithium salts to absorb the moisture [115].

More innovative works at the time employed two triphenylamine-based HTMs containing butadiene derivatives which they labelled as HTM<sub>1</sub> (11.34% efficiency) and HTM<sub>2</sub> (11.63% efficiency) which performed comparably to cells with Spiro-MeOTAD (12.08% efficiency). The results of the stability assessment under the conditions of ambient air/ 7 days/dark, showed HTM<sub>1</sub> retained its efficiency to 0.2% of the initial measurement and 0.9% reduction for HTM<sub>2</sub> [116]. The ease of synthesis, good hole mobility, low cost and good performance are factors that make them promising candidates [116].

Other works on HTMs include using poly(tetraphenylbenzidine) (PTPD) containing (hydrophobic side chains/hydrophilic side chains) PTPD(4/2) which were assessed with a dopant of 10 wt% Co(III)-complex, LiTFSI and tBP as additives; conditions: five months, nitrogen atmosphere, oxygen rest content 30 ppm. They are not available for purchase and would need to be synthesised.

External quantum efficiency measurements and UV-Vis absorption were improved with doping and also showed that over 5 months, there was up to a 50% increase in the cell's photovoltaic parameters due to the perovskite changing over time.

This is possibly due to defects, but to confirm this requires further investigation. The increase also is attributed to absorbance reduction of the HTM allowing the perovskite to

absorb the HTM's unabsorbed light. This is possibly resulting from oxidation, attributed to the hydrophilic chains in the molecule. Doping PTPD showed better performance in efficiency [117].

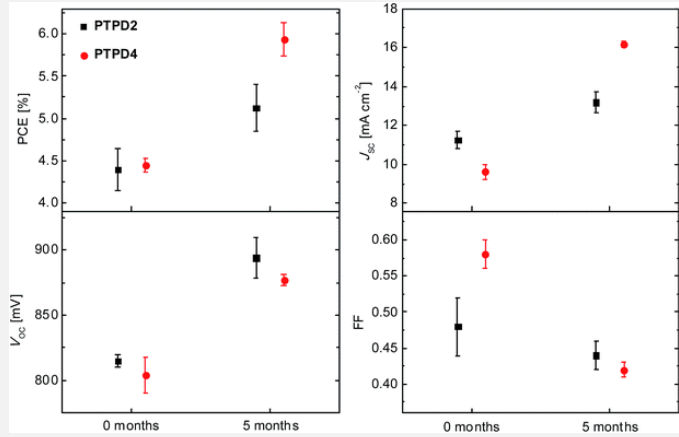


*Figure 27: Dependence of the mean power conversion efficiency, short circuit current density, open circuit voltage, and fill factor values of storage for PTPD2 (black squares) and PTPD4 (red circles). Both doped and containing the additives LiTFSI and TBP and measured in air (reproduced with permission from Ref. [117]). (K.Neumann and M. Thelakkat, (10.1039/C4RA05564K, RSC Adv., 2014, 4, 43550-43559) CC 3.0*

Table 2: Photovoltaic parameters using PTPD2 undoped, doped and doped containing LiTFSI and TBP as additives. The devices were measured directly after preparation and under ambient conditions. The parameters for the best devices and the average values for seven cells are given [117]. (K.Neumann and M. Thelakkat, (10.1039/C4RA05564K, RSC Adv., 2014,4, 43550-43559) CC 3.0

	$J_{sc}$ [ $\text{mA cm}^{-2}$ ]	$V_{oc}$ [mV]	FF	PCE [%]	$R_s$ [ $\Omega \text{cm}^2$ ]	$R_{SH}$ [ $\Omega \text{cm}^2$ ]
(A) Undoped (best)	9.25	685	0.57	3.59	15	408
Average value	8.05	715	0.59	3.37	14	891
RMS deviation	$\pm 0.8$	$\pm 50$	$\pm 0.04$	$\pm 0.39$	$\pm 2$	$\pm 580$
(B) Doped (best)	9.58	795	0.63	4.78	12	608
Average value	9.72	775	0.57	4.22	13	340
RMS deviation	$\pm 1.4$	$\pm 52$	$\pm 0.05$	$\pm 0.58$	$\pm 2$	$\pm 120$
(C) Doped + LiTFSI, tBP (best)	10.54	805	0.60	5.10	12	272
Average value	11.24	815	0.48	4.39	15	149
RMS deviation	$\pm 0.9$	$\pm 10$	$\pm 0.08$	$\pm 0.50$	$\pm 3$	$\pm 66$

(See sub-sections 5.5.1 and 6.2.2 of the current review on further information for Ref. [117]).

In order to address Spiro-MeOTAD degradation as a result of the lithium migration and moisture stability problems, a hydrophobic HTM was used; 9-(2-ethylhexyl)-*N,N,N,N*-tetrakis(4-methoxyphenyl)-9*H*-carbazole-2,7-diamine (EH44), which was additionally doped with the HTM EH44, and mixed with silver bis(trifluoromethanesulfonyl)imide (AgTFSI) to make (EH44-ox) [118]. The optimal EH44 thickness for the cell architecture: FTO/TiO<sub>2</sub>/(CH<sub>3</sub>IN<sub>2</sub>)<sub>x</sub>(CH<sub>3</sub>NH<sub>3</sub>)<sub>y</sub>Cs<sub>1-x-y</sub>Pb(I<sub>z</sub>, Br<sub>1-z</sub>)<sub>3</sub>/EH44/Au, was 60 nm, with tBP and EH44-ox. The stability test on the devices was static resistive load at approximately 510 Ω, 30°C, 160 h, 1 sun, voltage scan 60 mV/s every 30 min from forward to reverse bias, 12-22% humidity, ambient atmosphere.

The initial performance of the Spiro-MeOTAD cells was  $17.32 \pm 0.26\%$  efficient while the EH44 cells were  $16.35 \pm 0.23\%$  efficient. There was an initial degradation seen with both dropping to 80% of initial efficiency after 20 h, after which Spiro-MeOTAD based cells degraded faster than the EH44 cells. The degradation curves were fitted with a bi-exponential equation providing degradation time constants of 171 h for Spiro-MeOTAD and for EH44, 749 h.

This study was generally altering different parts of the cells so that stability would be improved at each step (see sections 7.4.2, 8.4 and 0 of the current paper for further information).

#### 4.1.3 An inexpensive spiro-MeOTAD alternative

A very cheap alternative to Spiro-MeOTAD such as copper iodide (CuI) has been proposed with experimental results indicating promising stability; after 1 h of light soaking in ambient conditions unsealed cells showed a decay in  $V_{oc}$  by 20% but had constant current, while Spiro-MeOTAD based cells had a  $J_{sc}$  reduction by 20%. A table

summarising the  $J_{sc}$  and  $V_{oc}$  changes is illustrated below [119]. The cost from the supplier is about  $70.50 \text{ € g}^{-1}$ .

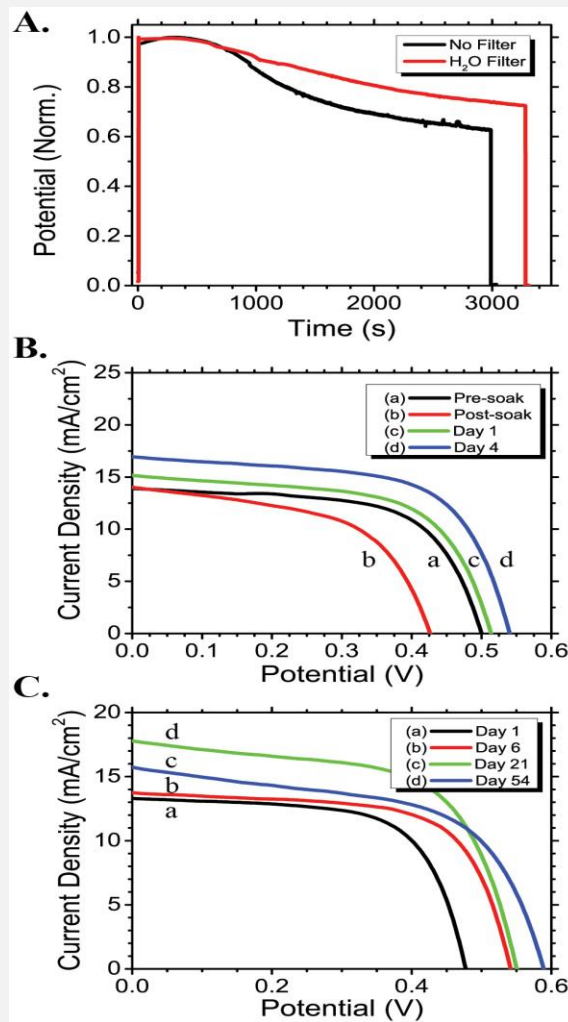


Figure 28: Reprinted (adapted) with permission from (J. Am. Chem. Soc., 2014, 136 (2), pp 758–764). Copyright (2014) American Chemical Society. (A) Normalized open-circuit voltage of CuI solar cell upon continuous  $100 \text{ mW/cm}^2$  illumination with and without a water filter. (B) J-V curve (a) before illumination, (b) immediately following 1 h continuous illumination at  $V_{oc}$ , and after (c) 1 and (d) 4 days storage in the dark. (C) J-V curve evolution upon storage in ambient conditions with no encapsulation over a period of 54 days (left) (reproduced with permission from Ref. [119]).

Table 3: Reprinted (adapted) with permission from (J. Am. Chem. Soc., 2014, 136 (2), pp 758–764). Copyright (2014) American Chemical Society. Storage of unsealed CuI HTM based perovskite solar cells stored under ambient conditions [119]

No. Days in ambient storage	Approximate $V_{oc}$ (mV)	Approximate $J_{sc}$ ( $\text{mA cm}^{-2}$ )
1	$\approx 475$	$\approx 13.1$
6	$\approx 540$	$\approx 13.9$
21	$\approx 550$	$\approx 15.9$
54	$\approx 580$	$\approx 17.8$

#### 4.1.4 Inverted structure and HTM comparison

An inverted structure for solar cells starts off with the electrode material, followed by the hole transporter, photosensitizer, blocking layer and then the anode, hence the name inverted, as it is built in the opposite order.

Inverted solar cell architectures are used in organic solar cell technologies and, usually due to the materials involved, need low temperature fabrication techniques. Hence, one of the main advantages is the low fabrication temperatures, and also the low hysteresis observed when applied to perovskites solar cells [120].

Inverted structures using nickel oxide ( $\text{NiO}_x$ ) as a HTM with a little copper doping at 5% result in a high performance of up to 15.4% efficiency [121]. This is due to greater photon to electron conversion, better conductivity and perovskite crystallization. Without doping, the performance was lower in comparison to the cell using PEDOT:PSS. The stability of the cell with  $\text{CH}_3\text{NH}_3\text{PbI}_3/\text{HTM Cu:NiO}_x$  compared to  $\text{CH}_3\text{NH}_3\text{PbI}_3/\text{HTM PEDOT:PSS}$  is significant as seen in Figure 29.

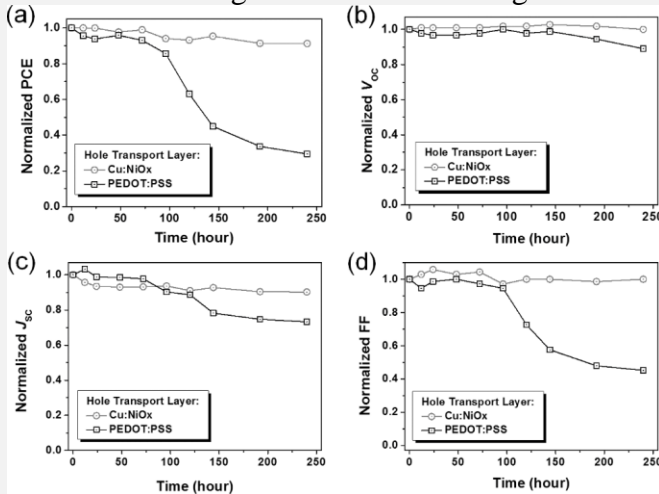


Figure 29: Normalized power conversion efficiency a) open-circuit voltage b), short-circuit current density c), and fill factor d) of perovskite solar cells based on PEDOT:PSS(squares) and Cu:NiO<sub>x</sub> (circles) holes-transporting layers as function of storage time in air (reproduced with permission from Ref. [121]). (Need guidance on how to reference/cite properly)

The cells were stored in air for 240 h and it is believed that the acidic properties of PEDOT:PSS degrade the ITO and perovskite layers, the structure of the device being: ITO/HTM/  $\text{CH}_3\text{NH}_3\text{PbI}_3/\text{ETL/Ag}$  (see Figure 29) To test the performance difference they also compared the cells with a bromine mixed perovskite  $\text{CH}_3\text{NH}_3\text{Pb}(\text{I}_{0.6}\text{Br}_{0.4})_3$ , finding that the inorganic HTM was better than the PEDOT:PSS mixture (see Table 4).

Table 4: Summarized solar cell parameters based on different HTMs reproduced (adapted) with permission from Ref. [121] (Need guidance on how to reference/cite properly)

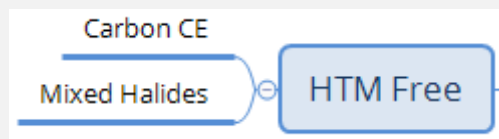
HTM layer	V <sub>oc</sub> (V)	FF (%)	J <sub>sc</sub> (mA cm <sup>-2</sup> )	PCE (%)
PEDOT:PSS	$0.9 \pm 0.01$	$73 \pm 1$	$16.64 \pm 0.55$	$10.87 \pm 0.29$ (11.16)
NiO <sub>x</sub>	$1.08 \pm 0.01$	$58 \pm 1$	$14.13 \pm 0.29$	$8.73 \pm 0.13$ (8.94)
5 at % Cu:NiO	$1.11 \pm 0.01$	$72 \pm 1$	$18.75 \pm 0.42$	$14.98 \pm 0.33$ (15.4)
Average values with standard deviation (maximum values in parenthesis)				

From the supplier, the  $\text{NiO}_x$  cost depending on the purity is 90 € for 100 g or as high as 66.50 € for 5 g and the cost of PEDOT:PSS for 5 g is 46.60 €.

## 4.2 HTM-free solar cells: is the HTM necessary?

Does a solar cell structure require a HTM layer? Despite their higher performance, the simple answer is no, and many other papers have suggested this; at least three are described in the sub-sections below. (See sub-section 4.2 on the benefits of not having an HTM layer).

Due to PSC stability being related to the degradation of the HTM, investigations without HTMs have been demonstrated.



Scheme 4-6

### 4.2.1 HTM free standard PSC

One such investigation using titanium diisopropoxidebis(acetylacetone) (TiDIP) in ethanol as a blocking material on top of the  $\text{TiO}_2$  electron acceptor layer, with an optimum thickness of  $620 \pm 25$  nm,  $\text{CH}_3\text{NH}_3\text{PbI}_3$  perovskite fabricated via the two-step deposition method (optimum waiting time for second step 3 mins) and utilizing a gold electrode attained 10.85% efficiency,  $\text{FF} = 68\%$ ,  $V_{oc} = 0.84$  V, and a  $J_{sc}$  of  $19 \text{ mA cm}^{-2}$ .

They found that the larger the depletion region of the electron acceptor (thickness of area where there are no free charge carriers available) improves charge transport. Comparing XRD diffraction data from a fresh cell and after a month in the dark, there was very little change in the crystallographic structure of the perovskite, indicating how effectively stable they are without a HTM [122].

### 4.2.2 Carbon counter electrode

Similarly to what was discussed earlier, a stability investigation was carried out without a hole transporter and fabricated in ambient conditions (no vacuum chamber/nitrogen/dry air) with the structure of glass/FTO/compact  $\text{TiO}_2$  (630 nm)/mp- $\text{TiO}_2/\text{CH}_3\text{NH}_3\text{PbI}_3/\text{carbon}$  was assessed for 800 h/encapsulated/ambient conditions. The stability was extremely good, initially from  $\text{PCE} = 7.31\%$  finishing at 7.42%, and averaging at 7.57%,  $J_{sc} = 16.65 \text{ mA cm}^{-2}$ ,  $V_{oc} = 0.89$  V and  $\text{FF} = 53\%$  [123]. (For more information in the current paper with carbon electrodes, see paragraph three of 3.2.2 for Ref. [95] as well as section 5.5.3.1 regarding Ref. [94].)

### 4.2.3 Mixed halide perovskite

A study of a PSC with different mixed halide ratios of bromine and iodine ( $\text{CH}_3\text{NH}_3\text{Br}:2\text{CH}_3\text{NH}_3\text{I}$ ), with  $\text{PbI}_2$  without the use of a HTM was performed; the stability over a period of 80 days in ambient conditions was assessed. The perovskite with the most stable halide ratio was  $\text{CH}_3\text{NH}_3\text{PbBr}_2\text{I}$ , retaining over 90% of its stability [76] (see section 2.2.1 for further information).

### 4.3 Summary of section 4

Initially, liquid electrolyte redox couples in DSCs were replaced by solid-state HTMs which proved successful, one HTM being Spiro-MeOTAD which is still very common and easily available although it is inherently unstable and expensive.

Different dopants have been investigated for their effect on performance and stability, and other fabrication conditions to produce better results.

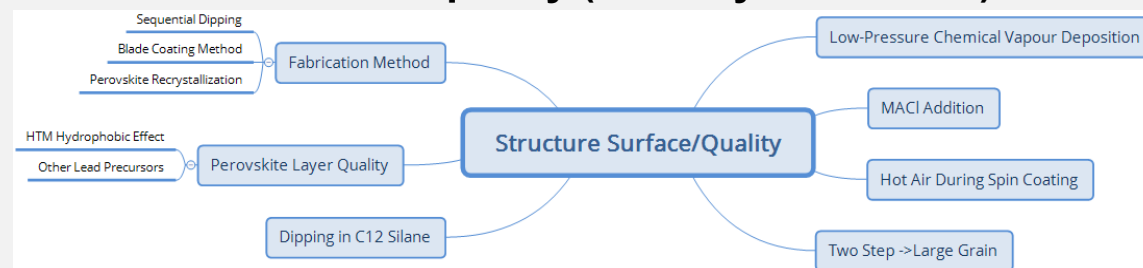
Alternative HTMs have been produced which have higher stability with less efficiency and although cheaper they are not mainstream on the commercial market or necessarily available and may require synthesis.

Hydrophobic HTMs have been developed which inherently resist moisture and produce significant results but these are still very costly solutions.

Inverse solar cell structures also use different HTMs and show promise for future commercial use provided the materials used are low cost.

A means to reduce the cost of solar cell production is to try to make cells without the HTM. However, the performance is not as optimal as those with a HTM, but have produced relatively stable results. Considering this, there is potential for further investigation, especially on the cells with carbon electrodes.

## 5 Surface structure/quality (stability as a result)



Scheme 5

Other aspects affecting stability in PSCs are film quality. The better the surface interface between each of the layers, the higher the performance and also the stability.

Often surfaces with small holes such as the perovskite layer or blocking layer can lead to shunt currents which reduce the performance of the solar cell and thus lead to early destruction of the solar cell. Various methods are listed below which are non-exhaustive to say the least but offer some perspectives on how some groups have dealt with this issue.

### 5.1 $\text{CH}_3\text{NH}_3\text{Cl}$ addition

The addition and careful removal of  $\text{CH}_3\text{NH}_3\text{Cl}$ , results in very good film quality, hence stability. Use of a vacuum to do this with the perovskite layer ( $60^\circ\text{C}$ , vacuum annealing) has been implemented to create a more stable  $\text{CH}_3\text{NH}_3\text{PbI}_3$  cell (ITO/PEDOT:PSS/ $\text{CH}_3\text{NH}_3\text{PbI}_3$ /PCBM/poly9,9-bis(*N,N,N*-trimethylammonium)hexylfluorene-alt-co-phenylenebromide (PFN-Br)/Al). Residues of  $\text{CH}_3\text{NH}_3\text{Cl}$  showed  $J_{\text{sc}}$  degradation (unencapsulated, ambient, 45 to 50% humidity,  $25^\circ\text{C}$ ,

1 sun 1.5 AM) in 2 h, whereas the vacuum  $\text{CH}_3\text{NH}_3\text{Cl}$  removed cells lasted over 10 days and the films remained black [124].

## 5.2 Two-step → large grain

Stored PSCs with large grains produced from the two-step deposition procedure on  $\text{TiO}_2$  showed generally good stability. Their storage conditions were: dark/ambient air/over a month/less than 30% humidity; the efficiency started at 14%, with  $V_{oc}$  remaining stable, an initial increase of FF which affected the efficiency positively but returned to 13% followed by a gradual decline to 12%. At about 25 days the efficiency declined even further to 11.5% [125].

In sections 4.1, 4.2, and 4.2.3 the two-step deposition technique was also carried out in the mixed halide paper referred to therein which also showed stability improvements [76].

## 5.3 Hot air during spin coating

The effect of blowing hot air during the perovskite spin coating deposition was assessed for efficiency and stability. Fabrication of solar cells occurred under ambient conditions with humidities of 30-90%.

Hot air during spin coating of the perovskite layer causes only the mesoporous structure to have a thin layer of perovskite over the  $\text{TiO}_2$  without a capping layer. When the cell structure was FTO/ $\text{TiO}_2/\text{CH}_3\text{NH}_3\text{PbI}_3/\text{Au}$  hot air drying led to poorer performance.

The addition of CuSCN as a hole transporter indicated that performance is higher with hot air drying. In comparison to stability tests (illuminated/ambient/unencapsulated/16 h) the opposite effect was seen.

The effects on the stability of the cell under light exposure involve reduced hole transport resistance, low recombination resistance of the thin perovskite layer, and  $\text{CH}_3\text{NH}_3^+$  cations escaping the perovskite structure; considering the fabrication conditions, humidity was not as important as initially thought. Understanding of the interface between the perovskite and HTM layer was suggested as a further set of investigations that they had to undertake [126].

## 5.4 Dipping in $\text{C}_{12}$ -silane

Dipping unsealed PSCs in a 0.1 M isopropanol solution of  $\text{C}_{12}$ -silane on the perovskite layer before the HTM is applied to the perovskite layer has been shown to increase recombination resistance and hydrophobicity of the perovskite surface while at the same time increasing current and voltage. Stability measurements under conditions of >600 h and 45% relative humidity showed results to within 85% of its original efficiency compared to the untreated cell being at 65% of its original efficiency [127].

## 5.5 Perovskite layer quality

If the layer of the perovskite interface is of good quality, then higher efficiency and stability can be achieved. Below, different methods have been utilized in producing good interfaces between these layers. Some methods involve exploiting the properties of HTMs, investigating the perovskite precursors (chemicals used in the reaction to make the perovskite) and applying different fabrication methods.

### **5.5.1 HTM hydrophilicity effects**

Hydrophobicity and hydrophilicity can help in different ways in the PSC layers. The hydrophilic chains on HTM PTPD4 showed greater wettability for  $\text{TiO}_2$  infiltrated with perovskite, thus the performance and surface of the interface demonstrates better results (see sections **Error! Reference source not found.** and 6.2.2 for further information on HTM hydrophilicity).

### **5.5.2 Other lead precursors**

As mentioned in section 2.2.2, different elements affect perovskite performance [79]. This investigation highlighted the effect on the cell stability and performance of the lead precursor due to the resulting film morphology;  $\text{Pb}(\text{OAc})_2$  showed smaller crystals on the  $\text{TiO}_2$  surface compared to  $\text{PbCl}_2$ . The performance of  $\text{Pb}(\text{OAc})_2$  was lower as well as the stability. Despite this, it was suggested that the deposition method was not optimal (optimized parameters used to deposit  $\text{PbCl}_2$ ), therefore possible further optimization of this method for  $\text{Pb}(\text{OAc})_2$  could result in a higher performance of efficiency and stability.

### **5.5.3 Fabrication method**

#### **5.5.3.1 Sequential Dipping**

A group that studied sequential dipping for producing a good perovskite layer, encapsulated under argon, carried out long term testing (500 h/45°C/constant illumination at 100 mW cm<sup>-2</sup>/held at maximum power point). They started with an efficiency over 8%, and after the stress, it decreased to almost 7% [65]. In section 3.2.2, another group using this method is described. As previously mentioned, the cell structure FTO/ $\text{TiO}_2$ / $\text{ZrO}_2$ /carbon showed that over 35 days starting from 6.64% efficiency, an insignificant decrease was observed [94].

#### **5.5.3.2 Blading method**

Blading and spin coating of a perovskite in short term measurements showed a significant increase in stability (stored 5 days, air humidity not specified) [128]. XRD and visual results showed no change with blade coating as well as with spin coated substrates, both resulting in the formation of  $\text{PbI}_2$  most likely as a result of the degraded perovskite during the perovskite formation phase under ambient conditions. All parameters indicated blade coating was higher; comparison of the two (spin (best):  $V_{\text{oc}} = 0.36 \pm 0.01 \text{ V}$   $J_{\text{sc}} = 6.99 \pm 0.24$ , FF =  $0.49 \pm 0.02$  PCE =  $1.23 \pm 0.06\%$  (1.3%); blade (best):  $V_{\text{oc}} = 0.92 \pm 0.01 \text{ J}_{\text{sc}} = 15.4 \pm 0.47$  FF =  $0.66 \pm 0.01$  PCE =  $9.29 \pm 0.21$  (9.52)).

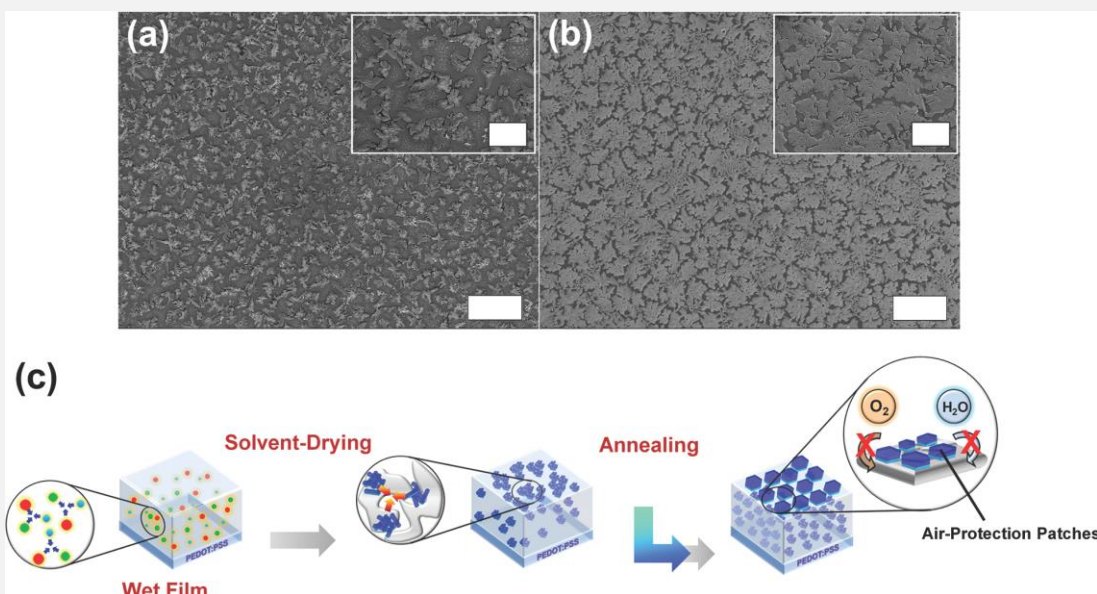


Figure 30: Scanning electron microscopy images of perovskite films prepared by a) spin-coating and b) blade-coating methods. Scale bar: 50 $\mu$ m; insets are magnified images for each film and scale bar is 20 $\mu$ m. c) Schematic diagram of structural evolution of large crystal domains during blade coating (reproduced with permission from Ref. [128]). Need guidance on how to acknowledge reference from Wiley

Stability from blade coating is suggested to be due to the formation of larger crystal sizes, hence air and moisture have a lower surface area to react with.

#### 5.5.3.3 Perovskite recrystallization

Another study on ‘recrystallization’ of the perovskite surface resulting from dissolving and annealing cycles, following single-step deposition of the perovskite solution, showed significant improvement in the surface morphology and reduced roughness [129]. Due to the better morphology/crystallinity, there was improved absorption, charge transfer and shunt resistance. The optimum repetition found was six cycles giving  $10.25 \pm 0.9\%$  efficiency compared to a 5.16% non-recrystallized substrate.

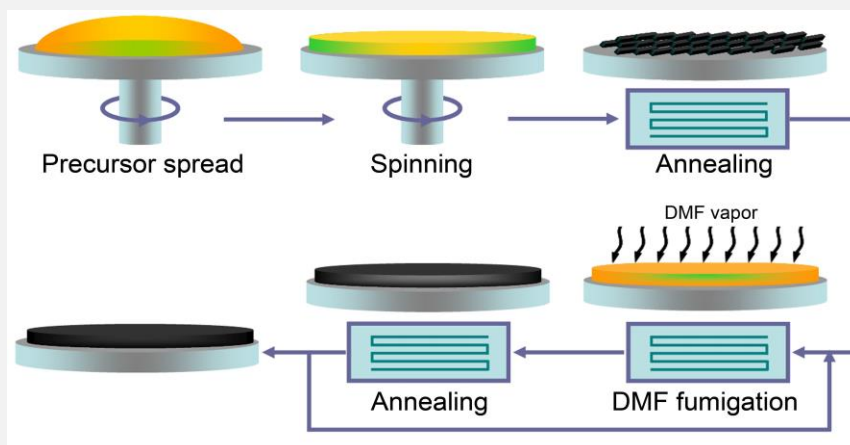


Figure 31: Schematic procedure for preparation of  $\text{CH}_3\text{NH}_3\text{PbI}_3$  film and preparation of  $\text{CH}_3\text{NH}_3\text{PbI}_3$  film and recrystallization via DMF vapour fumigation Reproduced (“Adapted” or “in part”) from {Nanoscale, 2015, 7, 5427-5434} (or Ref. [129]) with permission of The Royal Society of Chemistry.

#### 5.5.3.4 Low-pressure chemical vapour deposition

Another method has included fabrication with low-pressure chemical vapour deposition under open air conditions at 60% humidity [130]. This technique made the PSC more stable to Raman lasers. In general, the spectrum of  $\text{CH}_3\text{NH}_3\text{PbX}_3$  was found to be stable under a Raman laser at 70°C measurements even though it looked similar to that of  $\text{PbI}_2$ . Following heating up to 145°C after 5 min resulted in the crystal structure being in the initial stages of destabilization; at 180°C it was completely gone.

The other significant point is that this achieved a record efficiency of 12.73% reverse bias and 11.1% forward bias scan of a cell produced while at such a high humidity. Overall, efficiencies > 9%,  $V_{oc}$  890-960 mV,  $J_{sc}$  17.5-21.8 mA cm<sup>-2</sup> and FF of 50-66% were obtained; the optimal annealing time of 30 min resulted in 12.73% efficiency,  $V_{oc}$  of 910 mV,  $J_{sc}$  21.7 mA cm<sup>-2</sup> and FF of 64.5%.

The advantage of this method is in removing the residues of  $\text{CH}_3\text{NH}_3\text{Cl}$  formed from the precursors  $3\text{CH}_3\text{NH}_3\text{I}:\text{PbCl}_2$  via vacuum assisted annealing. It is also shown to improve films and increase stability in  $\text{CH}_3\text{NH}_3\text{PbI}_3$  while at the same time having a very low hysteresis. The structure of the unsealed cell:

ITO/PEDOT:PSS/ $\text{CH}_3\text{NH}_3\text{PbI}_3$ /PCBM/poly(9,9- bis[30 -(*N,N*-dimethyl)-*N*-ethylammonium-propyl-2,7-fluorene]-alt-2,7-(9,9dioctylfluorene)]-dibromide-electrolyte (PFN-Br)/Ag >10 h in ambient air (lighting not stated) (45 to 50% humidity, 25°C) attained an almost 15% efficiency without any sign of degradation.

### 5.6 Summary of section 5

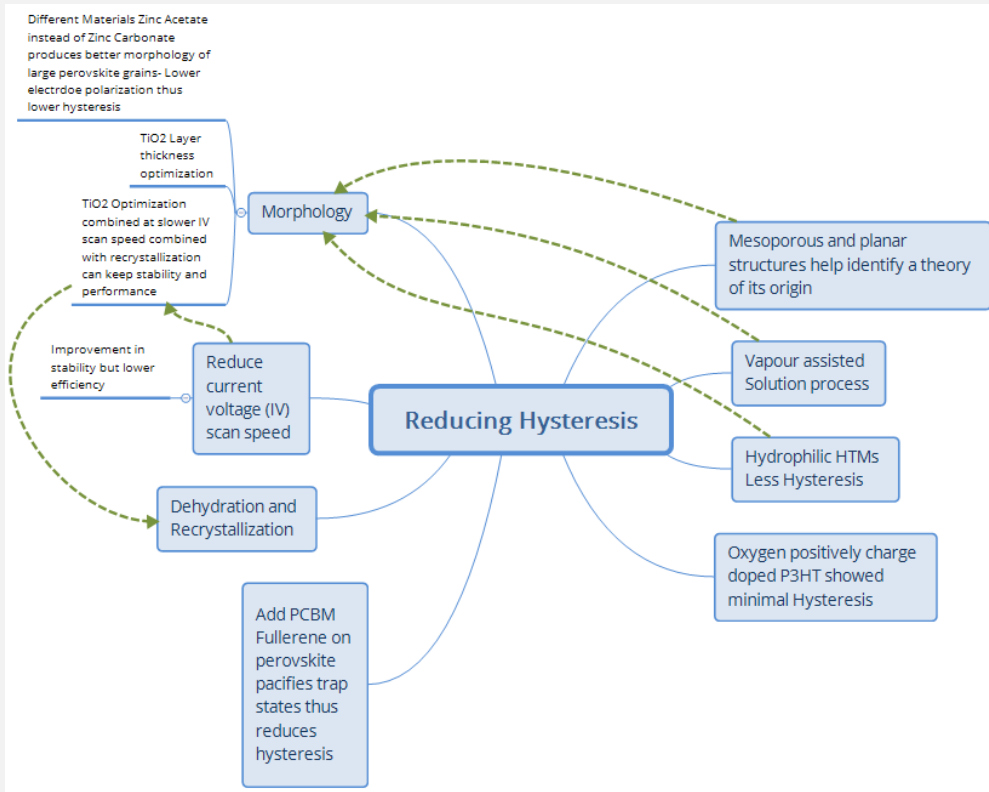
Film quality of the different layers produces improvements in both efficiency and stability. Addition and removal of  $\text{CH}_3\text{NH}_3\text{Cl}$ , two-step deposition/sequential deposition, blowing hot air, dipping the perovskite layer in  $\text{C}_{12}$  silane, blading and perovskite recrystallization as well as low-pressure chemical vapour deposition have all shown improvements compared to the control cells.

Possibly, a combination of some or all of the techniques would show even better stability and performance, for example, blade coating, dipping in  $\text{C}_{12}$  silane then blowing with hot air. Optimization of a combination of different methods is worth investigating. Since the time of writing, additional research has been carried out on different fabrication procedures; it would be worth studying those too.

## 6 Investigations to reduce hysteresis in IV scans of PSCs

In order to improve stability and obtain truer IV scans of solar cells, knowing why hysteresis occurs is important. When understood, the means to reduce this can be implemented. Many of the techniques used have an effect on the morphology of the layers, thus changing the way charge flows in the system, and hence reducing or increasing this phenomenon.

As a side note, what is negative for one technology is a benefit for another, e.g., hysteresis for memory based devices/switches is a useful property and has been incorporated for such use [98].



Scheme 6

## 6.1 Doping

The use of dopants has been described in Ref. [131]. The author recommends this as a means to understand dopants for improvement in stability.

### 6.1.1 Oxygen P doping

Perovskite solar modules demonstrated 1200 h of stability in the dark in a dry box during a test of their shelf life; the devices had very low hysteresis with an initial 3.45% efficiency, increasing to about 5.25% after 144 h due to oxygen p-doping (positive charge) of the P3HT HTM; following this, investigators sealed the modules with cyanoacrylate glue, which led to the efficiency decaying to 4.96%; at 300 h a reduction was shown in the  $J_{sc}$  from 9.8 to 8.9 mA cm<sup>-2</sup> due to possible de-doping and after a further 970 h a decrease from 4.4 to 4.3% efficiency.

Analysing its current-voltage/current-density voltage (IV/JV) scan with a delay time of 250 Ms and at 80 mV/s showed extremely minimal hysteresis. Further testing comparing Spiro-MeOTAD and P3HT (>350 h, 1 sun/dry box/40°C) resulted in efficiency reduction by 55% in the first 100 h with Spiro-MeOTAD, and 75% with P3HT. Spiro-MeOTAD continued at 55- 60% of the original normalized efficiency for a further 250 h [132] (see section 9.3.1 for further information on this reference).

## 6.2 Other methods of reducing hysteresis

### 6.2.1 Comparison of mesoporous and planar PSC Structures

Another study comparing planar and mesoporous structures using a modified vapour assisted solution process, to create a fully covered perovskite surface with microscale grain size, showed that the ferroelectric polarization of the dipoles in the perovskite is related to hysteresis [133].

Furthermore, investigators found that light soaking affects the planar structures whereas mesoporous structures showed little or no hysteresis regardless of light soaking.

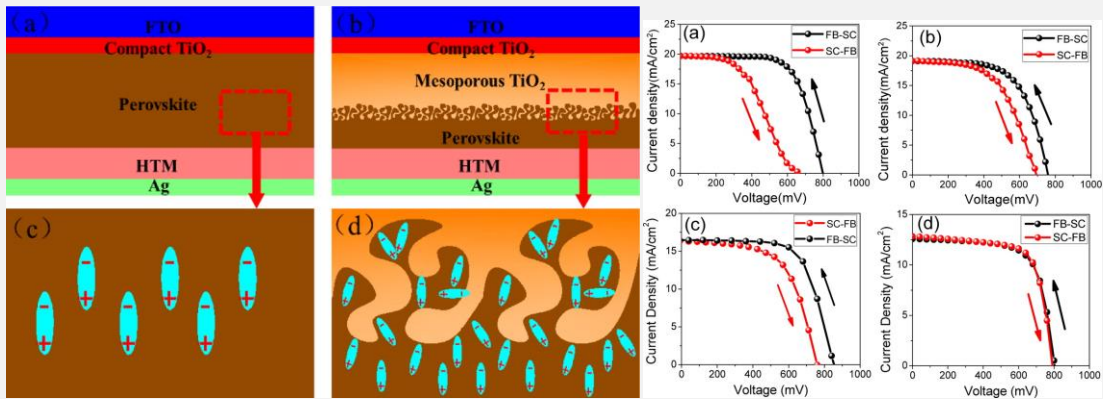


Figure 32: Reprinted (adapted) with permission from (ACS Appl. Mater. Interfaces, 2015, 7 (17), pp 9066–9071). Copyright (2015) American Chemical Society. Schematic Mechanism illustration of the polarization in (a) planar-structured solar cell and (b) mesoporous-structured solar cell under reverse biases; (c) and (d) are the magnified images of the corresponding regions in (a) and (b) respectively (Left), Influence of solar cell architecture upon current-voltage hysteresis. Forward bias to short circuit (FB-SC) and short circuit to forward bias (SC-FB) current-voltage curves measured under simulated AM 1.5 100mW cm<sup>-2</sup>sunlight for (a) solution-processed planar-structure-structured TiO<sub>2</sub>-based solar cell, (b) solution-processed mesoscopic TiO<sub>2</sub>-based solar cell, (c) vapour-assisted planar-structured TiO<sub>2</sub>-based solar cell, and (d) vapour-assisted mesoscopic TiO<sub>2</sub>-based solar cell (right). Images and captions (reproduced with permission from Ref. [133]).

### 6.2.2 HTMs with hydrophilic nature have less hysteresis

What is interesting is that hydrophobic HTMs have shown an increase in hysteresis in comparison to hydrophilic ones [117] (see near the end of section 4.1.2 on PTPD).

The PTPD4 (hydrophilic) HTM on the perovskite, after 5 min of illumination, resulted in almost zero difference in the JV scan in the forward and reverse directions, while the PTPD2 HTM (non-hydrophilic) demonstrated higher hysteresis  $\Delta J_{sc} > 5 \text{ mA cm}^{-2}$  and  $\Delta V_{oc} 40 \text{ mV}$  [117] (as suggested in section 5.5.1).

### 6.2.3 Slower IV scans are more stable

A distinct difference in the JV curves for reverse bias direction compared to forward bias has been measured to be coming from the interface between the perovskite and charge collection surfaces [134].

Researchers documented that JV scans indicating photovoltaic parameters should display both the forward and reverse scan, showing on the graph the scan rate in V/s. Hysteresis between the two directions can be avoided, but only if carried out at a very slow and impractical rate. With this information, groups should also present a graph showing the

stabilized power output at the maximum power point, supporting the ascertained efficiency and its stability.

#### 6.2.4 Morphology layer interface

The thickness of the  $\text{TiO}_2$  layer can be optimised to reduce hysteresis in the *IV* curve on the reverse and forward bias, and found that decreasing the voltage scan rate without the  $\text{TiO}_2$  lowers hysteresis but at the cost of efficiency [135]. One way to mitigate this was discovered surprisingly via recrystallization, as discussed in the current review in section 5.5.3.3, due to improved crystallinity/morphology and layer interface [129].

Hysteresis minimization can also be achieved via changing materials, such as using a caesium acetate dopant layer instead of caesium carbonate. Placing this coating on top of the  $\text{ZnO}$  blocking layer as part of a low temperature ITO inverse PSC structure has proved effective. This produced a smoother, more hydrophobic surface and large grains in the perovskite film, which reduced electrode polarization and thus, hysteresis [136]. This relates to the effects seen in the previous section on how to change and improve the layer quality of the cell (see section 5).

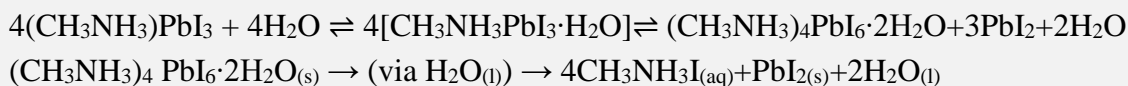
The higher performance was thought to be due to greater conductivity and better band gap energy matching of the layers. The acetate-based cell had smoother morphology and thus fewer shunt paths leading to lower current leakage and higher performance.

#### 6.2.5 Pacifying trap states using organic/inorganic layers

The use of a PCBM fullerene HTM on the top of the perovskite film has been shown to reduce hysteresis significantly as a result of pacifying trap states, due to surface decomposition in the  $\text{CH}_3\text{NH}_3\text{PbI}_3$  perovskite layer that was annealed at 100°C for 2 h. Increased annealing time of the PCBM layer at 100°C from 15-45 min further minimized this phenomenon [137].

#### 6.2.6 Dehydration and recrystallization effects on hysteresis

Contact with moisture results in the formation of perovskite hydrated crystals and after drying (with  $\text{N}_2$  or dry air at 30% relative humidity) they return close to their previous photovoltaic properties and to their original dehydrated structure. Hysteresis increases significantly after dehydration, indicating it is possibly linked with the recrystallization process although the authors of that work do suggest it is a means to obtain better film morphology provided optimum protocols are followed. The mechanisms by which this happens are illustrated below as well as the irreversible direction when excess humidity is applied [138].



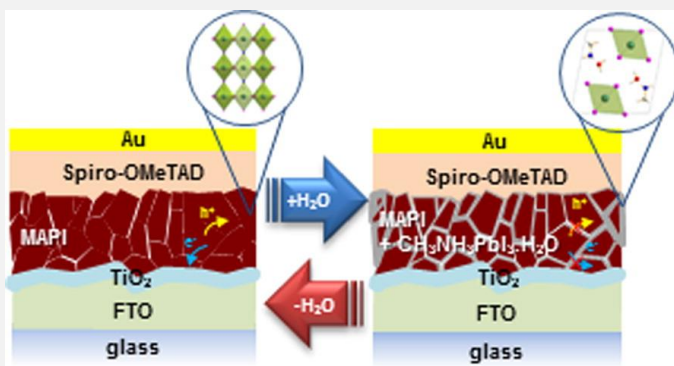


Figure 33: Presumed microscopic degradation model of  $\text{CH}_3\text{NH}_3\text{PbI}_3$  thin films under partial hydration Reproduced ("Adapted" or "in part") from { J. Mater. Chem. A, 2015, 3, 5360-5367 } or Ref. [74] with permission of The Royal Society of Chemistry

### 6.3 Summary of section 6

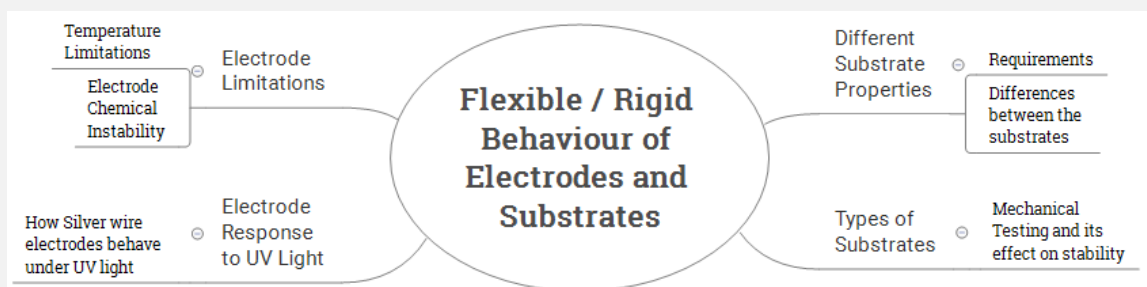
Hysteresis will affect the efficiency value of the PSCs and the smaller this effect is, the better. Observations of doping through different means have shown this to be effective. The structure of solar cells demonstrates that if there is a mesoporous layer, the hysteresis of JV scans is reduced in comparison to that of planar devices.

Some HTMs with hydrophobic properties show more stable results in the IV forward and backward scan, while the morphology of the layers has also been found to improve the measurement.

Another solution would be to pacify possible trap states; also removing moisture and recrystallizing the perovskite crystal would help repair and create better morphology although hysteresis is increased.

## 7 Flexible/rigid behaviour of electrodes and substrates

The different properties that flexible substrates for BIPV or other applications would need to have are high transparency, conductivity (low electrical resistance), flexibility without losing performance, and a cost-effective facile method of fabrication. There are many types of substrates that could meet this need, e.g., ITO sputtered polymers, metal nanowire meshes, and carbon-based substrates constituted of nanotubes and graphene. Since the majority of the substrates are used as part of the electrode, these two subjects are contained in this section.



Scheme 7

This section could in itself be the subject of a thorough review paper of at least 30 pages length, listing the different properties for use in photovoltaics, i.e., advantages, disadvantages, and the properties required, depending on where the device is to be

implemented. This section will just cover the initial thoughts of the author and suggest a few references which describe some of these properties.

## 7.1 Different substrate properties

### 7.1.1 Substrate requirements

The main function of the substrate for solar cells is to support the device throughout its fabrication (unaffected by strong polar solvents used in each of the layers during deposition, temperature of annealing the different layers). A homogeneous conductive layer enabling the electrical circuit to operate and remain connected throughout its life is also important.

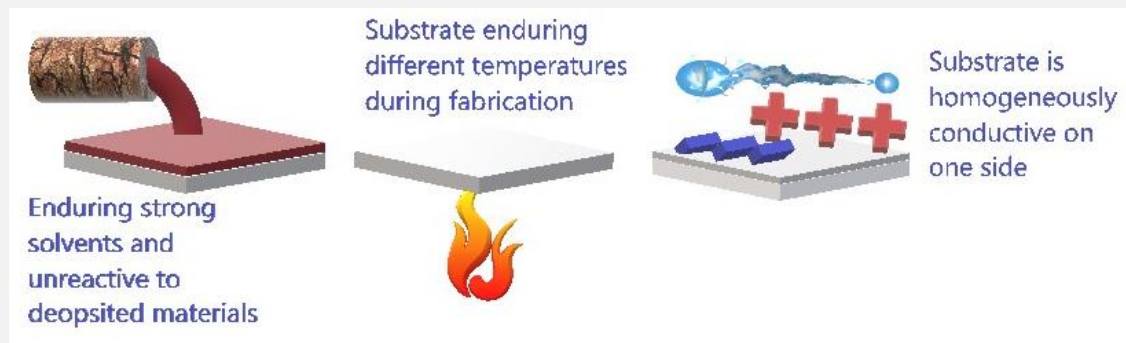


Figure 34: A few of the stability requirements for substrates to have during fabrication

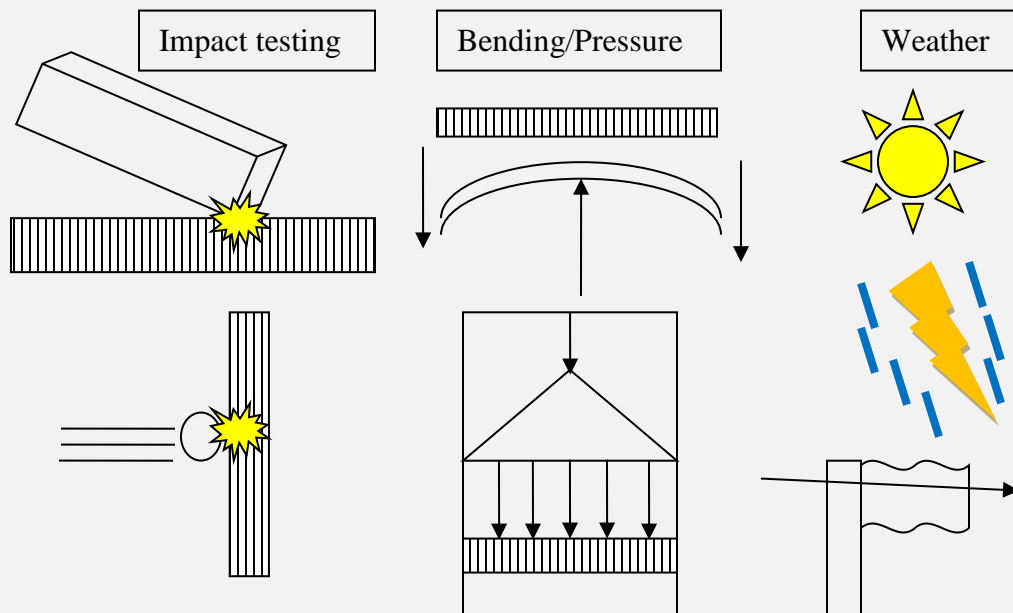


Figure 35: Some images for Substrate lifetime requirements

The substrate will need to endure stress throughout its working lifetime: transport to and from the point of manufacture, followed by delivery to the commercial vendor, and finally to its end destination. Throughout, it must be able to endure the impact of being dropped accidentally during transit, endure changes in air pressure, and impacts of unexpected objects such as stray balls, e.g., children playing in their gardens and accidentally hitting a ball onto the solar panel. The material will need to withstand

meteorological factors such as strong winds, mechanical resonance, harsh heat, humidity, cold temperatures and hailstones during storms. Thus, once it has passed thorough testing, the likelihood of the system failing from severe weather or any of the above is lowered.

Regarding the requirements for when the product is no longer functional due to age or not being able to be repaired, it is vital that it can be safely recycled or disposed of. If the substrate is to be part of transparent materials, then it needs to have adequate transparency and transmissivity to visible light of the solar spectrum, possibly filtering out UV light (depending on whether it cannot be harnessed instead).

A variety of tests that the substrates and photovoltaic systems need to undergo for harsh conditions are described in different assessments which cover many health and safety and operational procedures [139–142].

### 7.1.2 Substrate differences

Rigid substrates are often made from materials such as glass and silicon. Flexible substrates are usually made from polyethylene terephthalate (PET) or poly(ethylene 2,6-naphthalate (PEN), or in rare cases, metal depending on the thickness.

More often than not, hard substrates which are made from glass, are able to endure higher heat loads if coated with FTO, which can endure temperatures beyond 550°C, in contrast to ITO, which with annealing at or above 300°C damages or destroys the conductive layer.

The method by which the conductive material is deposited onto the substrate is often via sputtering. The substance to form this can be dispersed/dissolved in a liquid. Thus, by dipping the substrate into this solution, removing it and evaporating the solvent (dip coating), the substrate can become an electrode with low resistivity. This is one of the methods employed in nanowire electrode fabrication [143]. The substrate needs to adapt to the stress endured, and a homogeneous layer must form in order to make a good conductor.

Flexible substrates have temperature limits, usually from the material being a polymer, which degrades at temperatures in excess of 250°C.

## 7.2 Types of substrate

Much of the literature already deals with rigid substrates using transparent glass coated with a conductive metal oxide. FTO is usually sputtered on the glass surface, which comes in different dimensions, with the property of resistivity. The size, material and conductivity of the surface affect the price: Length × Width × Thickness 50 mm × 50 mm × 3 mm, surface resistivity  $\sim 10 \Omega m^{-2}$  five pack 59.60 € – Length × Width × Thickness 100 mm × 100 mm × 2.2 mm, surface resistivity  $\sim 13 \Omega m^{-2}$ , five pack 87.90 €. ITO similarly: 75 mm × 25 mm × 1.1 mm – 15-25  $\Omega/m^2$  25 pack 853 €, and if the resistance range is 8 – 12  $\Omega m^{-2}$  1320 €. The move to go from rigid ITO/FTO based substrates to plastic flexible materials has been an ongoing area of research. Nanowire meshes are a competing technology to metal oxide electrodes. They have the potential to meet many needs, i.e., they are inexpensive, flexible (if needed), transparent, easy to manufacture, and the method of manufacturing is less damaging to the substrate than sputtering metal oxide conductors on substrates [144].

Flexible plastic substrates with multilayer graphene, or one to four layer graphene, and carbon nanotubes have also demonstrated promise as cathode and anodes in organic solar cells which can be also applied to perovskites [145]. Like the metal wire meshes, they have transparent properties for BIPV. A summary from a chart in Ref. [146] shows the progress they have made in transparency and conductivity; it is a very good read where they also write about the methods of fabrication in their bibliography.

### 7.2.1 Mechanical testing and effect on efficiency

A review paper (see section 3 of Ref. [147]) lists the cell parameter results before and after a great deal of different mechanical tests, with various PSC architectures, layer materials, and methods of fabrication. Also listed are bending radii and deformation cycles; it provides a good summary for one to assess the various attempts at overcoming this issue.

They also review distorting flexible PSCs and fibres. One of the two they mention are investigations of cycles of crumpling a flexible substrate. There is stretching out uniaxially/radially the elastic substrate to be flat on which the cell is deposited, and then allowing it to relax, thus forming creases due to compressive strain.

In one test of the aforementioned review [147], the substrate was allowed to relax, decreasing to 44% of its initial area after it was stretched radially, which led to minimization of the area of the substrate caused by the compressive strain. The open circuit voltage and fill factor were hardly affected, while the  $I_{sc}$  decreased to around 65% the original value.

Similar results from uniaxial compressive strain at 50% were observed with an even lower drop of 30% for the short circuit current.

Looking at figure S19 in the supporting information from Ref. [148] and mentioned in Ref. [147], applying 25% linear compressive strain after 25 cycles demonstrated unchanged performance; after 100 cycles a 30% reduction was observed, which was due to lowered fill factor and open circuit voltage as a result of either loss of contact or cell defects due to the mechanical distortion, which led to short-circuited diodes.

Among one of the wire-based PSCs (PEN-ITO/TiO<sub>2</sub>/CH<sub>3</sub>NH<sub>3</sub>PbI<sub>3</sub>/carbon nanotubes), the device is fabricated on a wire substrate, thus becoming a concentric solar cell surrounding the wire. As a form of stress, it is tied in a knot, having a screw pitch of 3 mm and radius of curvature of 7.5 nm, the knotting being repeated for 500 cycles; an initial efficiency of 9.49% gave good stability reducing only by 10%. As well as this, they also highlight the piezo-phototronic effect for flexible PSCs, improving the efficiency 12.8-fold (0.0216 to 0.298%) under compressive strain during the flexing, using piezoelectric ZnO microwires (see section 3 in the aforementioned review for further information). Another review on the use of graphene compares results of ITO and graphene-based PSCs (see section 4 of Ref. [147]).

One of their references mentions that after 1000 cycles of bending radius 6, 4 and 2 mm, ITO cells lost between 70-90% of their original efficiency as a result of increased sheet resistance. ITO was unable to cope with the 2 mm bending assessment and show no results for that; graphene cells, on the other hand, retained 90% of their efficiency for all the tests.

Among the other materials for electrodes are indium zinc oxide (IZO) on PET, PEDOT:PSS substrates, and silver nanowires (NW), which have also been investigated in comparison to ITO. A brief summary of their mechanical endurance is listed in Table 6.

Table 5: Mechanical stress tests for PSCs with flexible electrodes ( $\eta$  = efficiency (%),  $\eta_0$  = initial efficiency,  $\Delta$  = difference)

Electrode	Stress Test	Observation	Ref.
PEDOT:PSS/ $\text{CH}_3\text{NH}_3\text{PbI}_3$	Bent over 50 times	( $\Delta\eta = 7\% \dots 6.9\%$ ) ( $\Delta\text{FF}: 0.474 \dots 0.464$ )	[149]
IZO PET	500 bending cycles at 20 rpm curvature of radius at 15.8 mm	80% of its original value (around $10.6 \pm 1.2\%$ bending test only relative $\eta$ average value)	[15]
	8.7 mm curvature up to 300 cycles	$\eta$ just <, 200 cycles $\Delta\eta = -0.4\eta_0$ , 300 <sup>th</sup> device failure possibly due to damage to the IZO	[15]
ITO based flexible electrodes	1 Hz with ‘a bending length and radius of 15 mm and 5 mm, respectively’	473% change after 10 cycles	[150]
Ag NW/FZO nanowires on a flexible substrate coated with FZO	1 Hz with ‘a bending length & radius of 15 mm & 5 mm respectively’	1000 cycles, $\Delta\Omega = 0$ , $\eta = 3.29\%$ compared to FTO’s 2.95% electrodes	[150]

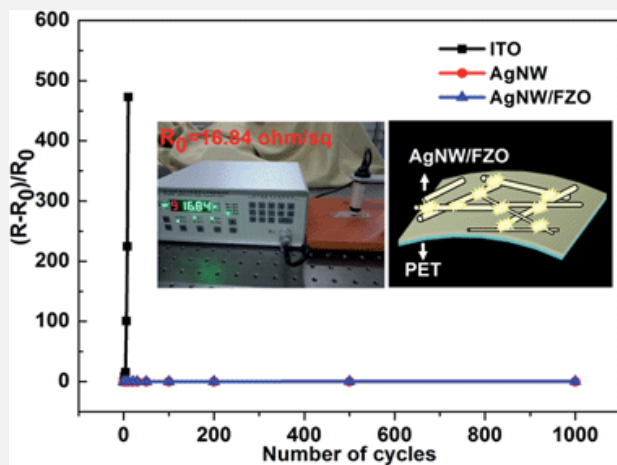


Figure 36:  $(R-R_0)/R_0$  vs. the number of cycles for the various electrodes on PET. The inset shows the  $R_0$  and schematic diagram of the bending Ag NW/FZO composite electrode (reproduced from Ref. [150] with permission from the Royal Society of Chemistry). Reproduced (“Adapted” or “in part”) from {J. Mater. Chem. A, 2015, 3, 5375-5384} (or Ref XX) with permission of The Royal Society of Chemistry.

## **7.3 Electrode response to UV light**

### **7.3.1 Silver nanowire electrodes**

Silver nanowires were assessed for deterioration under UV light and thermal effects. The wires had a protective coating of polyvinylpyrrolidone and were illuminated in an atmosphere of ozone (UV/O<sub>3</sub>) [151].

During the first 30 min the protective layer was degraded, releasing oxygen gas and leaving a nitrogen layer behind. This formed silver nitride on the nanowire surface, then the silver nitride decomposed explosively into silver and nitrogen, the energy producing this explosion arising the UV radiation.

Damaged caused by small explosions was observed, which reduced resistance. After nitrogen was depleted, oxides from polyvinylpyrrolidone formed with the silver creating silver oxide and gave way to smaller explosions caused by decomposition of the silver oxide to silver and oxygen. The breakage of the nanowires from these explosions caused the connections to break, thus increasing the resistance.

One means to prevent this was coating it with a graphene oxide layer, which helped to decrease the resistance by 50% despite lowering the transmission from 94 to 88%.

During UV/O<sub>3</sub> treatment for 10 min, a gradual degradation in resistance was observed; after this initial behaviour, it gradually increased for 40 min, followed by a rapid rise for a further 2 h; no breakage of the nanowires occurred during the assessment, until the 3 h point, because they could no longer take a resistance measurement.

## **7.4 Electrode limitations**

### **7.4.1 Temperature limitations**

The electrodes made with metal nanowires or other materials can be degraded due to their limitation resulting from thermal stress. Silver nanowires on a silicon substrate, starting from 85°C, showed a reduction in resistance, due to part of the mesh network melting, thus decreasing the contact resistance between them [151]. The lowest resistance was observed at 160°C, due to the contact points of the nanowires melting. The surface of the nanowires melted after further heating to above 205°C, which above 160°C, damaged what they call the percolation network and caused spheres to form, which resulted in a rise in resistance. Above this temperature, data could not be obtained, owing to the destruction of the network.

### **7.4.2 Electrode chemical instability**

The electrode is usually the layer that sits on top of the perovskite film or hole transporter. This needs to be inert to the coatings below, lest degradation occurs through the electrode reacting with the iodine in the perovskite. Finding a replacement which is more stable needs to be done carefully in order to avoid reducing efficiency from(2.5-6%, down to 2%, as shown by one study, yet using alternatives can also deliver comparable results [110,118].

Investigating electrode stability, using secondary ion mass spectrometry, showed atoms in the anode/cathode interact with the iodide in the perovskite due to particles migrating to the photosensitive layer [118]. The group stated that this is not only observed by them

and included other references; their solution was using a thin (15 nm) molybdenum oxide and (200 nm) aluminium electrode layer, resulting in an interaction, which acts as a barrier against electrode migration.

The FTO substrate's surface was inhomogeneous and contained a  $>1.5 \mu\text{m}$  step at the edge of the cell; subsequently, the aluminium migrated to the rest of the cell structure causing degradation to failure at 120 h in an ambient environment, thus they replaced it with an ITO layer with a step of less than  $0.4 \mu\text{m}$ ; this phenomenon that was observed was described as step edge induced degradation..

For improving stability further, they suggested a molybdenum oxide layer with an optimum thickness of 15 nm to avoid stability reduction from what they state from other references they cite in their paper. The cell architectures were ITO/TiO<sub>2</sub>/(CH<sub>3</sub>IN<sub>2</sub>)<sub>x</sub>(CH<sub>3</sub>NH<sub>3</sub>)<sub>y</sub>Cs<sub>1-x-y</sub>Pb(I<sub>z</sub>, Br<sub>1-z</sub>)<sub>3</sub>/EH44/MoO/Al and gave an initial efficiency of  $13.73 \pm 0.67\%$  (four devices) or ITO/SnO<sub>2</sub>/(CH<sub>3</sub>IN<sub>2</sub>)<sub>x</sub>(CH<sub>3</sub>NH<sub>3</sub>)<sub>y</sub>Cs<sub>1-x-y</sub>Pb(I<sub>z</sub>, Br<sub>1-z</sub>)<sub>3</sub>/EH44/MoO/Al, resulting in an initial efficiency of  $12.19 \pm 0.11\%$  (15 devices).

With the TiO<sub>2</sub> ETL, the cells quickly decayed to 85% initial efficiency in less than 100 h leading to a gradual decline to 80% of their initial efficiency after 300 h, followed by a faster degradation during 700 h to 60% [118]; stability was improved significantly when SnO<sub>2</sub> was used in place of TiO<sub>2</sub> under conditions of static resistive load at  $\approx 510 \Omega/30^\circ\text{C}$  /1 sun no UV filter /voltage scan 60 mV/s every 30 min from forward to reverse bias/12-22% humidity/ambient atmosphere/1000 h; initially decreasing to 90% almost at the start of the measurements, increasing to 100%, and retaining this value for 200 h, then gradually taking up to a further 800 h to degrade to 80% initial efficiency.

## 7.5 Summary of section 7

There are many challenges for flexible substrates and electrodes; the substrates/electrodes need to endure the fabrication methods. Regarding the temperature of annealing methods, carbon electrodes can endure high temperature processes while polymer-based electrodes cannot and would require low temperatures. Materials used in the layers of PSCs have properties that would require different fabrication steps. Among thermal limits for ETLs, heating during cell construction, e.g., TiO<sub>2</sub>, requires temperatures above 300°C to harden the material to perform well. Another alternative is ZnO which does not require tempering but is less stable in comparison to TiO<sub>2</sub>; and SnO<sub>2</sub> can replace TiO<sub>2</sub> which increases stability by being less reactive to the ion migration at the perovskite interface.

Substrates would need to be chemically stable during assembly and be able to retain their conductivity after any of the steps of the process. HTMs such as PCBM and PEDOT:PSS affect stability as mentioned earlier in the review due to their acidic properties, which degrades ITO electrodes. Other challenges are the solvents and deposition methods which the substrates can withstand without disturbing their performance.

Solar cells/modules need to have mechanical endurance while in operation during their lifetime; their use could be applied to clothes (wire based) or flexible surfaces which will undergo mechanical stress, such as bags or hats worn by people, etc. Testing of such rigid/flexible substrates would need to take into account high impact or environmental testing. These factors need to be incorporated into their assessment for suitability of commercial/industrial use.

The chemical stability of the electrode on the substrate under illumination also plays a role. A case to show this was UV light illumination of silver nanowire electrodes. Other factors are how the counter electrode material can migrate into the perovskite layer such as aluminium forming aluminium iodide due to electrode morphology, resulting from step edge induced degradation.

These topics in themselves can be a subject of a separate review paper alone.

## 8 The role of various stress types on solar cell parameter stability

There are various parameters/properties to assess solar cell performance and stability; one of these is the fill factor which is a property that is affected by the resistances in the solar cell, which affects how current flows.

The greater the current, the lower the resistance; where there is zero voltage, the cell is at maximum current. This point is called the short circuit value  $I_{sc}$  or  $J_{sc}$  (depending on whether it is referred to as short circuit current ( $I_{sc}$ ) or short circuit current density ( $J_{sc}$ )). This can be affected by electrons that recombine with their initial site or other sites within the lattice of the semiconductor material.

Recombination of electrons would reduce the current, so the property to describe this resistance is known as recombination resistance. In addition, there is the current that leaks out of the cell into other regions, which is prevented by shunt resistance.

There is also the chemistry which is affected by band gaps (energy required to excite electrons from their ground state (valence band) into their conduction band (where electrons can travel to other atoms); see Figure 37), which gives rise to the value of the open circuit voltage ( $V_{oc}$ ).

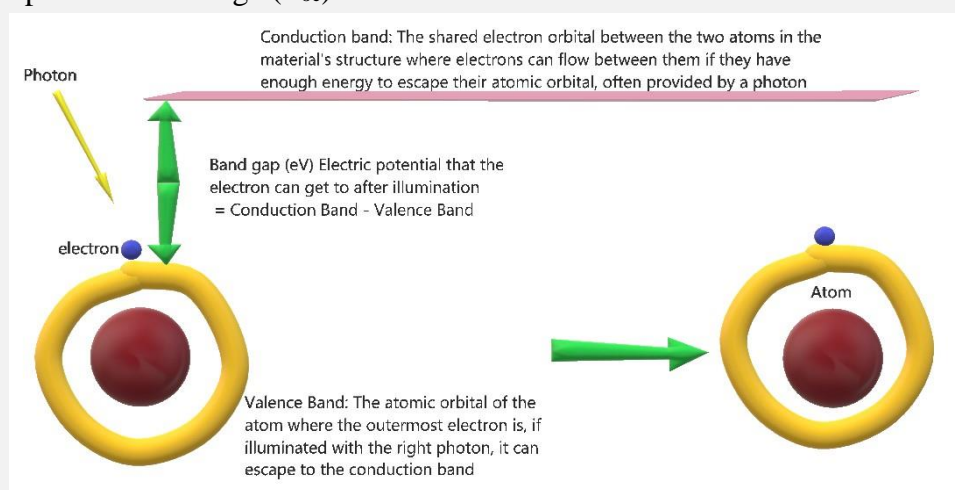


Figure 37: Describing valence and conduction band for the open circuit voltage ( $V_{oc}$ )

This value occurs when the current in the cell is zero; it is the potential energy that can be given to the flow of the electricity in the cell, which contributes to the performance. The efficiency is the overall contribution of all the parameters, i.e., the amount of photonic energy hitting the cell, compared to the amount of energy being transformed into electricity.

When the cell is being assessed, a current/current density voltage curve (*IV/JV* curve) is produced. The product of the current and voltage values along this scan is known as the power of the cell. The short circuit value and open circuit voltage are at the points in the cell where there is zero power.

When the product of these values is at a peak, the value and position of this on the graph denotes the maximum power point of the operating cell. The theoretical and measured maximum power points ( $M_{pp}$ ) are different. The ratio of the two of these is the percentage which is called the fill factor. A square drawn with the edges at the short circuit current/current density  $I_{sc}/J_{sc}$  and open circuit voltage  $V_{oc}$  is compared to the square drawn from the  $M_{pp}$ . The fraction of the area that this square fills is called the fill factor.

The basic equation to work out the fill factor of the solar cell is the following:

$$FF = (M_{pp})_{\text{measured}} / (J_{sc} \times V_{oc})$$

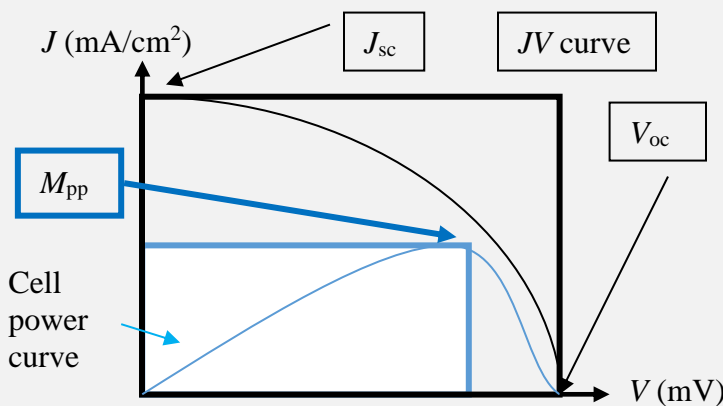
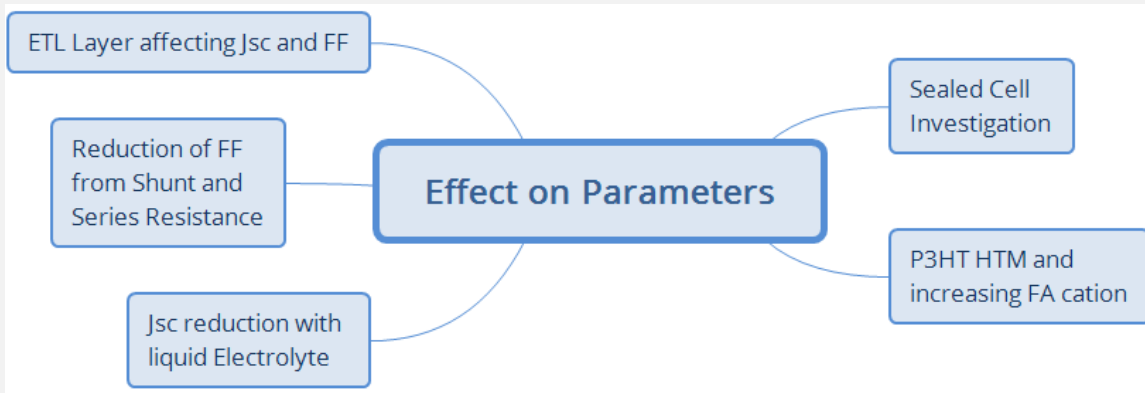


Figure 38: Description of Fill Factor

All these parameters are measured in stability tests, and change over time in different ways, which are caused by changes in the internal parts of the cells mentioned elsewhere in this review.

Different concentrations of perovskite in the solution can also affect the deposition layer, which in turn improves the absorption, and thus the  $J_{sc}$  can increase with a simultaneous reduction of  $V_{oc}$  from intercalation of the different layers of a cell into each other, due to the photoactive layer showing a porous nature [110]. Thus, the parameters arise as a result of different cell properties such as the photoactive layer, morphology, absorbance spectra, crystal structure, and so on.



Scheme 8

### 8.1 *$J_{sc}$ reduction from liquid tri-iodide*

As discussed in sections 1 and 4.1.1, one of the problems due to the presence of a tri-iodide electrolyte in DSCs is its corrosiveness. An increase of stability for a 9% solar cell was achieved in 2012 using a perovskite sensitized solid-state solar cell [28].

The decay was caused by the liquid electrolyte, damaging the perovskite in the solar cell, and led to a decrease in  $J_{sc}$ , resulting from a loss in the photosensitivity of the perovskite.

### 8.2 *Sealed cell, decay due to $V_{oc}$ reduction: $R_{sh}$ degrades with different illuminations*

One of the tests in a PhD thesis on the methylammonium lead iodide perovskite based cell, with Spiro-OMeTAD as the HTM [40], had the cells sealed with a 50 nm heat melted polymer spacer and microscope cover slip in an argon atmosphere; during testing they were kept at their maximum power point at a temperature of 45°C. Measurements were acquired every 2 h for over 500 h (20 days and 20 h) with intensity levels of 0, 0.1, 0.5 and 1 sun. Their results showed promising stability, by retaining 80% of the efficiency, with reduction from approximately 9% down to 7.2%.

The short circuit current stayed the same and this implied that the perovskite material transporting charges had no stability issues in this test. The reason for the decay was attributed to the decrease of the  $V_{oc}$  and FF. Reduction in the open circuit voltage was assumed to be due to the decrease in the shunt resistance.

### 8.3 *P3HT $V_{oc}$ and FF increase with formamidinium as a cation*

Using formamidinium as a cation with iodine and chlorine halides in a lead perovskite has shown that chlorine improved the performance, in general generating good stability for 30 days of ageing in ambient light/inert atmosphere with a P3HT HTM, with an efficiency increase (0.91%) from 6.6 to 7.51%. It was not clear why this performance boost occurred, which subsequently produced the improvement in  $V_{oc}$  and FF [86] (see sections 2.4.2 and 4.1.2.1 for further information on this reference).

## **8.4 Reduction of FF and shunt resistance $R_{sh}$ , $R_{sh}$ affects $V_{oc}$**

Mixed halides containing bromine were observed to have greater stability (30 days/N<sub>2</sub>/dark); although more efficient without bromine, the stability shows a steady drop whereas with bromine, there is a rise and decrease, thus maintaining the efficiency at the same level.

The mixture of different halides (I, Cl and Br) provided a reduction in non-luminescent charge recombination, thus increasing  $V_{oc}$  and improving efficiency [78].

## **8.5 ETL layer affecting $J_{sc}$ and FF**

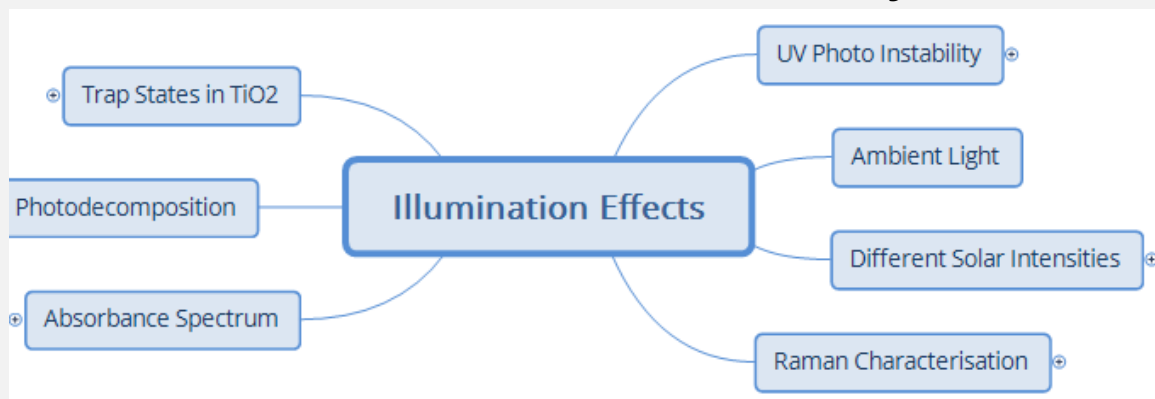
The use of TiO<sub>2</sub> as an ETL layer showed that it was susceptible to UV photoinduced catalysis degrading the perovskite (see section 0). The effects of degradation consisted of a decay in both  $J_{sc}$  and FF over a period of 1000 h. Using SnO<sub>2</sub> instead in the cell structure, SnO<sub>2</sub> or TiO<sub>2</sub>/(CH<sub>3</sub>IN<sub>2</sub>)<sub>x</sub>(CH<sub>3</sub>NH<sub>3</sub>)<sub>y</sub>Cs<sub>1-x-y</sub>Pb(I<sub>z</sub>, Br<sub>1-z</sub>)<sub>3</sub>/EH44/MoO<sub>x</sub>/Al, abolished this decay, leading to TiO<sub>2</sub> devices with an initial efficiency of 13.73 ± 0.67% and for SnO<sub>2</sub> cells 12.19 ± 0.11%. The overall stability seen from a test under static resistive load at ≈ 510 Ω, 30°C, 1000 h, 1 sun, no UV filter, voltage scan 60 mV/s every 30 min from forward to reverse bias, 12-22% humidity, ambient air resulted in the TiO<sub>2</sub> cells degrading to 60% of their initial efficiency, while the SnO<sub>2</sub> cells during that time held to a staggering 88 ± 0.4% of their initial efficiency for 1000 h (this is also mentioned above at the end of section 7.4.2).

## **8.6 Summary of section 8**

This section was a brief description of the different parts of the solar device giving rise to parameters which can cause changes to solar cell activity; and subsequently, to the efficiency, and as these different aspects change over time, the stability.

The liquid electrolyte redox couple was corrosive and lowered the  $J_{sc}$ . The effects of illumination impacting the shunt resistance changes the  $V_{oc}$  value. Chlorine produces a rise in the  $V_{oc}$  and FF and if halides are mixed the non-luminescent charge recombination is reduced, resulting in increased  $V_{oc}$ . Different layers affect the parameters of the cell through various degradation mechanisms. TiO<sub>2</sub> ETL cells undergo UV induced photocatalysis, hence damaging part of the device on an atomic/molecular scale, measured via FF and  $J_{sc}$  decay, although changing to SnO<sub>2</sub> significantly increased the stability of the system by preventing interaction between the perovskite and ETL.

## 9 The effects of illumination on cell stability

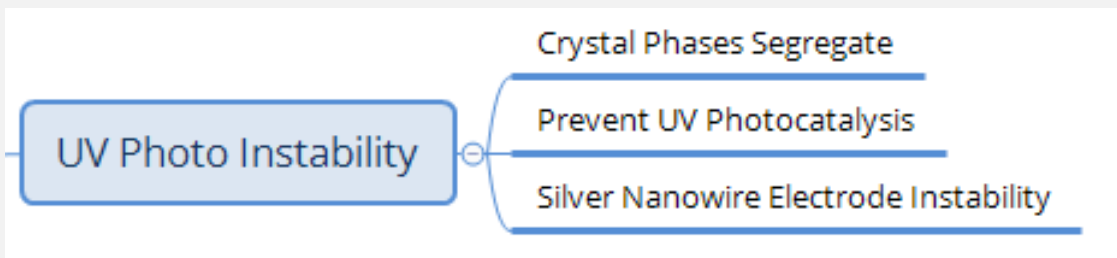


Scheme 9

### 9.1 UV photo induced instability

The solar spectrum has areas of it which can help in the performance of perovskite solar cells but, depending on the materials that make up the different layers, will affect which region of the incoming light may or may not damage.

The UV light section of the spectrum causes numerous effects in solar cells, several of which are listed below, describing how this is detrimental to cell performance and the need to protect against this.



Scheme 9-1

#### 9.1.1 Photo related segregation of halide crystal phases

Mixed halide perovskite studies using XRD and photoluminescence techniques showed reversible band gap reduction from 1.95 to 1.68 eV, and segregation of the different halide crystal phases under illumination, thus explaining why  $V_{oc}$  values of  $\text{CH}_3\text{NH}_3\text{PbBr}_x\text{I}_{3-x}$  perovskites are not as high as expected, this phenomenon being referred to as ‘reversible photo-induced trap formation’ [152].

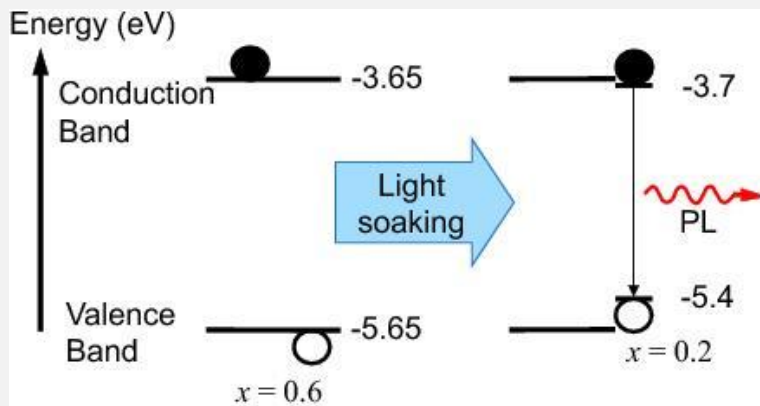


*Figure 39: Schematic of the proposed mechanism for photo-induced trap formation through halide segregation. Photogenerated holes or excitons may stabilize the formation of iodide-enriched domains which then dominate the photoluminescence. The valence band (VB) and conduction band (CB) energies with respect to vacuum were estimated by interpolation of published values obtained from ultraviolet photoemission spectroscopy (UPS) and inverse photoemission spectroscopy (IPES) for the endpoint stoichiometries (E.T. Hoke, D.J. Slotcavage, E.R. Dohner, A.R. Bowring, H.I. Karunadasa and M.D. McGehee Chem. Sci., 2015, 6, 613-617, 10.1039/C4SC03141E, RSC) CC 3.0 from Ref. [152]*

### 9.1.2 Preventing UV photocatalysis of perovskite

Indirectly, UV light affects the interaction of  $\text{TiO}_2$  with the perovskite. It could be a key problem in the stability of PSCs; it might be required to do away with the  $\text{TiO}_2$  mesoporous layer altogether and use the  $\text{Al}_2\text{O}_3$  mesoporous layer which is better [153]. They tested cells without the  $\text{TiO}_2$  mesoporous layer and found that they had over 1000 h of stability.

A  $\text{Sb}_2\text{S}_3$  blocking layer prevents UV light photo-induced catalysis of the perovskite  $\text{CH}_3\text{NH}_3\text{PbI}_3/\text{TiO}_2$  [153,154], thus increasing stability, efficiency, FF and  $J_{sc}$ , via increased PCE. Change in efficiency ( $\Delta\eta$ : air and light, 12 h) without the blocking layer drops from 4 to 0%; with this blocking layer, the efficiency is more stable falling from 6 to 4% [154].

One means for reducing the UV related perovskite catalysis due to the  $\text{TiO}_2$  UV light interaction was changing the ETL from  $\text{TiO}_2$  to  $\text{SnO}_2$  [118]. The device structure was either FTO/ $\text{TiO}_2$ / $(\text{CH}_3\text{NH}_3)_x(\text{CH}_3\text{NH}_3)_y\text{Cs}_{1-x-y}\text{Pb}(\text{I}_z, \text{Br}_{1-z})_3/\text{EH44}/\text{Au}$  or (FTO/ $\text{SnO}_2$ / $(\text{CH}_3\text{NH}_3)_x(\text{CH}_3\text{NH}_3)_y\text{Cs}_{1-x-y}\text{Pb}(\text{I}_z, \text{Br}_{1-z})_3/\text{EH44}/\text{Au}$ , and stability test under a static resistive load at  $\approx 510 \Omega$ ,  $30^\circ\text{C}$ , 160 h, 1 sun, voltage scan 60 mV/s every 30 min from forward to reverse bias, 12-22% humidity, ambient atmosphere.

Assessing the absorbance spectrum showed a decay that was constant along the whole spectrum in  $\text{SnO}_2$ , indicating UV light degradation was not occurring. The absorbance spectrum in the case of  $\text{TiO}_2$  degraded from 500 nm and lower wavelengths, demonstrating UV induced catalysis perovskite degradation. This was part of a study to assess the layers individually from the HTM to the electrodes, dopants and more (see sections 4.1.2, 7.4.2, and 8.5).

Another way to improve performance is adding a layer of sodium hexametaphosphate capped with  $\text{YVO}_4:\text{Eu}_3^+$  nanophosphor, which absorbs the UV light and simultaneously transforms it into longer wavelengths, contributing towards an increase in the absorbed radiation, which can be taken advantage of by the photosensitive perovskite layer [155].

An increase in  $V_{oc}$  and  $J_{sc}$  of approximately 1 mV and 1 mA/cm<sup>2</sup>, despite a loss of about 0.5% fill factor, led to the efficiency improving by approximately 0.5%. Stability was greater as a result of minimizing UV-induced photocatalysis, or by absorbing it and downshifting it to the visible spectrum, thus increasing the photocurrent.. The raised photocurrent in the PSCs (24 of them) is due to the increased absorption in the 300-450 nm region of the solar spectrum as seen in the IPCE data. Conditions during the stability assessment were temperature and humidity of 25 to 31°C and 25 to 40%, respectively, illumination for 12 h without a UV filter in a solar simulator at 1 sun and unencapsulated/ambient air (they discuss the presence of oxygen). The efficiency is stable for 4 h, followed by 2 h of strong decline after which a constant reduction to 50% of the initial efficiency was measured over the period of a further 6 h. During the 6 h protection where the first 4 h showed very little change, there is an increase in hydrophilicity of TiO<sub>2</sub> owing to the UV light in the presence of oxygen; moisture therefore accumulates, increasing degradation and ‘UV generated deep trap sites’ begin to form, and thus the perovskite begins to degrade after 4 h.

As described in the previous paragraph, research groups used a layer to absorb UV light, creating greater photocurrent. A dual function coating deposited on the non-conductive side of FTO glass, which incorporated phosphor particles with yttrium oxide, doped with europium (Y<sub>2</sub>O<sub>3</sub>:Eu<sup>3+</sup>) to absorb UV light and convert it to visible light, followed by a gold monolayer to amplify absorbed/converted light, improved both performance and stability under 1 solar illumination for 24 h while unencapsulated.

Efficiency increase was seen to be from 15.2-16.1% and instead of a 0.9% relative efficiency drop during the ageing assessment, a 0.6% relative fall in efficiency was observed due to reduced UV light absorbance [156].

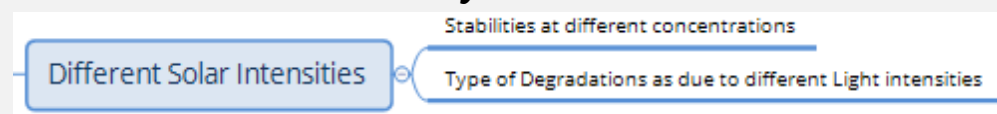
### 9.1.3 Silver nanowire electrode instability

Silver nanowires are one alternative to FTO or ITO electrodes, providing good performance when considering flexible substrates [151]. When illuminated with UV radiation, the nanowires underwent degradation, induced by radiative energy, which led to minor chemical explosions of reactive by-products with the nanowires’ polymer coating. A stable electrode was achieved through employing a graphite oxide coating. For a more detailed description, see section 7.3.1.

## 9.2 Ambient light and inert atmosphere

As mentioned earlier, tests performed with ambient light are numerous, together with the effect of an inert atmosphere; we in theory observe only photo-induced effects ( for further information see sections 8.2 for Ref. [40] and 0 for other works).

## 9.3 Solar intensity effect



*Scheme 9-0*

### 9.3.1 Degradation as a function of light intensity

PSCs are surprisingly capable of enduring light intensities up to 40 solar equivalents for 63 h [157]. The intensity of light correlates to the number of photons per second, so for 40 suns, the number of equivalent hours at one solar equivalent would be  $40 \times 63 = 2580$  h (100 days). The group was able to simulate this without the high temperature costing less than \$1000 using a LED light simulator, which does not produce IR radiation. Thus, the temperature of the setup can be kept fan cooled to less than or equal to 80°C.

At higher solar intensities than 1 sun A.M 1.5, reduced IR radiation leads to a difference between the applied voltage and cell voltage. This causes the device to go into forward bias due to a reduced electric field between the layers. To compensate, a combination of: substrate series resistance, top electrodes and resistance of the leads to the cell, called external resistance ( $exR_{ser}$ ), is added to provide a true current value; thus, with this in mind, true short circuit current ( $tJ_{sc}$ ) is introduced to compensate for this and enable true comparison at the different solar concentrations.

At increasing solar equivalents (SE) from 1 to 41 with an ( $exR_{ser}$ ) of  $10\ \Omega$ , a true photocurrent density increase was measured. From 1 to 19 SE, a linear rise was observed, at 20 SE, a sub-linear photocurrent density growth was detected, and at 41 SE the increase became 88% linear.

At high solar illumination, a 41 SE JV rounded curve compared to a JV curve at 1 SE showed charged dependent loss mechanisms grew in importance, using a  $23\ \Omega$  compensation  $exR_{ser}$ .

An increase in photocurrent was observed initially, starting with concentrated solar cell tests over a period of 63 h at 40 SE on a PSC with the structure encapsulated/FTO/TiO<sub>2</sub>/CH<sub>3</sub>NH<sub>3</sub>PbI<sub>3</sub>/OMeTad/Au, which was held in air/ $\leq 80^\circ\text{C}/\approx 40\%$  humidity. The  $tJ_{sc}$  was initially at  $0.29\ \text{A/cm}^2$ , dropped to 0.24, then increased to 0.29 during a couple of hours, followed by a gradual decrease.

This behaviour was typical of the TiO<sub>2</sub>/CH<sub>3</sub>NH<sub>3</sub>PbI<sub>3</sub>/OMeTad structure. The overall reduction of 8% photocurrent density was calculated to be at a rate of -0.2%/h, and ended at  $0.26\ \text{A/cm}^2$ . The JV curve at 41 SE showed a photovoltage change of -180 mV with a 420 nm cut-off filter and  $10\ \Omega$   $exR_{ser}$ . At 1 SE, the shift was slightly greater at -190 mV with a drop in 7% of the photocurrent, although after adjustment for this  $V_{oc}$  loss, the photocurrent was practically the same.

Heating the sealed cells in air to  $60^\circ\text{C}$  in the dark for 5 days was not responsible for any shift in photovoltage, as seen from the charge density (electrons per cm<sup>3</sup>) vs  $V_{oc}$  graphs whereas the observation of the -180 mV shift is detected after 40 SE for 63 h. From the IV curves in the supporting information, they state that high light intensity and heat show no negative effect on charge generation.

The loss in  $V_{oc}$  is attributed to ‘a decrease in band edge offsets at either the TiO<sub>2</sub>/CH<sub>3</sub>NH<sub>3</sub>PbI<sub>3</sub> or CH<sub>3</sub>NH<sub>3</sub>PbI<sub>3</sub>/OMeTAD interfaces (or both)’. They say it arises from a change in the ions adsorbed at the interface and suggested that the likely reason for this was due to ion migration, which probably comes from the Li<sup>+</sup> ion in the OMeTAD.

Testing other HTMs, P3HT and poly[2,5-bis(2-octyldodecyl)-3,6-di(thiophen-2-yl)pyrrolo[3,4-c]pyrrole-1,4(2H,5H)-dione]-alt-thieno[3,2-b]thiophene (known as DPPTTT), showed poor linearity for high solar equivalents and low stability.

Without encapsulation, the concentrated solar test caused degradation in the perovskite crystal, going from dark brown to yellow over a period of hours at 40 SE, while at 0.25 SE, it took a number of days.

Flat cells without a mesoporous structure present lower stability in the dark. The cells with mesoporous ETL using  $\text{Al}_2\text{O}_3$  are also unstable under the same conditions, whereas the  $\text{TiO}_2$  mesoporous layers were stable under both zero lighting and illumination.

The paper also compares organic solar cells and DSCs, and in general, concludes that not one technology stands out above the others in this harsh solar test.

In general, the author highly recommends this paper due to the uniqueness in its assessments which will help to eliminate unstable materials in a short space of time.

Their findings relating to the improvement in photocurrent, due to the degradation as a result of 63 h of illumination of 40 SE (illumination was passed through a 420 nm long pass filter), followed by, heating to 60°C, demonstrated the photovoltage transient lifetime to be constant; this is quite impressive!

The high intensity/focused light tests are important for potential use in concentrated solar power plants which already exist in commercial energy facilities. Perovskite solar modules have also managed to show 1200 h of stability in the dark in a dry box, to test shelf life; they produced very low hysteresis with an initial 3.45% efficiency, increasing to about 5.25% after 144 h owing to oxygen p-doping of the P3HT HTM, followed by the modules being sealed with cyanoacrylate glue; this led to the efficiency dropping to 4.96%; subsequently at 300 h, a reduction was measured in the  $J_{sc}$  from 9.8 to 8.9 mA cm<sup>-2</sup>, due to possible de-doping, and after a further 970 h a decrease in efficiency from 3.4 to 3.3%.

Further testing with cells containing the Spiro-MeOTAD HTM (>350 h, 1 sun/dry box/40°C), showed efficiency decay by 55% in the first 100 h, whereas P3HT fell by 75% of its original efficiency, Spiro-MeOTAD remaining at the same value for a further 250 h [132].

Additionally, concentrated solar testing up to 100 suns showed that mixed halide concentration increased the degradation rate of perovskites, resulting from an increase in defects rather than perovskite composition [158]. Degradation dependence on heat and light for low intensity to 1 sun indicated that perovskites bode well for concentrated light testing [159].

In another research article, scientists discovered that atoms in the crystal structure of the perovskite  $\text{CH}_3\text{NH}_3\text{PbBr}_3$  have a stronger bond than those in  $\text{CH}_3\text{NH}_3\text{PbI}_3$ ; this was attributed to the smaller atomic orbitals of Br. This led to the film of the bromide perovskite showing very little change under 100 suns illumination at 40 to approximately 55°C for 1 h as compared to the iodide perovskite which displayed evidence of decomposition; XRD data evidenced the aforementioned phenomena. The iodide-based film had a better absorption spectrum although degradation was ascribed to illumination and heating. They hypothesise that a combination of the high stability offered by the bromide perovskite can be combined with the better absorption of the iodide perovskite

to form a crystal that will be both stable and have good absorbance at high temperatures and more intense illumination [160]..

Other works included adding pseudo-halides such as thiocyanate (SCN) to perovskites, which has had a positive impact on the stability under conditions of 4 h/95% relative humidity/closed chamber/dark/open air/ambient laboratory light. Harsh humidity at 95% did not show any effect on the perovskite  $\text{CH}_3\text{NH}_3\text{PbI}(\text{SCN})_2$  after 4 h, while comparing that to the standard  $\text{CH}_3\text{NH}_3\text{PbI}_3$  based perovskite, XRD data showed degradation to  $\text{PbI}_2$  within 1.5 h

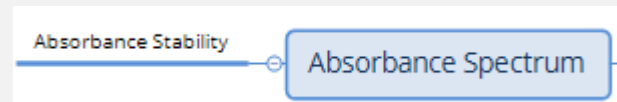
Performance of the perovskite with Spiro-MeOTAD as the HTM showed 8.3% efficiency while that of  $\text{CH}_3\text{NH}_3\text{PbI}_3$  was 8.8% efficient due to a higher  $J_{sc}$ .

In long term testing for 14 days at 20 to 40% relative humidity, the pseudo-halide perovskite only showed 0.9% absolute reduction in efficiency and  $\text{CH}_3\text{NH}_3\text{PbI}_3$  displayed 1.9% absolute reduction within 7 days, with complete failure after 14 days; other tests in their absorbance spectra show similar stability trends [80].

#### 9.4 Raman characterisation breakdown

Raman spectroscopy on perovskites is difficult to observe due to decomposition under the laser even though minimal power is used, although a combination of the two precursors has been used to simulate such spectra. The use of a mixed halide standard  $\text{CH}_3\text{NH}_3\text{PbCl}_{3-x}\text{I}_x$  perovskite held in atmospheric air, humidity and temperature not specified but weather dependent, for 30 days, showed improved efficiency performance from 1.65 to 2.26% after the fourth day; subsequently, after a month, it fell to 0.94% due to a loss in  $V_{oc}$  [161].

#### 9.5 Absorbance spectrum



Scheme 9-2

A perovskite layer ( $\text{CH}_3\text{NH}_3\text{PbI}_{3-x}\text{Cl}_x$ ) and undoped P3HT were deposited on plain glass in an ambient environment of 50% or greater humidity. The device without the electrode was compared to the bilayer perovskite/HTM, indicating a great similarity of shape and absorption peaks; the main difference was in the absorbance magnitude being slightly lower for the device. Higher concentrations of perovskite solution 40 wt% as opposed to 30 wt% showed greater coverage and absorbance. The absorbance spectrum over the cell that was fabricated again in >50% humidity, with the architecture

FTO/TiO<sub>2</sub>/CH<sub>3</sub>NH<sub>3</sub>PbI<sub>3-x</sub>Cl<sub>x</sub>/P3HT, showed absorption of magnitudes between 0.2-0.3 at the wavelengths of 350 to 650 nm, with a broad peak at 520 nm. After one month, this changed to 0.2 to 0.3 and the peak was no longer there.

Initially, the longer wavelengths 650-750 nm showed an absorbance of 0.2, and decreased to zero on going from 750 to 800 nm. After one month, the absorbance in this region altered minimally, possibly only displaying a slight redshift in the broad peak which almost was non-existent. The mechanism causing the change was attributed to the degradation of the P3HT layer, while the perovskite coating remained intact.

After six months, the remnant of the peak disappeared leaving two small peaks at approximately 420 and 480 nm, respectively. The absorbance over the wavelength range of 500 to 650 nm depicted a slope which decreased gradually towards 0, remaining there for the longer wavelengths [110]. The decrease was attributed to the breakdown of the P3HT and further to that, the reaction of the silver electrode with the iodide (see sections 4.1.2 and 7.4.2 regarding this reference).

## 9.6 Photodecomposition

### 9.6.1 The $\text{CH}_3\text{NH}_3^+$ cation with $\text{PbX}$ is photosensitive and can decompose



Scheme 9-3

The theory and mechanisms of the photodecomposition of the metal halide molecule have been investigated in a review, highlighting the instability of lead halides recorded in 1893 [162]. It discussed the complete motion of the hole at the different lattice sites, interacting with the halides and metal in the centre of the structure, which can be ionized and, if so, reduce semiconductor properties.

The need to study the dynamic behaviour of charges formed from incident photons in the different perovskites, as well as the traps formed from ions of lead on the regular lattice sites, was also suggested (this paper contains much more information that would interest someone analysing/working on photodecomposition of lead halides).

## 9.7 Traps states in $\text{TiO}_2$



Scheme 9-4

### 9.7.1 Al doped $\text{TiO}_2$ to reduce deep trap states and the phenomena explained

Sealed solar cells illuminated for 14 h with UV light caused significant normalized PCE decay from 1.0 to 0.25% of the initial performance. Unsealed cells actually improved over time. The theory they state suggests the following:

$\text{TiO}_2$  anatase lattice from the removal of oxygen due to defects results in  $2x\text{Ti(III)}$  which is unstable becoming  $\text{Ti(IV)}^+ + \text{e}^-$  and acts as an electron trap site. The  $\text{Ti(III)}$  forms shallow (0.7-1 eV) energy levels below the conduction band. The oxygen combines with the  $\text{Ti(III)}^+$  to form a complex of  $\text{Ti(IV)}^+ + \text{e}^- - \text{O}_2^-$ , where the superoxide is stable. This pacifies the  $\text{Ti(III)}$  electron trap and occurs at the surface of the lattice where the oxygen defects are located.

When illuminated by UV light, electron hole pairs are produced; the hole produced in the valence band recombines with the electron on the superoxide  $O_2^-$ . The titanium oxygen complex then reverts back to Ti(III), causing the deep defect energy levels; thus the electrons in the conduction band, which would go to the electrode, recombine with these holes in these trap states.

When the cells are unsealed, the oxygen titanium complex can reform, whereas in an encapsulated cell this is prevented, and thus the complexes are reduced to almost nothing. This causes the recombination rate to reach a point where the cell can no longer operate.

The overall results showed that doping with aluminium using a sol-gel method increased the  $V_{oc}$  slightly, although it lowered the  $J_{sc}$ . The conductivity was found to rise due to the passivation effects, although above 0.5% the conductivity was lower due likely to charge scattering.

It was found that the number of sub-band gap states were pacified, or significantly reduced with aluminium doping. With aluminium, the conduction band is raised, and an increase in the band gap occurs as their observations showed. At an optimised doping of 0.3% mol, a significant improvement in the stability of the PSC was observed, going from an efficiency of 11.13% undoped, to 13.80% doped.

Stability improvement under conditions of 30 h, encapsulated, and illumination in an inert atmosphere was observed for the solid-state DSC. The undoped encapsulated cell lost 80% of its initial efficiency after 5 h, whereas the doped cell showed a decrease of 70% after 30 h [163]. It is a significant improvement, showing how in sealed cells, aluminium can be used to passivate trap states and increase performance.

## 9.8 Summary of section 9

The phenomenon known as reversible photo-induced trap formation causes cell performance issues. Various materials have been used to either pacify the photocatalysis of the perovskite, or increase UV light absorbance, so as to reduce photocatalysis. Concentrated solar testing shows the potential for PSCs being used in solar power plants and how different perovskites deteriorate. Raman analysis highlights their instability under laser light observation and how this occurs.

The photosensitivity of the perovskite cation and anion is affected by hole motion ionising the metal halide, which reduces semiconductor properties. Understanding has also been gained on how stability is affected through trap formation and recombination by UV light, and pacification of sealed and unsealed cells with aluminium via a sol-gel method of doping.

This all suggests that illumination alone, with or without an atmosphere, using different parts of the spectrum, is a subject worth investigating. It is also important to gain insight into the effects of lighting on device performance, and the respective degradation mechanisms. Via these potential discoveries, more techniques to increase stability can be implemented.

## 10 Challenge to find non-toxic alternatives to lead and other toxic perovskite precursors

Perovskite precursors are usually halide or heavy metal based. These materials pose a risk to the environment. It is important that the solar energy community carefully monitors the dangers of these materials and finds successful alternatives.

'Lead-free' perovskites as a search topic in Scopus produced an outcome of 79 results since the time of writing, including seven reviews, three of those being open source.

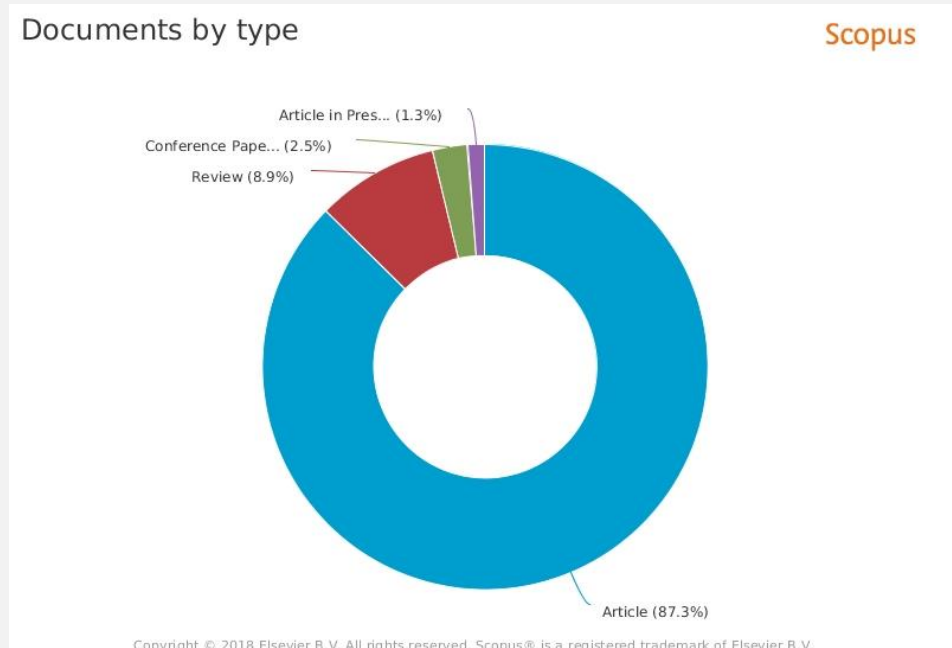


Figure 40: 'Lead-free' perovskite solar cells as a key words in a Scopus document type percentage analysis (74 articles)

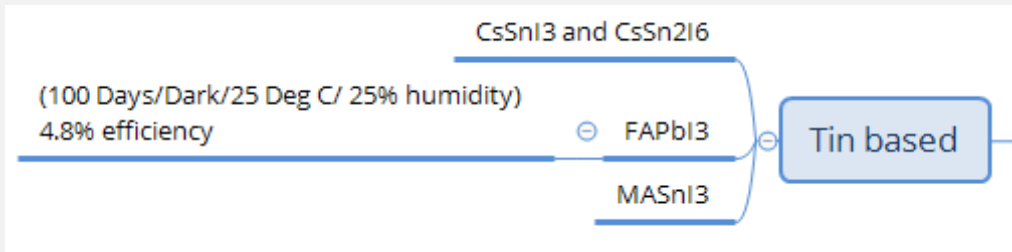
A few of these papers are described below

Despite interest in tin alternatives for replacing lead, a recent study found that the tin halide precursor does more harm due to its greater degradation rate to form hydroiodic acid which, when leaked into the ecosystem, negatively impacts the pH of the environment in which water based organisms live [164].

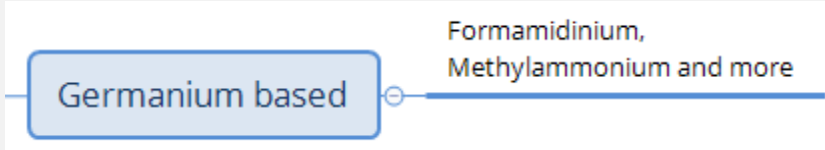
Thus, thanks to this study, the need to find other materials for perovskites is strongly emphasized, despite the push to use tin alternative perovskites, unless tin based perovskites which do not decompose into harmful tin precursors are discovered! Below, various investigations into trying to find lead alternatives are described.



Scheme 10



Scheme 10-1: MA and FA represent methylammonium and formamidinium cations



Scheme 10-2



Scheme 10-3: MA represents the methylammonium cation

The durability of the perovskite material under operational conditions was analysed for tin and lead based methylammonium tri-iodide perovskites.

Lead based perovskites showed greater stability than tin. They are stable in air for months, since the inner structure is unaffected, and only their outer layer loses its shiny appearance when exposed to humidity, after a couple of weeks.

When compared to the lead-based perovskites in that article, those based on tin are both air and moisture sensitive, and after 2 h of exposure begin to degrade; within a day they completely decompose [57].

Lead free cells with the structure FTO/blocking layer/CsSnI<sub>3</sub>+ 20 mol% SnF<sub>2</sub>/4,4'-4"-tris[phenyl(*m*-tolyl)amino]triphenylamine (*m*-MTDATA)/Au were tested over a period of 0, 6, 7 and 11 days in a nitrogen filled glove box. Their *JV* curves showed very little difference of 1 mV or 1 mA [165] (see their supporting information).

Another article on a lead-free perovskite based on CH<sub>3</sub>NH<sub>3</sub>SnI<sub>3</sub> was found to crystallize at room temperature after spin coating [166]. This affects the performance and also shows greater instability when compared to the lead-based perovskite since, after encapsulation, the cell still shows degradation when placed in ambient conditions, indicating the sealing method was not satisfactory, or simply that the perovskite material was chemically unstable.

As with the lead based CH<sub>5</sub>N<sub>2</sub>PbI<sub>3</sub>, there is the equivalent tin analogue CH<sub>5</sub>N<sub>2</sub>SnI<sub>3</sub> [167]. Assessments showed very promising stability [168] with devices which were prepared and encapsulated in a nitrogen glove box providing encouraging results for stability test under the conditions of dark storage/ambient conditions with humidity ≈ 25%, temperature ≈ 25°C (see Figure 41).

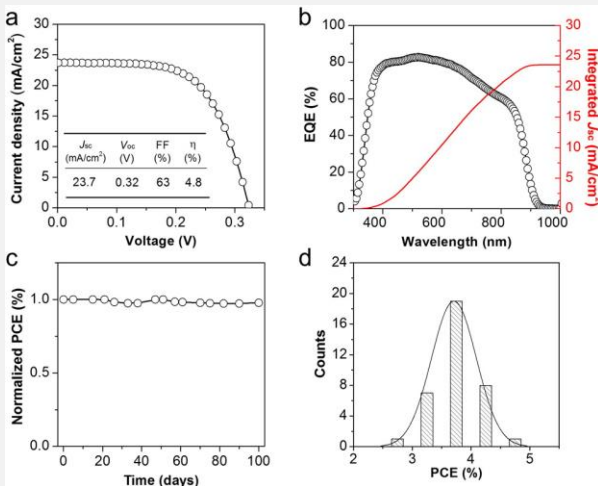


Figure 41: (a) J-V curve and (b) external quantum efficiency (EQE) spectrum and integrated  $J_{sc}$  for the optimized  $\text{FASnI}_3$  PSC. (c) Normalized PCE of the encapsulated  $\text{FASnI}_3$  PSC under ambient condition for over 100 days and (d) histogram of PCE obtained for 36 devices Ref. [168] (reprinted (adapted) with permission from (*J. Am. Chem. Soc.*, 2016, 138 (12), pp 3974–3977). Copyright 2016 American Chemical Society. FA = formamidinium).

Greater intrinsic perovskite stability was obtained in tin based perovskites as an HTM, consisting of the already oxidized  $\text{SnI}_4^+$  in ethanol and CsI in water/DMF, the cells being fabricated under ambient conditions [169]. Characterisation of its many properties (photovoltaic, band gap, electronic) indicate that it still undergoes degradation, albeit being more stable [170].

Another very promising +4 oxidation state metal perovskite employs Ti, which shows very good stability, and band gap tuning from 1.3 eV to 1.8 eV. Theoretical and experimental data indicate that it holds potential for use in PSCs but no cells were fabricated in that article [171].

Perovskite degradation while acting as a photo-absorber was measured owing to possible HTM P3HT decay, or from applied bias, and possible interaction with other materials in the cell at their interfaces [172]. Other perovskites have been theorised or produced in the laboratory, incorporating germanium [173,174], bismuth [175,176], bismuth with titanium or sodium [177], bismuth and silver [178], and copper [179].

A bismuth based perovskite  $\text{Cs}_3\text{Bi}_2\text{Br}_9$  with quantum dot properties was prepared using an environmentally ‘green’ method employing ethanol as the main solvent; the researchers found good stability and the wavelength could be tuned from 393 to 545 nm [180]. The possible tuning of such perovskites could be an interesting matter of research in finding non-toxic materials which do not destabilize into environmentally harmful substances. In this paper, there was no application of such materials in solar cell devices. A review paper dedicated to bismuth perovskite is available for the reader, if need be including literature from 2018 reporting its use in devices (one in particular using nanocrystals and boasting 4.3% efficiency): the authors present a table of bismuth perovskites and their crystal structures and efficiencies which is very useful [181].

Another review with a table on various, mostly lead-free perovskites can also be obtained for further analysis on what has been researched on this topic; a tin based device reached 7.8% efficiency using a tin perovskite as a hole transporter [182].

For a review discussing potential lead-free perovskites for photovoltaics, see Ref. [45]

## 10.1 Summary of chapter 10

There is an ongoing search for perovskites which will be useful for photovoltaics having stability, good efficiency and are safe for people to handle. Having perovskite systems without the lead and stable forms of tin are aspects of research, although it is rather the precursors entering the environment which will cause the damage. So, to find more intrinsically stable perovskites which will not break down is key.

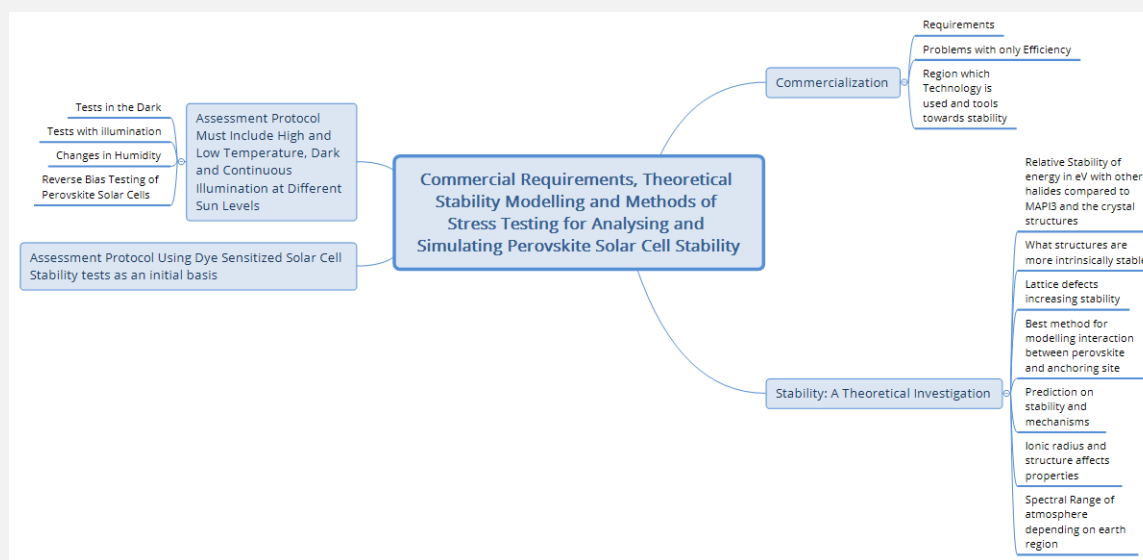
Theoretical investigations also provide evidence of which direction a research study could go to in order to start synthesising photosensitive stable perovskites. Then their abilities could be tested in their use for photovoltaics in HTM, photosensitizers or other applications, etc.

While much effort has been made to find a useful lead-free perovskite, the devices made with these materials have not yet received enough attention, such that the research community would stop experimenting with lead-based devices; if the research is intensified, potential stability and efficiency of lead-free devices is within reach.

## 11 Commercial requirements, theoretical stability modelling and methods of stress testing for analysing and simulating PSC stability

Many tools with potential applications in PSC stability will need to be incorporated to match the commercialization requirements for PSCs. Theoretical effort helps experimental work in researching in which direction to go.

An open source program needs to be created which researchers employ to simulate various test conditions, incorporating the numerous methods of cell manufacture, and thus build up a database, which will contribute towards the search for the optimal parameters and materials experimented with in the past. This will take experimental stability tests as a guide and subsequently implement them as a rule for how cell parameters decay. Therefore, the different effects can be calculated to produce a map for future stable devices.



Scheme 11

## **11.1 Commercialization**

### **11.1.1 Requirements**

Without too much enquiry and just basic thinking, one can envisage the following criteria that would be necessary for new solar technology to come to fruition.

- Be safe for the end user throughout its lifetime
- Be cheap enough to be able to produce enough energy to become cost effective over its lifetime
  - The indirect financial benefits would be the need to recover the cost and energy that they were made with
  - Currently solar panel energy recuperation figures can range from 2.9 to 5.4 years
  - Have the added benefit of reduced CO<sub>2</sub> emissions, which also helps to lower a country's expenditure regarding fees for the amount of CO<sub>2</sub> produced; also for sound reduction
  - Last for at least 20 years for the cost to be matched with the energy generated depending on the region, type of investment and incentives provided by the government
    - Finland showed that at present, with the current incentives, the time is 20 years and could go down to 10, whilst in Iran it is still not competitive unless various incentives are introduced, and other countries have similar issues, although India possibly had a pay-back time of 6 years [183–187].
- Be stable enough to endure the conditions of oxygenated atmosphere, pollution, dirt, rain, humidity, mechanical strain
- If possible, be aesthetically pleasing for building integrated photovoltaics, and even in other sectors.
- Be easily available and manufacturable
- Have a recyclable end cycle for when the device begins to drop below acceptable performance, otherwise it could possibly pose a health and safety hazard to the end user

### **11.1.2 Problems with focusing only on efficiency**

Each of the above points could be the focus of a review paper. Solar cell efficiency alone, while testing the limits of short-term performance, cannot result in commercialization; to achieve this, the greatest attention needs to be paid to stability.

If a cell's high efficiency only lasts a year at most, and degrades significantly thereafter, then the technology does not serve its purpose. It will not be able to produce enough energy in its lifetime to justify the energy consumed during manufacture.

There are problems with only focusing on the highest efficiency for solar cells. Despite groups reporting high efficiencies, the surface area of the solar cells quoted is very low; on increasing to larger surface areas, falls in performance are expected due to defects in layer quality and increase in resistances. Stability testing of these designs on large panels is as yet not part of the main research directions.

Perovskite solar panels may or may not reach required efficiencies. It is possible that through hybridization of a silicon solar panel using both silicon and perovskite crystals, its efficiency can be improved from 19 to 23%; subsequently, the cost of fabrication and payback time are lowered. Again, the challenge would be the stability of the system.

### **11.1.3 Considering the region where the technology is to be used and tools towards achieving stability**

Another aspect is that scientists/industrialists working on solar cell technology need to take into account the latitude at which their devices will be implemented, since the solar panels' performances will be affected. This arises from the angle of the incident solar radiation, hitting the Earth in that region due to the Sun's zenith angle. This also changes throughout the year and if this is modelled, it could be a tool in predicting long-term performance for solar cells.

A theoretical simulation tool, called the simple model of the atmospheric radiative transfer of sunshine (SMARTS), has been used to address this issue. It has been used for different latitudes on the surface of the Earth. This was implemented for high concentrator multi-junction photovoltaics on how they would perform in that region [188].

A simulation on the spectral losses/gains involving the reduced/improved solar radiation absorption in comparison to that from a reference cell in a laboratory calculated from factors such as annually average values of air mass, aerosol optical depth at 555 nm ( $\tau_{0.55}$ ) Ångström exponent  $\alpha$  (non-dimensional) and precipitable water (w) in cm) in different parts of the world and its applicability to PSCs was carried out.

The presented spectral gains were only in certain geographical regions, while spectral losses were observed in other places around the world. Solar photovoltaics would need to be tailored for the region that they are going to be sold in (e.g., see section 11.2.7).

On a similar topic, a review on various spectral techniques analysing the performance of cells with respect to the atmospheric conditions, can provide further information for interested readers [189]. Some of these tools in the aforementioned reference would be useful regarding the concept of forming a stability performance modelling package. It would include the place in which the cell is being tested.

Regarding tools for applications towards stability, a Marie Curie research group has set up a degradation database, which has been implemented for organic solar cells and is soon to be employed for perovskites too, as seen in the Marie Curie meeting presentation in Ref. [190]

The author's opinion would be a suggestion of possibly more specific additional adaptations to the database, if possible, such as in Figure 42 (link to the aforementioned database: <http://plasticphotovoltaics.com/lifetime-predictor.html>).

Using a skeleton of a table like Table 6 below, one could classify the references in terms of the stability points. A graph of a similar test has been done in the previous reference where the type of testing is a line chart and each stress is a different line. The combination of such could prove informative.

To illustrate the assessment score for the different stabilities, line charts can be implemented. Other methods could be 3D-mapping, depending on the stress conditions involved, for pictures and 4D-mapping (animation), for a more sophisticated understanding of change over time for all the stress different factors. Combining that with several 4D-charts, a scientist would be able to see the behaviour of the parameters with respect to each other.

*Table 6: Map of Stability tests, C indicates cycling of the parameter (not exhaustive) It needs to be visual somewhat closer to the top right the better, I have found papers who have tables of tests, would be good to visualise it possibly.*

Stress para-meters	Time: normalized efficiency drop > 20%: {hours (h), days (d), weeks (w), months (m), years (y)}					Time: normalized efficiency drop > 10%: {hours (h), days (d), weeks(w), months(m), years (y)}					Ref erence
	h	d	w	m	y	H	d	w	m	Y	
Concentrated solar intensity 1+ sun 1.5 AM											
1 sun											
100 suns											
Solar intensity less than 1 sun 1.5 AM											
0.99 sun											
0.5 sun											
Dark/Storage											
Electrical											
Open circuit											
Short circuit											

Reverse bias (V or I)								
Atmosphere								
Argon								
Nitrogen								
Oxygen								
Ambient								
Humidity								
Approximately dry < 1ppm								
10%								
20%								
30%								
Etc. up to 100%								
Thermal								
200 K (Antarctica)								
273.5K (Freezing point of water)								
373.5K (Boiling point of water)								
>373.5K Above waters boiling point								
Mechanical								
Oscillation								

Direct impact											
Long term gravity effects											
Corrosion											
Likely fumes											
Worst case scenario e.g. fire											
Magnetic interference											

It is likely that such testing methodology and risk factor analysis has already been incorporated in health and safety and manufacturing for the consumers' wellbeing. Much of this is likely to be in many International Electrotechnical Commission (IEC) directives, reports and protocols such as RoHS (Restriction Of Hazardous Substances), REACH (Registration, Evaluation, Authorisation and Restriction of Chemicals), SVHC (substance of very high concern), etc.; most would be applicable for various circumstances, and this would also depend on the materials involved in building and manufacturing the perovskite solar panels.

Before panels are made, the device testing scenario would depend on the types of cells, and whether they are encapsulated; it may also incorporate testing prior to any encapsulation as well as final testing.

One can see a more visual diagram for cell testing in the mind map below, which will be incorporated into module/panel manufacture, although it is outside the scope of this review but is mentioned here for the sake of completeness.

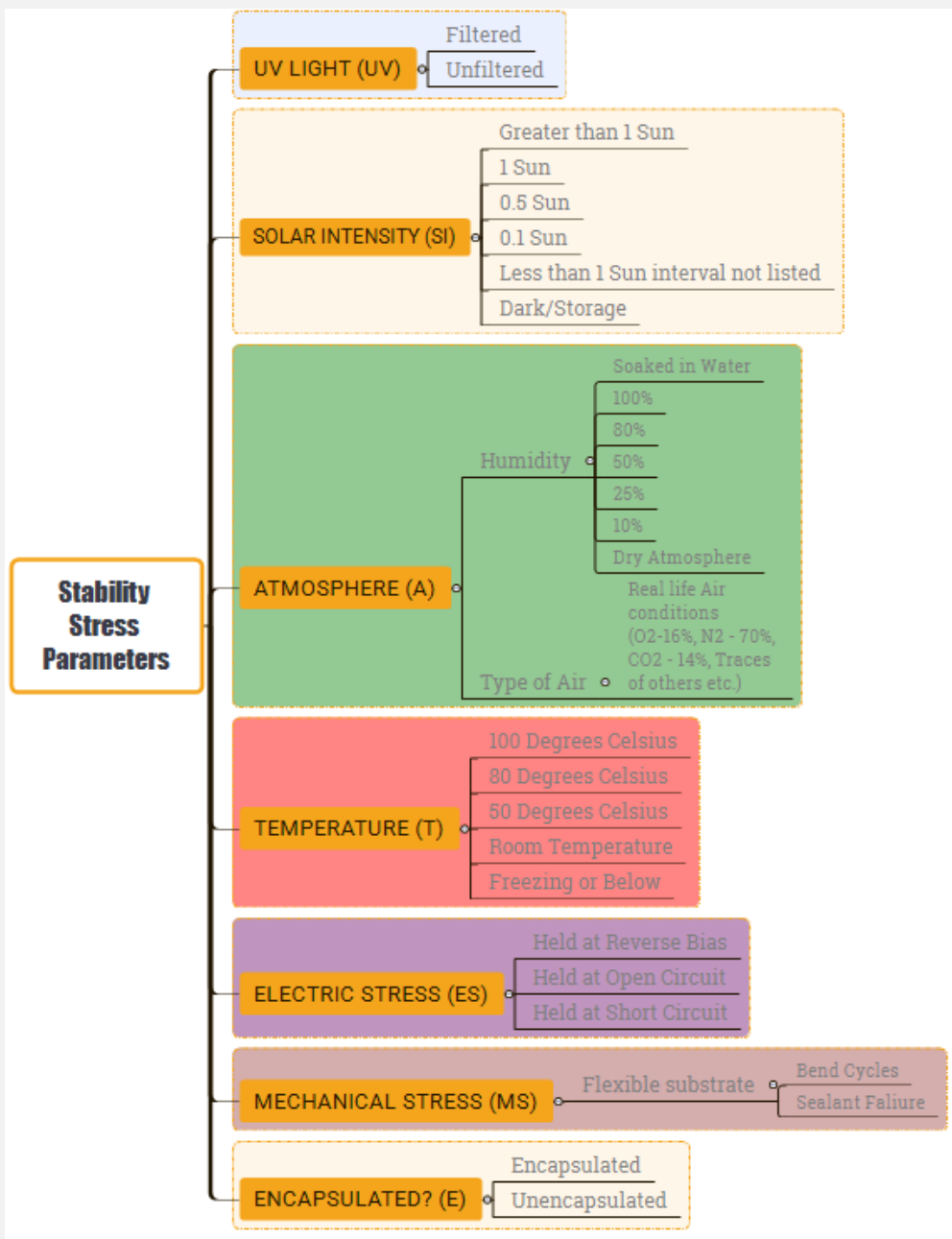


Figure 42: Mind map of what the stress parameters are for a stability test

## 11.2 Stability: a theoretical investigation

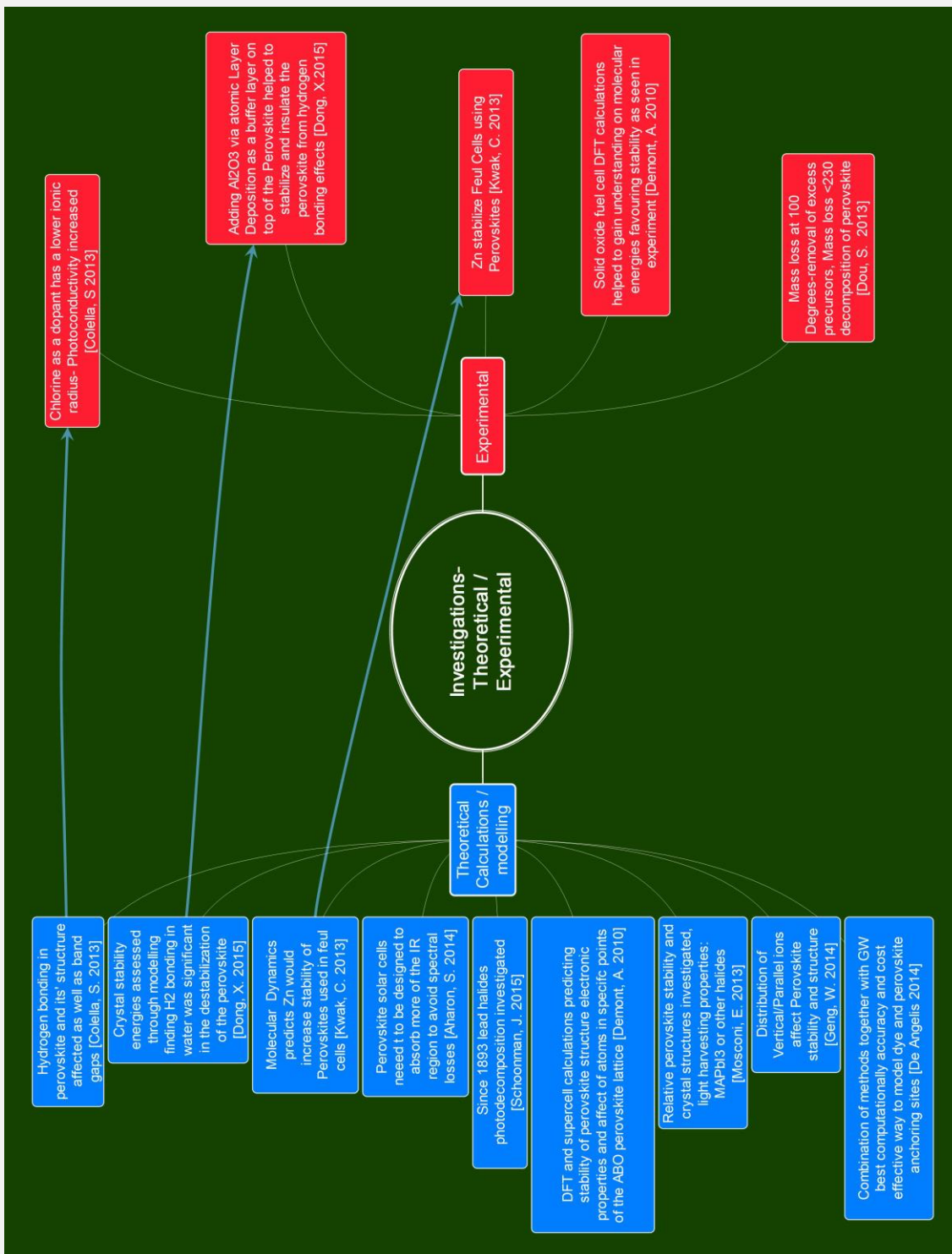


Figure 43: Summary of a combination of theoretical (in this section) and its links to experimental work which are mentioned in other sections of the review

There are a number of reviews/articles published covering theoretical subtopics on perovskite solar cells, as follows: properties of perovskite crystals [191,192], ETL-

perovskite interface investigations and the role of chlorine [193], different computational and theoretical methods [194], lead-free perovskites [45], the source of hysteresis [134] and the instability of perovskites with regard to humidity [74] (see section 1.4 in the present paper for a list of some of reviews, you can also find some referenced in some of the other sections 10, 11.1.3 and 11.2.3).

### **11.2.1 Relative stability in eV of other halides to $\text{CH}_3\text{NH}_3\text{PbI}_3$ and the crystal structures**

The light harvesting properties of a perovskite are related to the relative energy stability in eV of other halides compared to  $\text{CH}_3\text{NH}_3\text{PbI}_3$  crystal structures and band gaps, as discussed in a theoretical investigation [191].

### **11.2.2 What structures are more intrinsically stable**

Cubic perovskite structures under normal lighting conditions have been shown to be more stable than tetragonal ones [77]. The greater the intensity of solar illumination, the fewer the defects in the crystal film and the better the stability [158–160] (see section 9.3.1 for further information on this topic and references therein). The orthorhombic structure has been calculated to be the most stable and, in general, the distribution of parallel or vertical methylammonium ions affects the stability as well as its electronic structure [75].

### **11.2.3 Lattice defects can also improve stability**

It has been observed, ‘contrary to naive thinking’, that defects in the perovskite crystal lattice improve stability. This has been noted with chlorine in the perovskite lattice; the theory to explain this has suggested it is due to the binding energy, and reduced bond length in the mixed halide between the I-Cl, mentioned in the text of this review [193]. One still needs to understand, that as mentioned before, under high intensity illumination stress of 40 SE, this is untrue.

### **11.2.4 Best method for modelling the interaction between the perovskite and anchoring site**

In order for investigators to predict and understand stability mechanisms, accurate and computationally efficient models need to be used. Scientists model different sections of the solar cell; perovskite anchoring, the anchoring site and interface, can affect stability. Calculating this though has used different computing models. The GW method (a technique using the Green function and the screened coulomb interaction  $W$  [195]) has been found to be the most accurate and useful for the dyes and perovskites, although for interfaces it becomes computationally expensive.

At the current level of computing power, other techniques have less accuracy but are more practical. In order to overcome this, a combination of different models is suggested as a route forward, until greater computing power is available [194].

### **11.2.5 Prediction on stabilities and mechanisms**

At present, a key problem for efficient photosensitive perovskite crystals is their degradation via water molecules. It only requires one to two water molecules to weaken the bonds [74]. For three or more water molecules, the perovskite crystals are strongly affected.

Calculations have shown that the high polarity of water causing hydrogen bonding is responsible; thus, encapsulation is recommended if and where possible.

Some studies have shown that the chlorine doped PSCs display elevated efficiencies as opposed to undoped PCSS [196]. In this work, this increase was attributed to one of two properties: (remove highlight? Does increase and the comma help?) the excitons generated by photons or the crystal orientation; further investigation was needed to identify which one was responsible. The investigators were unable to detect chlorine in the energy dispersive XRD spectroscopy measurement.

Regarding similar research on the same dopant, theoretically, chlorine can at most constitute 4% of the crystal structure. These defects affect the lattice structure and hydrogen bonding with the organic and inorganic parts of the crystal, thus affecting energy band gaps, and as mentioned in a previous paragraph, stability [197].

They find the ionic radius of the halide atom affects the formation of a solid solution, while a mixed halide solution increases the photoconductivity.

Other theoretical work on additives using molecular dynamics shows that Zn dopants have been predicted to improve stability. Experimentation has confirmed this in a perovskite structure implemented in fuel cells [198]; one could possibly apply this to photovoltaics.

### **11.2.6 Ionic radius and structure affect properties**

Among many computational tools used to identify various properties of perovskites, density functional theory simulations were applied on a different perovskite ( $\text{Ba}_{1.6}\text{Ca}_{2.3}\text{Y}_{1.1}\text{Fe}_5\text{O}_{13}$ ) which is employed for solid oxide fuel cell cathodes; it was calculated to have a 2D structure, and predicted molecular energies in the ‘frontier electronic states’ in the top and bottom section of the valence and conduction bands. These electronic states are favourable for stability as judged from the amount of ‘A site disorder’ and other useful properties, such as conductivity and catalytic ability, etc. Their experimental observations have shown how band gaps affected the materials’ properties, as well as much more. There were other computational tools involved, which were used for other aspects of the perovskite, such as ‘spin-polarized GGA’ for approximating the magnetic moments, which showed good agreement with experimental data [199]. Theoretical effort applying these techniques to the field of photovoltaics, to obtain more stable photosensitive materials, would contribute a lot to the work of synthetic chemists.

### **11.2.7 Spectral range of atmosphere depending on earth region**

Industrial applications of perovskite photovoltaics through modelling SMARTS (see section 11.1.3 for further information on this computational technique) suggest that PSCs, due to having strong UV absorption, will suffer from high spectral losses; thus, tuning the solar cell absorption properties, to account for the UV range in the particular country it is deployed, will need to be incorporated.

Only in places such as Alta Floresta in Brazil would a spectral gain be produced [200], and in cities like Edinburgh in Scotland, which is far from the equator, large spectral losses of up to 10% would occur. They suggest that the perovskites used will need to be tuned so that they have greater IR absorption [200].

### **11.3 Assessment protocol: DSC stability tests initially**

Much information can be gained from stability studies of the DSCs and organic solar cells. The stability on DSCs has come a long way, with harsh testing environments. This can be ascertained when reading a recent review paper of cells undergoing accelerated testing [20]: long term with full sunlight illumination, as well as outdoor testing of modules, and testing different electrolytes such as  $\gamma$ -butyrolactone and the dye  $C_{42}H_{52}N_6O_4RuS_2$  (Z907) at 95°C. Reverse bias stress on modules was carried out by the group of Aldo di Carlo [201,202].

In their documentation, they carried out harsh testing of over 250 mA reverse bias stress on DSCs showing a drop in the fill factor to be the main problem.

Raman spectroscopy and photo-spectroscopy were carried out in order to clarify the degradation mechanism which exhibited tri-iodide bleaching and strong interactions of triiodide with dye-thiocyanate groups.

Harsh high-temperature long-term stability testing has also been performed with liquid DSCs in our group at Demokritos for DSCs [24,27,203], which needs to also be implemented with PSC assessment.

Looking at the tools available to be used for polymer solar cells, a large number would be beneficial for observing the degradation mechanisms in PSCs (see Table 1 in Ref. [204]).

Such thorough characterization can be applied to PSCs for simulating real time stress conditions. A very good progress report on thin film solar cell stress testing criteria could also be implemented to develop an understanding for an initial PSC standard [205].

A paper was published on the assessment of bulk heterojunction organic solar cells under harsh temperature and lighting conditions (1 sun/60-70°C/ $N_2$  environment), which demonstrated lifetimes of 3000-5000 h, with a reduction of nearly 55% efficiency, although in one circumstance, the device in combination with one of the materials they assessed, lost more than 60% of performance after 500 h [206].

In an organic solar cell stability study, morphology evolution can affect stability, and such a review was conducted to identify what was implemented to address this issue [207].

Various reviews have also been written for DSC research, which also include their degradation mechanisms, module performance, limitations and commercial potential, as well as many other useful topics related to stability [23,47,208]

Among the many procedures that are available, one could devise additional testing protocols that may not currently be in use.

It is common for academic groups to only select a few of the tests that stability testing protocols recommend for industrial use. So, checking and tailoring it to suit the technology are important.

High temperature ageing tests in the dark with different electrolytes, dyes or redox couples have been carried out, which indicate the stress endurance criteria that need to be met [27,209,210]

There are also tests where the HTM is the tin based lead free perovskite [211–213] which indicate it is worth further investigation. The cell uses a dye for the photoabsorber, which would also need testing and incorporating into various protocols.

While there could be many more features to check for PSCs, as a foundation, one can at least start with what is available, and so employing the available tools to characterize them can be implemented to assess how the cell degrades. A general prediction of linear efficiency or other parameter decay after the initial drop or rise that is commonly seen would be useful, and if possible, also predict non-linear changes over time (see Figure 44).

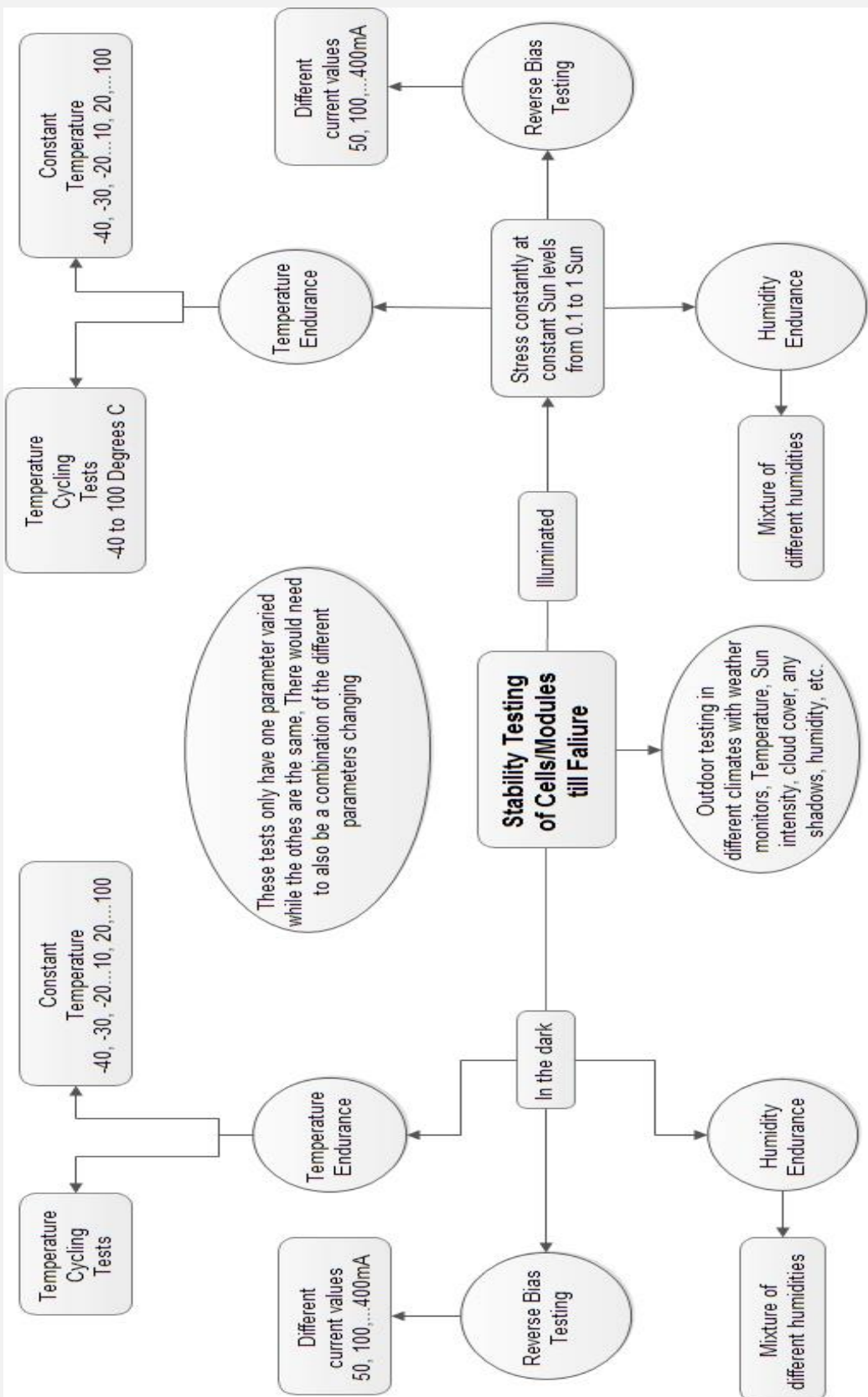


Figure 44: Initial stability test procedure for PSCs

## **11.4 Protocol must include high and low temperature, dark and continuous illumination at different sun levels**

The stress that cells undergo in the real world involves different light levels, variations of humidity levels, and temperature changes which can be extreme, such as those encountered in deserts.

- A tool box where Raman analysis, cyclic voltammetry, photospectroscopy, intensity-modulated photocurrent spectroscopy (IMPS), intensity-modulated photovoltage spectroscopy (IMVS), impedance spectroscopy, to name a few, implemented by different groups will be useful in characterizing the aging mechanisms, and accelerate the commercialization of this technology; such a toolbox was recommended for DSC stability testing [20], so why not PSCs too?
- A testing duration for up to a year will be a good start, observing PSC efficiency and monitoring at which point the cell loses more than 10% of its initial efficiency.

At present, researchers are still trying to understand the various operational mechanisms of different PSCs, employing theory and other spectrometric methods; the ageing may help to provide more information for them.

### **11.4.1 Tests in the dark**

Tests in the dark will be a way to isolate how the cells behave with regard to temperature alone.

- Identifying differences and effects of holding batches of cells at different temperatures: one set at RT with a temperature and humidity monitor, to correlate changes in combination with the effects seen on the parameters of the cells.
- Temperature cycling from -40 to 95°C simulating the harsh environments that some solar panels could experience, for example, spacecraft or research stations in the Antarctic, or deserts such as the Sahara where it is hot during the day and very cold at night.
- In all cases of testing, the measurements of the radiation levels would range from zero to 1 solar illumination, possibly greater if the facilities can produce such lighting for obtaining different efficiencies.

### **11.4.2 Tests with illumination**

- Undertaking tests at RT first in combination with different solar intensities, starting from 0.1 sun. Each test getting harsher, by increasing the solar illumination by a set amount, and then followed by a combination of elevated or lower temperatures, with low to high sun levels, keeping each parameter constant whilst measuring the effect.
  - For example, holding a cell/module at -30°C with 0.5 sun illumination for a year, and measuring its performance at all variations of solar intensities whilst carrying out other tests.
  - Cycling temperatures at continuous illumination levels, e.g., having a cell at 1 sun and increasing the temperature from -30°C to 90°C.

- Cycling temperatures with different sun levels:
  - Tests above 1 sun: as there are solar plant facilities where they focus the light in a particular module, as this has been found to be more efficient; one such company has noted very high efficiencies with their 36.4% silicon solar module with a solar concentrator mechanism [214].
- Outdoor testing is one of the areas that needs to be carried out in different regions' measurement of the weather conditions, in order to observe the real-life performance. This would require a database of the different environmental conditions of the regions around the world, which the cells or solar panels would need to be tested for.

#### **11.4.3 Changes in humidity**

In all the above, it would be good to incorporate tests with the parameter of the percentage of humidity involved, since PSCs are very sensitive to moisture, again, keeping other parameters constant, and testing under various water vapour levels from 0 to 100%, using condensing, as well as non-condensing environments.

#### **11.4.4 Reverse bias testing of PSCs**

Reverse bias testing of PSCs needs to be carried out such that if a part of a module was covered, the other section would be affected, and ageing would occur. This would be useful to observe the effect of different sun levels on the parts of the same cell.

If possible, one should investigate the effects of various intensities of current flow over different temperature ranges, as this would also be of use in simulating the effect that may happen in different climates with modules in positions such that they are only partly illuminated (e.g., clouds passing overhead, tree branches over urban installations).

#### **11.4.5 Open source stability modelling idea**

The author believes that it would significantly help groups around the world if the theoretical departments of each team in the research centres teamed up to produce a simulation of the most efficient, stable and environmentally friendly, perovskite crystal structure, as well as the other elements of the cell, such as the optional HTM, blocking layer, including the band gaps and crystal structures, as well as ionic radii and hole transport properties.

If a free GNU open software program could be created to fulfil the above sub-sections on assessment protocols, then this would accelerate progress of the research teams in focusing their investigations towards applications to the relevant areas predicted by the software. Like all models, however, this would not necessarily be able to cover all device structures, unless it was designed for that purpose. It would need to have flexibility programmed into it; this way, properties could be added, and being open source, would also have groups checking the accuracy of the information, debugging the software, and contributing to it to keep it up to date.

In general, the map of the program should contain something like the structure below:

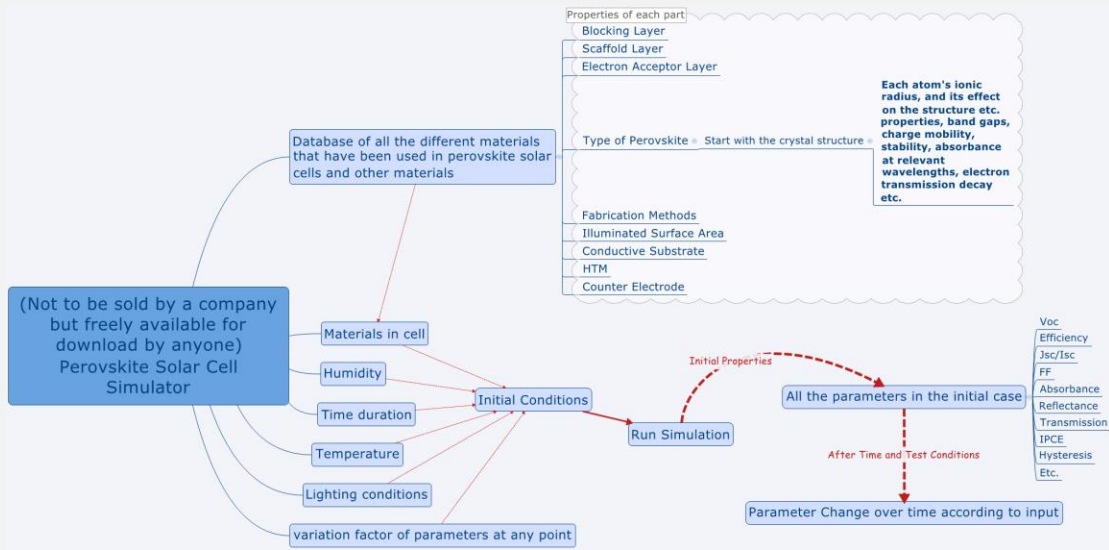


Figure 45: Recommended open source solar cell simulator program with parameters and stability

The stress tests which would be included in the program would need to be backed up by studies; thus, further research focusing on stability, rather than efficiency, will need to be performed. Once degradation mechanisms are further understood, researching on how to improve the efficiency can be then be carried out. The plethora of materials available and discoveries in literature, which highlight various efficiency enhancement techniques, will aid in creating stable, inexpensive, efficient, solar devices.

There is a perspective paper which highlights the need for real life practical testing of PSCs [141], using information from IEC tests and other protocols: electrode performance, different layers of materials and atmospheres involved, various intensities of illumination, multiple temperatures, etc. In order to identify the degradation mechanisms that would need to be assessed with this technology, they examine the external factors which would need to be taken into consideration, such as harsh sand winds eroding the cells, soiling and pollution. As they state ‘There are currently no commonly applied standardized qualification tests for mechanical wear (such as erosion due to blown sand), soiling and pollution, though evaluations are being performed for the development of future standards.’ Other environmental areas needed for testing, illumination and atmospheric testing with and without electrical load. Further evaluations, which are similar to technical assay standards described in various reports, will also need to be incorporated so that one can evaluate how well they perform in real life scenarios, which is also emphasized in the above works [139–142].

## 11.5 Summary of section 11

Commercialization of PCS is possible if they have potentially lower costs. It is still vital that stability should be a focus of photovoltaic research, otherwise the vision of PSC becoming a reality will not come to fruition. Government incentives can help with cost recovery, and the potentially lowered expenses in the materials that are used in PCS can contribute to this aim.

Looking at where solar cells are going to be used in the world and how they will perform will also be important and this has been assessed using a tool called SMARTS.

Theoretical investigations have been utilized in helping scientists find means to stabilize systems. In perovskites, they have been employed to determine how the energies in crystal structures are affected. Hypothetically, greater intrinsic stability is found in certain crystal structures, as well as from calculations of lattice defects in perovskites.

How the perovskite connects to the ETL/HTM has been modelled in an effort to understand its degradation; mechanisms of decomposition have been simulated in other studies in order to gain knowledge on its stability. Properties of different ions, such as their ionic radius and its effect on the perovskite, are used in conceptual studies, which help to clarify how stability can be improved.

In carrying out stability testing, solar cell research groups/industry will need to use various stability tests from silicon and thin film technology for perovskites. Also, DSC architecture, which shares similar properties to that of PSCs, can have its stability assessments applied to PSCs.

All sorts of analyses will be required:

- Temperature
- Illumination
- Humidity
- Atmospheres
- Electrical load

It would be important having this data in a system to exist freely for all scientists, so that modelling can be applied to elucidate how certain parameter combinations would perform, e.g., harsh climate like sandstorms or cold and ice with various cell architectures.

Again, it is key that research groups begin to focus on stability, rather than boosting efficiency, and that without there having been any significant leap in knowledge of this topic, PSC technology will be only limited to the laboratory.

## 12 Conclusion

Since as early as 2009, perovskites have been used as photosensitizers, with the potential for being included as solar cells in BIPV.

Recently, the scientific community has begun to focus on the issue of stability for PSCs for the industry; this is positive, as the performance alone does not mean anything without it. Some recent advances have been made in the understanding of the theory, as well as phenomenological studies, which help with the selection of other elements, for the production of various perovskites with higher intrinsic stability.

Metal toxicity needs to be addressed in perovskite solar cells, with lead-free alternatives. The recent discovery of tin perovskite being more dangerous than lead due to its higher instability after its decomposition into different chemicals has suggested that we need other alternatives to perovskite photoabsorbers, unless they can be prevented from undergoing decomposition, and while a few substitutes have been found which have

potential, there is still a lot of work to be done in synthesis and computation for other properties, ideally in order to discover materials which are intrinsically stable, to produce decent performance.

There are numerous ways to stabilize perovskites: from adding different chemicals after the initial layer, to adding a mixture of different precursors and halides; containing different cations and anions, to be more intrinsically/resilient to ambient environments.

Measures to avoid degradation resulting from humidity require understanding of the mechanisms involved with the parameters of light, humidity, and various atmospheres. Ways to prevent such phenomena through various layers, dopants, and other ideas have been suggested, such as sealing the solar cell in different ways, and implementing carbon as protection against humidity. There are different metal oxides employed, functioning as a buffer against photocatalysis, or being a barrier minimizing the effects of humidity, such as  $\text{Al}_2\text{O}_3$ . Deposition techniques, such as ALD in applying  $\text{Al}_2\text{O}_3$  as an obstacle to humidity, have been found to be advantageous, although manufacturing via this deposition method in industry may be a problem.

Spiro-MeOTAD, which is the standard HTM of most laboratories worldwide has issues with stability, as well as being very costly. Investigations regarding doping various HTMs with different materials have been performed, and each HTM may need a different concentration of materials and dopants to be made more stable. Understanding the role of dopants, which are used in conjunction with HTMs, and the effect of the different environments on their stability, also help towards progressing this technology, to commercialization.

Many groups have worked on much cheaper alternatives to Spiro-MeOTAD, which have comparable performance, although their availability for purchase is limited at the present time of writing. To prevent stability, and issues of extra expense, some groups fabricate cells without the HTM; their tests indicated promising results, and while performance is not as good, it shows potential for further investigation.

Different structures of and within solar cells (nanorods/nanotubes, surfaces, perovskite layer quality, interface with respect to the perovskite and HTM) affect performance and stability, with hydrophobic and hydrophilic aspects offering different advantages in each case. Various techniques to fabricate the perovskite layers and improve the stability have been suggested as each have their impact on the quality of the perovskite layer and its sensitivity to the environment.

The *IV* scans of solar cells in perovskites showing hysteresis also show links to the solar cell structure, and some promising fabrication techniques can minimize the effects. It is at present believed to be due to cation and anion migration during the flow of current, mesoporous structures being more stable in this regard.

Mechanical testing of cells is also important for electrodes and substrates, and how this affects perovskite performance; as a result, different materials need to be investigated for their efficacy, for objects such as flexible/rigid photovoltaics with PSCs in mind.

Raman measurements have been made of various perovskites, although the common  $\text{CH}_3\text{NH}_3\text{PbI}_3$  would break down upon laser illumination to  $\text{PbI}_2$ . Ways to observe the perovskites with different tools and developing perovskites which do not break down under such measurements, could increase our level of understanding towards more stable materials.

Multiple illumination tests suggest instability resulting from various mechanisms, such as, photocatalysis, cation and anion migration, and degradation of electrode types. Numerous perovskites have varying abilities to endure concentrated radiation levels such as 40 to 100-fold solar intensity, e.g., a perovskite device architecture FTO/TiO<sub>2</sub>/CH<sub>3</sub>NH<sub>3</sub>PbI<sub>3</sub>/OMeTad/Au, in air/<= 80°C/≈ 40% humidity having photocurrent at 0.29 A/cm<sup>2</sup> dropping to 0.24 A/cm<sup>2</sup> in a couple of hours, followed by a gradual decline, or a P3HT device under 40SE goes from dark brown to yellow over a period of hours whereas at 0.25SE this change took a number of days.

Several stress testing methods have been applied, and during the time of writing this review, one has been specified for PSCs, showing promise for translating this technology from the laboratory through to the end user; assessments would be enhanced by additional measures indicated in the current review paper. It would be important to have some specialized evaluations for this type of material, in terms of efficiency and stability.

A recommendation for a free, open source, stability prediction and efficiency testing software platform, accessible for researchers worldwide, is also recommended in assisting scientists to decide which direction of exploration to embark upon.

This review has covered various areas where research communities have carried out stability investigations. This involved different materials, layers, electrodes, dopants, experimenting with sealing methods, illumination conditions, intrinsic and external humidity resistance, theory and more. Many review papers have been written which investigate these areas in more detail, some of which are referenced. It is hoped that the reader will become more aware of these topics, so that he/she can decide in which direction to pursue his/her goals.

It should be borne in mind that the priority now is stability; i.e., to use real world test conditions, which would ensure that the cells, which eventually progress/evolve to panels, which are developed, will be suitable for their application in the environment in which they will be used. We as a community are responsible for achieving this, to try to focus the research on this topic, and to work together as a team; it is within our reach, and with this at the forefront of our minds, our own imagination is the limit!

## Acknowledgements

The research leading to these results has received funding from the European Union Seventh Framework Programme [FP7/2007-2013] under grant agreement 316494.

I would like to thank my supervisor Dr P. Falaras and other academic staff including Dr A.G. Kontos, who supported me in producing this review paper, and Andreas Georgiou for help and advice. I would also like to thank Andrew Kourdoulos for critical reading of the manuscript and suggestions/writing assistance.

## Bibliography

- [1] Worldometers.info, Worldometers, Dover, Delaware, U.S.A. (2018).  
<http://www.worldometers.info/faq/> (accessed June 19, 2018).
- [2] A. Louwen, W. van Sark, R. Schropp, A. Faaij, A cost roadmap for silicon heterojunction solar cells, Sol. Energy Mater. Sol. Cells. 147 (2016) 295–314.  
doi:10.1016/j.solmat.2015.12.026.

- [3] M. Cai, Y. Wu, H. Chen, X. Yang, Y. Qiang, L. Han, Cost-Performance Analysis of Perovskite Solar Modules, *Adv. Sci.* 4 (2017) 1–6.  
doi:10.1002/advs.201600269.
- [4] J. Kalowekamo, E. Baker, Estimating the manufacturing cost of purely organic solar cells, *Sol. Energy.* 83 (2009) 1224–1231. doi:10.1016/j.solener.2009.02.003.
- [5] S. Mozaffari, M.R. Nateghi, M.B. Zarandi, An overview of the Challenges in the commercialization of dye sensitized solar cells, *Renew. Sustain. Energy Rev.* 71 (2017) 675–686. doi:10.1016/j.rser.2016.12.096.
- [6] J.B. Baxter, Commercialization of dye sensitized solar cells: Present status and future research needs to improve efficiency, stability, and manufacturing, *J. Vac. Sci. Technol. A Vac. Surf. Film.* 30 (2012) 020801. doi:10.1116/1.3676433.
- [7] N.L. Chang, A.W.Y. Ho-Baillie, D. Vak, M. Gao, M.A. Green, R.J. Egan, Manufacturing cost and market potential analysis of demonstrated roll-to-roll perovskite photovoltaic cell processes, *Sol. Energy Mater. Sol. Cells.* 174 (2018) 314–324. doi:10.1016/j.solmat.2017.08.038.
- [8] R.E. Beal, D.J. Slotcavage, T. Leijtens, A.R. Bowring, R.A. Belisle, W.H. Nguyen, G.F. Burkhardt, E.T. Hoke, M.D. McGehee, Cesium Lead Halide Perovskites with Improved Stability for Tandem Solar Cells, *J. Phys. Chem. Lett.* 7 (2016) 746–751. doi:10.1021/acs.jpclett.6b00002.
- [9] A.-L. Anderson, S. Chen, L. Romero, I. Top, R. Binions, Thin Films for Advanced Glazing Applications, *Buildings.* 6 (2016) 37. doi:10.3390/buildings6030037.
- [10] G.E. Eperon, V.M. Burlakov, A. Goriely, H.J. Snaith, Neutral Color Semitransparent Microstructured Perovskite Solar Cells, *ACS Nano.* 8 (2014) 591–598. doi:10.1021/nn4052309.
- [11] K. Kapsis, V. Dermardiros, A.K. Athienitis, Daylight Performance of Perimeter Office Façades utilizing Semi-transparent Photovoltaic Windows: A Simulation Study, *Energy Procedia.* 78 (2015) 334–339. doi:10.1016/j.egypro.2015.11.657.
- [12] H. Yuan, W. Wang, D. Xu, Q. Xu, J. Xie, X. Chen, T. Zhang, C. Xiong, Y. He, Y. Zhang, Y. Liu, H. Shen, Outdoor testing and ageing of dye-sensitized solar cells for building integrated photovoltaics, *Sol. Energy.* 165 (2018) 233–239. doi:10.1016/j.solener.2018.03.017.
- [13] S. Mathew, A. Yella, P. Gao, R. Humphry-Baker, B.F.E. Curchod, N. Ashari-Astani, I. Tavernelli, U. Rothlisberger, M.K. Nazeeruddin, M. Grätzel, Dye-sensitized solar cells with 13% efficiency achieved through the molecular engineering of porphyrin sensitizers, *Nat. Chem.* 6 (2014) 242–247. doi:10.1038/nchem.1861.
- [14] K. Kakiage, Y. Aoyama, T. Yano, K. Oya, J. Fujisawa, M. Hanaya, Highly-efficient dye-sensitized solar cells with collaborative sensitization by silyl-anchor and carboxy-anchor dyes, *Chem. Commun.* 51 (2015) 15894–15897. doi:10.1039/C5CC06759F.
- [15] Y. Dkhissi, F. Huang, S. Rubanov, M. Xiao, U. Bach, L. Spiccia, R.A. Caruso, Y.-B. Cheng, Low temperature processing of flexible planar perovskite solar cells with efficiency over 10%, *J. Power Sources.* 278 (2015) 325–331. doi:10.1016/j.jpowsour.2014.12.104.

- [16] K. Hara, H. Arakawa, *Handbook of Photovoltaic Science and Engineering*, John Wiley & Sons, Ltd, Chichester, UK, 2003. doi:10.1002/0470014008.
- [17] M.I. Asghar, *Stability Issues of Dye Solar Cells*, Aalto University, 2012. <http://lib.tkk.fi/Diss/2012/isbn9789526046112/isbn9789526046112.pdf> (accessed February 6, 2017).
- [18] S. Hassing, K.D. Jernshøj, P.T. Nguyen, T. Lund, Investigation of the Stability of the Ruthenium-Based Dye (N719) Utilizing the Polarization Properties of Dispersive Raman Modes and/or of the Fluorescent Emission, *J. Phys. Chem. C.* 117 (2013) 23500–23506. doi:10.1021/jp406596p.
- [19] N. Kato, Y. Takeda, K. Higuchi, A. Takeichi, E. Sudo, H. Tanaka, T. Motohiro, T. Sano, T. Toyoda, Degradation analysis of dye-sensitized solar cell module after long-term stability test under outdoor working condition, *Sol. Energy Mater. Sol. Cells.* 93 (2009) 893–897. doi:10.1016/j.solmat.2008.10.022.
- [20] N. Jiang, T. Sumitomo, T. Lee, A. Pellarque, O. Bellon, D. Milliken, H. Desilvestro, High temperature stability of dye solar cells, *Sol. Energy Mater. Sol. Cells.* 119 (2013) 36–50. doi:10.1016/j.solmat.2013.04.017.
- [21] A.J. Huckaba, A. Yella, P. Brogdon, J. Scott Murphy, M.K. Nazeeruddin, M. Grätzel, J.H. Delcamp, A low recombination rate indolizine sensitizer for dye-sensitized solar cells, *Chem. Commun.* 52 (2016) 8424–8427. doi:10.1039/C6CC02247B.
- [22] X. Qin, Z. Zhao, Y. Wang, J. Wu, Q. Jiang, J. You, Recent progress in stability of perovskite solar cells, *J. Semicond.* 38 (2017) 011002. doi:10.1088/1674-4926/38/1/011002.
- [23] F. Sauvage, A Review on Current Status of Stability and Knowledge on Liquid Electrolyte-Based Dye-Sensitized Solar Cells, *Adv. Chem.* 2014 (2014) 1–23. doi:10.1155/2014/939525.
- [24] T. Stergiopoulos, A.G. Kontos, N. Jiang, D. Milliken, H. Desilvestro, V. Likodimos, P. Falaras, High boiling point solvent-based dye solar cells pass a harsh thermal ageing test, *Sol. Energy Mater. Sol. Cells.* 144 (2016) 457–466. doi:10.1016/j.solmat.2015.09.052.
- [25] T. Stergiopoulos, A.G. Kontos, V. Likodimos, D. Perganti, P. Falaras, Solvent Effects at the Photoelectrode/Electrolyte Interface of a DSC: A Combined Spectroscopic and Photoelectrochemical Study, *J. Phys. Chem. C.* 115 (2011) 10236–10244. doi:10.1021/jp2007864.
- [26] A.G. Kontos, T. Stergiopoulos, G. Tsiminis, Y.S. Raptis, P. Falaras, In situ micro- and macro-Raman investigation of the redox couple behavior in DSSCs, *Inorganica Chim. Acta.* 361 (2008) 761–768. doi:10.1016/j.ica.2007.06.018.
- [27] A.G. Kontos, T. Stergiopoulos, V. Likodimos, D. Milliken, H. Desilvestro, G. Tulloch, P. Falaras, Long-Term Thermal Stability of Liquid Dye Solar Cells, *J. Phys. Chem. C.* 117 (2013) 8636–8646. doi:10.1021/jp400060d.
- [28] H.-S. Kim, C.-R. Lee, J.-H. Im, K.-B. Lee, T. Moehl, A. Marchioro, S.-J. Moon, R. Humphry-Baker, J.-H. Yum, J.E. Moser, M. Grätzel, N.-G. Park, Lead Iodide Perovskite Sensitized All-Solid-State Submicron Thin Film Mesoscopic Solar Cell with Efficiency Exceeding 9%, *Sci. Rep.* 2 (2012) 591. doi:10.1038/srep00591.

- [29] M. Liu, M.B. Johnston, H.J. Snaith, Efficient planar heterojunction perovskite solar cells by vapour deposition, *Nature*. 501 (2013) 395–398. doi:10.1038/nature12509.
- [30] K.-T. Lee, M. Fukuda, S. Joglekar, L.J. Guo, Colored, see-through perovskite solar cells employing an optical cavity, *J. Mater. Chem. C*. 3 (2015) 5377–5382. doi:10.1039/C5TC00622H.
- [31] M. GRÄTZEL, N.-G. PARK, ORGANOMETAL HALIDE PEROVSKITE PHOTOVOLTAICS: A DIAMOND IN THE ROUGH, *Nano*. 09 (2014) 1440002. doi:10.1142/S1793292014400025.
- [32] M. He, D. Zheng, M. Wang, C. Lin, Z. Lin, High efficiency perovskite solar cells: from complex nanostructure to planar heterojunction, *J. Mater. Chem. A*. 2 (2014) 5994. doi:10.1039/c3ta14160h.
- [33] A. Hinsch, W. Veurman, H. Brandt, K. Flarup Jensen, S. Mastroianni, Status of Dye Solar Cell Technology as a Guideline for Further Research, *ChemPhysChem*. 15 (2014) 1076–1087. doi:10.1002/cphc.201301083.
- [34] T.C. Sum, N. Mathews, Advancements in perovskite solar cells: photophysics behind the photovoltaics, *Energy Environ. Sci.* 7 (2014) 2518–2534. doi:10.1039/C4EE00673A.
- [35] S. Patwardhan, D.H. Cao, S. Hatch, O.K. Farha, J.T. Hupp, M.G. Kanatzidis, G.C. Schatz, Introducing Perovskite Solar Cells to Undergraduates, *J. Phys. Chem. Lett.* 6 (2015) 251–255. doi:10.1021/jz502648y.
- [36] P. Gao, M. Grätzel, M.K. Nazeeruddin, Organohalide lead perovskites for photovoltaic applications, *Energy Environ. Sci.* 7 (2014) 2448–2463. doi:10.1039/C4EE00942H.
- [37] P. V. Kamat, Organometal Halide Perovskites for Transformative Photovoltaics, *J. Am. Chem. Soc.* 136 (2014) 3713–3714. doi:10.1021/ja501108n.
- [38] P.K. Nayak, D. Cahen, Updated Assessment of Possibilities and Limits for Solar Cells, *Adv. Mater.* 26 (2014) 1622–1628. doi:10.1002/adma.201304620.
- [39] J. Poppe, S.G. Hickey, A. Eychmüller, Photoelectrochemical Investigations of Semiconductor Nanoparticles and Their Application to Solar Cells, *J. Phys. Chem. C*. 118 (2014) 17123–17141. doi:10.1021/jp5016092.
- [40] J. Burschka, High performance solid-state mesoscopic solar cells, *École Polytechnique Fédérale De Lausanne*, 2013. doi:10.5075/epfl-thesis-6006.
- [41] P. Docampo, S. Guldin, T. Leijtens, N.K. Noel, U. Steiner, H.J. Snaith, Lessons Learned: From Dye-Sensitized Solar Cells to All-Solid-State Hybrid Devices, *Adv. Mater.* 26 (2014) 4013–4030. doi:10.1002/adma.201400486.
- [42] X. Guo, G. Niu, L. Wang, Chemical Stability Issue and Its Research Process of Perovskite Solar Cells with High Efficiency, *Acta Chim. Sin.* 73 (2015) 211. doi:10.6023/A14100687.
- [43] X.L.-X. Zhang Dan-Fei, Zheng Ling-Ling, Ma Ying-Zhuang, Wang Shu-Feng, Bian Zu-Qiang, Huang Chun-Hui, Gong Qi-Huang, D.F. Zhang, L.L. Zheng, Y.Z. Ma, S.F. Wang, Z.Q. Bian, C.H. Huang, Q.H. Gong, L.X. Xiao, Factors influencing the stability of perovskite solar cells, *Acta Phys. Sin.* 64 (2015) 7.

doi:10.7498/aps.64.038803.

- [44] G. Niu, X. Guo, L. Wang, Review of recent progress in chemical stability of perovskite solar cells, *J. Mater. Chem. A*. 3 (2015) 8970–8980.  
doi:10.1039/C4TA04994B.
- [45] P.P. Boix, S. Agarwala, T.M. Koh, N. Mathews, S.G. Mhaisalkar, Perovskite Solar Cells: Beyond Methylammonium Lead Iodide, *J. Phys. Chem. Lett.* 6 (2015) 898–907. doi:10.1021/jz502547f.
- [46] C. Zuo, H.J. Bolink, H. Han, J. Huang, D. Cahen, L. Ding, Advances in Perovskite Solar Cells, *Adv. Sci.* 3 (2016) 1500324. doi:10.1002/advs.201500324.
- [47] M.I. Asghar, K. Miettunen, J. Halme, P. Vahermaa, M. Toivola, K. Aitola, P. Lund, Review of stability for advanced dye solar cells, *Energy Environ. Sci.* 3 (2010) 418. doi:10.1039/b922801b.
- [48] T.M. Koh, B. Febriansyah, N. Mathews, Ruddlesden-Popper Perovskite Solar Cells, *Chem.* 2 (2017) 326–327. doi:10.1016/J.CHEMPR.2017.02.015.
- [49] C. Grätzel, S.M. Zakeeruddin, Recent trends in mesoscopic solar cells based on molecular and nanopigment light harvesters, *Mater. Today*. 16 (2013) 11–18.  
doi:10.1016/j.mattod.2013.01.020.
- [50] J.H. Rhee, C.-C. Chung, E.W.-G. Diau, A perspective of mesoscopic solar cells based on metal chalcogenide quantum dots and organometal-halide perovskites, *NPG Asia Mater.* 5 (2013) e68–e68. doi:10.1038/am.2013.53.
- [51] N.-G. Park, Organometal Perovskite Light Absorbers Toward a 20% Efficiency Low-Cost Solid-State Mesoscopic Solar Cell, *J. Phys. Chem. Lett.* 4 (2013) 2423–2429. doi:10.1021/jz400892a.
- [52] S.P. Singh, P. Nagarjuna, Organometal halide perovskites as useful materials in sensitized solar cells, *Dalt. Trans.* 43 (2014) 5247. doi:10.1039/c3dt53503g.
- [53] S. Gamliel, L. Etgar, Organo-metal perovskite based solar cells: sensitized versus planar architecture, *RSC Adv.* 4 (2014) 29012–29021. doi:10.1039/C4RA03981E.
- [54] H.J. Snaith, Perovskites: The Emergence of a New Era for Low-Cost, High-Efficiency Solar Cells, *J. Phys. Chem. Lett.* 4 (2013) 3623–3630.  
doi:10.1021/jz4020162.
- [55] P.P. Boix, K. Nonomura, N. Mathews, S.G. Mhaisalkar, Current progress and future perspectives for organic/inorganic perovskite solar cells, *Mater. Today*. 17 (2014) 16–23. doi:10.1016/j.mattod.2013.12.002.
- [56] Z. Hameiri, Photovoltaics literature survey (No. 144), *Prog. Photovoltaics Res. Appl.* 26 (2018) 688–693. doi:10.1002/pip.3064.
- [57] C.C. Stoumpos, C.D. Malliakas, M.G. Kanatzidis, Semiconducting Tin and Lead Iodide Perovskites with Organic Cations: Phase Transitions, High Mobilities, and Near-Infrared Photoluminescent Properties, *Inorg. Chem.* 52 (2013) 9019–9038.  
doi:10.1021/ic401215x.
- [58] G. Rose, Mineralogisch geognostische Reise nach dem Ural, dem Altai und dem Kaspischen Meere, Sander, Berlin, 1842. <https://books.google.gr/books?id=Tl1b31r8UwC> (accessed June 23, 2018).
- [59] R.J. Cava, Perovskite structure and derivatives, (n.d.).

<https://www.princeton.edu/~cavalab/tutorials/public/structures/perovskites.html>  
(accessed September 21, 2018).

- [60] Q. Fu, T. He, J.L. Li, G.W. Yang, Band-engineered SrTiO<sub>3</sub> nanowires for visible light photocatalysis, *J. Appl. Phys.* 112 (2012) 104322. doi:10.1063/1.4767229.
- [61] Q. Fu, J.L. Li, T. He, G.W. Yang, Band-engineered CaTiO<sub>3</sub> nanowires for visible light photocatalysis, *J. Appl. Phys.* 113 (2013) 104303. doi:10.1063/1.4794196.
- [62] T.R.N. Kutty, M. Avudaithai, Photocatalysis on Fine Powders of Perovskite Oxides, *Catal. Rev.* 34 (1992) 373–389. doi:10.1080/01614949208016318.
- [63] S. Murugesan, M.N. Huda, Y. Yan, M.M. Al-Jassim, V. (Ravi) Subramanian, Band-Engineered Bismuth Titanate Pyrochlores for Visible Light Photocatalysis, *J. Phys. Chem. C.* 114 (2010) 10598–10605. doi:10.1021/jp906252r.
- [64] F. Deschler, M. Price, S. Pathak, L.E. Klintberg, D.-D. Jarausch, R. Higler, S. Hüttner, T. Leijtens, S.D. Stranks, H.J. Snaith, M. Atatüre, R.T. Phillips, R.H. Friend, High Photoluminescence Efficiency and Optically Pumped Lasing in Solution-Processed Mixed Halide Perovskite Semiconductors, *J. Phys. Chem. Lett.* 5 (2014) 1421–1426. doi:10.1021/jz5005285.
- [65] J. Burschka, N. Pellet, S.-J. Moon, R. Humphry-Baker, P. Gao, M.K. Nazeeruddin, M. Grätzel, Sequential deposition as a route to high-performance perovskite-sensitized solar cells, *Nature*. 499 (2013) 316–319. doi:10.1038/nature12340.
- [66] T. Song, Q. Chen, H. Zhou, C. Jiang, H.-H. Wang, Y. (Michael) Yang, Y. Liu, J. You, Y. Yang, Perovskite solar cells: film formation and properties, *J. Mater. Chem. A*. 3 (2015) 9032–9050. doi:10.1039/C4TA05246C.
- [67] A. Kojima, K. Teshima, Y. Shirai, T. Miyasaka, Organometal Halide Perovskites as Visible-Light Sensitizers for Photovoltaic Cells, *J. Am. Chem. Soc.* 131 (2009) 6050–6051. doi:10.1021/ja809598r.
- [68] I. Chung, B. Lee, J. He, R.P.H. Chang, M.G. Kanatzidis, All-solid-state dye-sensitized solar cells with high efficiency, *Nature*. 485 (2012) 486–489. doi:10.1038/nature11067.
- [69] M.M. Lee, J. Teuscher, T. Miyasaka, T.N. Murakami, H.J. Snaith, Efficient Hybrid Solar Cells Based on Meso-Superstructured Organometal Halide Perovskites, *Science* (80-. ). 338 (2012) 643–647. doi:10.1126/science.1228604.
- [70] W. Li, J. Li, L. Wang, G. Niu, R. Gao, Y. Qiu, Post modification of perovskite sensitized solar cells by aluminum oxide for enhanced performance, *J. Mater. Chem. A*. 1 (2013) 11735. doi:10.1039/c3ta12240a.
- [71] D. Liu, T.L. Kelly, Perovskite solar cells with a planar heterojunction structure prepared using room-temperature solution processing techniques, *Nat. Photonics*. 8 (2014) 133–138. doi:10.1038/nphoton.2013.342.
- [72] J.H. Heo, S.H. Im, J.H. Noh, T.N. Mandal, C.-S. Lim, J.A. Chang, Y.H. Lee, H. Kim, A. Sarkar, M.K. Nazeeruddin, M. Grätzel, S. Il Seok, Efficient inorganic-organic hybrid heterojunction solar cells containing perovskite compound and polymeric hole conductors, *Nat. Photonics*. 7 (2013) 486–491. doi:10.1038/nphoton.2013.80.
- [73] J.A. Christians, P.A. Miranda Herrera, P. V. Kamat, Transformation of the Excited

State and Photovoltaic Efficiency of CH<sub>3</sub>NH<sub>3</sub>PbI<sub>3</sub> Perovskite upon Controlled Exposure to Humidified Air, *J. Am. Chem. Soc.* 137 (2015) 1530–1538. doi:10.1021/ja511132a.

- [74] X. Dong, X. Fang, M. Lv, B. Lin, S. Zhang, J. Ding, N. Yuan, Improvement of the humidity stability of organic–inorganic perovskite solar cells using ultrathin Al<sub>2</sub>O<sub>3</sub> layers prepared by atomic layer deposition, *J. Mater. Chem. A* 3 (2015) 5360–5367. doi:10.1039/C4TA06128D.
- [75] W. Geng, L. Zhang, Y.-N. Zhang, W.-M. Lau, L.-M. Liu, First-Principles Study of Lead Iodide Perovskite Tetragonal and Orthorhombic Phases for Photovoltaics, *J. Phys. Chem. C* 118 (2014) 19565–19571. doi:10.1021/jp504951h.
- [76] S. Aharon, B.-E. El Cohen, L. Etgar, Hybrid Lead Halide Iodide and Lead Halide Bromide in Efficient Hole Conductor Free Perovskite Solar Cell, *J. Phys. Chem. C* 118 (2014) 17160–17165. doi:10.1021/jp5023407.
- [77] J.H. Noh, S.H. Im, J.H. Heo, T.N. Mandal, S. Il Seok, Chemical Management for Colorful, Efficient, and Stable Inorganic–Organic Hybrid Nanostructured Solar Cells, *Nano Lett.* 13 (2013) 1764–1769. doi:10.1021/nl400349b.
- [78] B. Suarez, V. Gonzalez-Pedro, T.S. Ripples, R.S. Sanchez, L. Otero, I. Mora-Sero, Recombination Study of Combined Halides (Cl, Br, I) Perovskite Solar Cells, *J. Phys. Chem. Lett.* 5 (2014) 1628–1635. doi:10.1021/jz5006797.
- [79] F.K. Aldibaja, L. Badia, E. Mas-Marzá, R.S. Sánchez, E.M. Barea, I. Mora-Sero, Effect of different lead precursors on perovskite solar cell performance and stability, *J. Mater. Chem. A* 3 (2015) 9194–9200. doi:10.1039/C4TA06198E.
- [80] Q. Jiang, D. Rebollar, J. Gong, E.L. Piacentino, C. Zheng, T. Xu, Pseudohalide-Induced Moisture Tolerance in Perovskite CH<sub>3</sub>NH<sub>3</sub>Pb(SCN)<sub>2</sub>I Thin Films, *Angew. Chemie Int. Ed.* 54 (2015) 7617–7620. doi:10.1002/anie.201503038.
- [81] S.Y. Dou, L.T. Yan, Y.C. Liu, G. Du, P. Zhou, Preparation and performance of organic–inorganic halide perovskites, *J. Mater. Sci. Mater. Electron.* 24 (2013) 4862–4867. doi:10.1007/s10854-013-1489-3.
- [82] G.E. Eperon, S.D. Stranks, C. Menelaou, M.B. Johnston, L.M. Herz, H.J. Snaith, Formamidinium lead trihalide: a broadly tunable perovskite for efficient planar heterojunction solar cells, *Energy Environ. Sci.* 7 (2014) 982. doi:10.1039/c3ee43822h.
- [83] I.C. Smith, E.T. Hoke, D. Solis-Ibarra, M.D. McGehee, H.I. Karunadasa, A Layered Hybrid Perovskite Solar-Cell Absorber with Enhanced Moisture Stability, *Angew. Chemie Int. Ed.* 53 (2014) 11232–11235. doi:10.1002/anie.201406466.
- [84] H. Tsai, W. Nie, J.C. Blancon, C.C. Stoumpos, R. Asadpour, B. Harutyunyan, A.J. Neukirch, R. Verduzco, J.J. Crochet, S. Tretiak, L. Pedesseau, J. Even, M.A. Alam, G. Gupta, J. Lou, P.M. Ajayan, M.J. Bedzyk, M.G. Kanatzidis, A.D. Mohite, High-efficiency two-dimensional ruddlesden-popper perovskite solar cells, *Nature* 536 (2016) 312–317. doi:10.1038/nature18306.
- [85] C.C. Stoumpos, C.M.M. Soe, H. Tsai, W. Nie, J.-C. Blancon, D.H. Cao, F. Liu, B. Traoré, C. Katan, J. Even, A.D. Mohite, M.G. Kanatzidis, High Members of the 2D Ruddlesden-Popper Halide Perovskites: Synthesis, Optical Properties, and Solar Cells of (CH<sub>3</sub>(CH<sub>2</sub>)<sub>3</sub>NH<sub>3</sub>)<sub>2</sub>(CH<sub>3</sub>NH<sub>3</sub>)<sub>4</sub>Pb<sub>5</sub>I<sub>16</sub>, *Chem.* 2 (2017) 427–440.

- doi:10.1016/J.CHEMPR.2017.02.004.
- [86] S. Lv, S. Pang, Y. Zhou, N.P. Padture, H. Hu, L. Wang, X. Zhou, H. Zhu, L. Zhang, C. Huang, G. Cui, One-step, solution-processed formamidinium lead trihalide ( $\text{FAPbI}_{(3-x)}\text{Cl}_x$ ) for mesoscopic perovskite–polymer solar cells, *Phys. Chem. Chem. Phys.* 16 (2014) 19206–19211. doi:10.1039/C4CP02113D.
- [87] D.P. McMeekin, G. Sadoughi, W. Rehman, G.E. Eperon, M. Saliba, M.T. Horantner, A. Haghhighirad, N. Sakai, L. Korte, B. Rech, M.B. Johnston, L.M. Herz, H.J. Snaith, A mixed-cation lead mixed-halide perovskite absorber for tandem solar cells, *Science* (80-. ). 351 (2016) 151–155. doi:10.1126/science.aad5845.
- [88] L. Peedikakkandy, P. Bhargava, Recrystallization and phase stability study of cesium tin iodide for application as a hole transporter in dye sensitized solar cells, *Mater. Sci. Semicond. Process.* 33 (2015) 103–109. doi:10.1016/j.mssp.2015.01.023.
- [89] A. Fakharuddin, F. Di Giacomo, I. Ahmed, Q. Wali, T.M. Brown, R. Jose, Role of morphology and crystallinity of nanorod and planar electron transport layers on the performance and long term durability of perovskite solar cells, *J. Power Sources.* 283 (2015) 61–67. doi:10.1016/j.jpowsour.2015.02.084.
- [90] D. Bi, G. Boschloo, S. Schwarzmüller, L. Yang, E.M.J. Johansson, A. Hagfeldt, Efficient and stable  $\text{CH}_3\text{NH}_3\text{PbI}_3$ -sensitized  $\text{ZnO}$  nanorod array solid-state solar cells, *Nanoscale*. 5 (2013) 11686. doi:10.1039/c3nr01542d.
- [91] F.J. Ramos, D. Cortes, A. Aguirre, F.J. Castano, S. Ahmad, Fabrication and encapsulation of perovskites sensitized solid state solar cells, in: 2014 IEEE 40th Photovolt. Spec. Conf., IEEE, 2014: pp. 2584–2587. doi:10.1109/PVSC.2014.6925459.
- [92] F. Hao, C.C. Stoumpos, D.H. Cao, R.P.H. Chang, M.G. Kanatzidis, R.P.H.C.& M.G.K. Feng Hao, Constantinos C. Stoumpos, Duyen Hanh Cao, Lead-free solid-state organic–inorganic halide perovskite solar cells, *Nat. Photonics.* 8 (2014) 489–494. doi:10.1038/nphoton.2014.82.
- [93] Y. Han, S. Meyer, Y. Dkhissi, K. Weber, J.M. Pringle, U. Bach, L. Spiccia, Y.-B. Cheng, Degradation observations of encapsulated planar  $\text{CH}_3\text{NH}_3\text{PbI}_3$  perovskite solar cells at high temperatures and humidity, *J. Mater. Chem. A.* 3 (2015) 8139–8147. doi:10.1039/C5TA00358J.
- [94] Z. Ku, Y. Rong, M. Xu, T. Liu, H. Han, Full Printable Processed Mesoscopic  $\text{CH}_3\text{NH}_3\text{PbI}_3/\text{TiO}_2$  Heterojunction Solar Cells with Carbon Counter Electrode, *Sci. Rep.* 3 (2013) 3132. doi:10.1038/srep03132.
- [95] A. Mei, X. Li, L. Liu, Z. Ku, T. Liu, Y. Rong, M. Xu, M. Hu, J. Chen, Y. Yang, M. Gratzel, H. Han, A hole-conductor-free, fully printable mesoscopic perovskite solar cell with high stability, *Science* (80-. ). 345 (2014) 295–298. doi:10.1126/science.1254763.
- [96] X. Liu, H. Yu, L. Yan, Q. Dong, Q. Wan, Y. Zhou, B. Song, Y. Li, Triple Cathode Buffer Layers Composed of PCBM, C 60 , and LiF for High-Performance Planar Perovskite Solar Cells, *ACS Appl. Mater. Interfaces.* 7 (2015) 6230–6237. doi:10.1021/acsami.5b00468.

- [97] S. Guarnera, A. Abate, W. Zhang, J.M. Foster, G. Richardson, A. Petrozza, H.J. Snaith, Improving the Long-Term Stability of Perovskite Solar Cells with a Porous Al<sub>2</sub>O<sub>3</sub> Buffer Layer, *J. Phys. Chem. Lett.* 6 (2015) 432–437. doi:10.1021/jz502703p.
- [98] B. Hwang, J. Lee, Hybrid Organic-Inorganic Perovskite Memory with Long-Term Stability in Air, *Sci. Rep.* 7 (2017) 673. doi:10.1038/s41598-017-00778-5.
- [99] X. Gao, J. Li, J. Baker, Y. Hou, D. Guan, J. Chen, C. Yuan, Enhanced photovoltaic performance of perovskite CH<sub>3</sub>NH<sub>3</sub>PbI<sub>3</sub> solar cells with freestanding TiO<sub>2</sub> nanotube array films, *Chem. Commun.* 50 (2014) 6368–6371. doi:10.1039/C4CC01864H.
- [100] L. Loh, J. Briscoe, S. Dunn, Perovskite enhanced solid state ZnO solar cells, *J. Phys. Conf. Ser.* 476 (2013) 012008. doi:10.1088/1742-6596/476/1/012008.
- [101] J. Yang, B.D. Siempelkamp, D. Liu, T.L. Kelly, Investigation of CH<sub>3</sub>NH<sub>3</sub>PbI<sub>3</sub> Degradation Rates and Mechanisms in Controlled Humidity Environments Using in Situ Techniques, *ACS Nano.* 9 (2015) 1955–1963. doi:10.1021/nn506864k.
- [102] F. Hao, C.C. Stoumpos, R.P.H. Chang, M.G. Kanatzidis, Anomalous Band Gap Behavior in Mixed Sn and Pb Perovskites Enables Broadening of Absorption Spectrum in Solar Cells, *J. Am. Chem. Soc.* 136 (2014) 8094–8099. doi:10.1021/ja5033259.
- [103] W. Li, H. Dong, L. Wang, N. Li, X. Guo, J. Li, Y. Qiu, Montmorillonite as bifunctional buffer layer material for hybrid perovskite solar cells with protection from corrosion and retarding recombination, *J. Mater. Chem. A.* 2 (2014) 13587–13592. doi:10.1039/C4TA01550A.
- [104] A.D. Sheikh, A. Bera, M.A. Haque, R.B. Rakhi, S. Del Gobbo, H.N. Alshareef, T. Wu, Atmospheric effects on the photovoltaic performance of hybrid perovskite solar cells, *Sol. Energy Mater. Sol. Cells.* 137 (2015) 6–14. doi:10.1016/j.solmat.2015.01.023.
- [105] D. BI, G. BOSCHLOO, A. HAGFELDT, HIGH-EFFICIENT SOLID-STATE PEROVSKITE SOLAR CELL WITHOUT LITHIUM SALT IN THE HOLE TRANSPORT MATERIAL, *Nano.* 09 (2014) 1440001. doi:10.1142/S1793292014400013.
- [106] B. Xu, J. Huang, H. Ågren, L. Kloo, A. Hagfeldt, L. Sun, AgTFSI as p-Type Dopant for Efficient and Stable Solid-State Dye-Sensitized and Perovskite Solar Cells, *ChemSusChem.* 7 (2014) 3252–3256. doi:10.1002/cssc.201402678.
- [107] L. Badia, E. Mas-Marzá, R.S. Sánchez, E.M. Barea, J. Bisquert, I. Mora-Seró, New iridium complex as additive to the spiro-OMeTAD in perovskite solar cells with enhanced stability, *APL Mater.* 2 (2014) 081507. doi:10.1063/1.4890545.
- [108] Y. Zhang, W. Liu, F. Tan, Y. Gu, The essential role of the poly(3-hexylthiophene) hole transport layer in perovskite solar cells, *J. Power Sources.* 274 (2015) 1224–1230. doi:10.1016/j.jpowsour.2014.10.145.
- [109] J. Liu, Y. Wu, C. Qin, X. Yang, T. Yasuda, A. Islam, K. Zhang, W. Peng, W. Chen, L. Han, A dopant-free hole-transporting material for efficient and stable perovskite solar cells, *Energy Environ. Sci.* 7 (2014) 2963–2967. doi:10.1039/C4EE01589D.

- [110] M. Seetharaman S, P. Nagarjuna, P.N. Kumar, S.P. Singh, M. Deepa, M.A.G. Namboothiry, Efficient organic–inorganic hybrid perovskite solar cells processed in air, *Phys. Chem. Chem. Phys.* 16 (2014) 24691–24696. doi:10.1039/C4CP03726J.
- [111] M. Zhang, M. Lyu, H. Yu, J.-H. Yun, Q. Wang, L. Wang, Stable and Low-Cost Mesoscopic CH<sub>3</sub>NH<sub>3</sub>PbI<sub>2</sub>Br Perovskite Solar Cells by using a Thin Poly(3-hexylthiophene) Layer as a Hole Transporter, *Chem. - A Eur. J.* 21 (2015) 434–439. doi:10.1002/chem.201404427.
- [112] Y.S. Kwon, J. Lim, H.-J. Yun, Y.-H. Kim, T. Park, A diketopyrrolopyrrole-containing hole transporting conjugated polymer for use in efficient stable organic–inorganic hybrid solar cells based on a perovskite, *Energy Environ. Sci.* 7 (2014) 1454. doi:10.1039/c3ee44174a.
- [113] B. Cai, Y. Xing, Z. Yang, W.-H. Zhang, J. Qiu, High performance hybrid solar cells sensitized by organolead halide perovskites, *Energy Environ. Sci.* 6 (2013) 1480. doi:10.1039/c3ee40343b.
- [114] H. Choi, S. Park, S. Paek, P. Ekanayake, M.K. Nazeeruddin, J. Ko, Efficient star-shaped hole transporting materials with diphenylethenyl side arms for an efficient perovskite solar cell, *J. Mater. Chem. A.* 2 (2014) 19136–19140. doi:10.1039/C4TA04179H.
- [115] Y. Ma, Y.-H. Chung, L. Zheng, D. Zhang, X. Yu, L. Xiao, Z. Chen, S. Wang, B. Qu, Q. Gong, D. Zou, Improved Hole-Transporting Property via HAT-CN for Perovskite Solar Cells without Lithium Salts, *ACS Appl. Mater. Interfaces.* 7 (2015) 6406–6411. doi:10.1021/acsami.5b00149.
- [116] S. Lv, L. Han, J. Xiao, L. Zhu, J. Shi, H. Wei, Y. Xu, J. Dong, X. Xu, D. Li, S. Wang, Y. Luo, Q. Meng, X. Li, Mesoscopic TiO<sub>2</sub>/CH<sub>3</sub>NH<sub>3</sub>PbI<sub>3</sub> perovskite solar cells with new hole-transporting materials containing butadiene derivatives, *Chem. Commun.* 50 (2014) 6931. doi:10.1039/c4cc02211d.
- [117] K. Neumann, M. Thelakkat, Perovskite solar cells involving poly(tetraphenylbenzidine)s: investigation of hole carrier mobility, doping effects and photovoltaic properties, *RSC Adv.* 4 (2014) 43550–43559. doi:10.1039/C4RA05564K.
- [118] J.A. Christians, P. Schulz, J.S. Tinkham, T.H. Schloemer, S.P. Harvey, B.J. Tremolet de Villers, A. Sellinger, J.J. Berry, J.M. Luther, Tailored interfaces of unencapsulated perovskite solar cells for >1,000 hour operational stability, *Nat. Energy.* 3 (2018) 68–74. doi:10.1038/s41560-017-0067-y.
- [119] J.A. Christians, R.C.M. Fung, P. V. Kamat, An Inorganic Hole Conductor for Organo-Lead Halide Perovskite Solar Cells. Improved Hole Conductivity with Copper Iodide, *J. Am. Chem. Soc.* 136 (2014) 758–764. doi:10.1021/ja411014k.
- [120] L. Meng, J. You, T.-F. Guo, Y. Yang, Recent Advances in the Inverted Planar Structure of Perovskite Solar Cells, *Acc. Chem. Res.* 49 (2016) 155–165. doi:10.1021/acs.accounts.5b00404.
- [121] J.H. Kim, P.-W. Liang, S.T. Williams, N. Cho, C.-C. Chueh, M.S. Glaz, D.S. Ginger, A.K.-Y. Jen, High-Performance and Environmentally Stable Planar Heterojunction Perovskite Solar Cells Based on a Solution-Processed Copper-

- Doped Nickel Oxide Hole-Transporting Layer, *Adv. Mater.* 27 (2015) 695–701. doi:10.1002/adma.201404189.
- [122] S. Aharon, S. Gamliel, B. El Cohen, L. Etgar, Depletion region effect of highly efficient hole conductor free  $\text{CH}_3\text{NH}_3\text{PbI}_3$  perovskite solar cells, *Phys. Chem. Chem. Phys.* 16 (2014) 10512–10518. doi:10.1039/C4CP00460D.
  - [123] F. Zhang, X. Yang, H. Wang, M. Cheng, J. Zhao, L. Sun, Structure Engineering of Hole-Conductor Free Perovskite-Based Solar Cells with Low-Temperature-Processed Commercial Carbon Paste As Cathode, *ACS Appl. Mater. Interfaces.* 6 (2014) 16140–16146. doi:10.1021/am504175x.
  - [124] F.X. Xie, D. Zhang, H. Su, X. Ren, K.S. Wong, M. Grätzel, W.C.H. Choy, Vacuum-Assisted Thermal Annealing of  $\text{CH}_3\text{NH}_3\text{PbI}_3$  for Highly Stable and Efficient Perovskite Solar Cells, *ACS Nano.* 9 (2015) 639–646. doi:10.1021/nn505978r.
  - [125] K. Wu, A. Kogo, N. Sakai, M. Ikegami, T. Miyasaka, High Efficiency and Robust Performance of Organo Lead Perovskite Solar Cells with Large Grain Absorbers Prepared in Ambient Air Conditions, *Chem. Lett.* 44 (2015) 321–323. doi:10.1246/cl.140919.
  - [126] S. Ito, S. Tanaka, H. Vahlman, H. Nishino, K. Manabe, P. Lund, Carbon-Double-Bond-Free Printed Solar Cells from  $\text{TiO}_2/\text{CH}_3\text{NH}_3\text{PbI}_3/\text{CuSCN}/\text{Au}$ : Structural Control and Photoaging Effects, *ChemPhysChem.* 15 (2014) 1194–1200. doi:10.1002/cphc.201301047.
  - [127] J. Zhang, Z. Hu, L. Huang, G. Yue, J. Liu, X. Lu, Z. Hu, M. Shang, L. Han, Y. Zhu, Bifunctional alkyl chain barriers for efficient perovskite solar cells, *Chem. Commun.* 51 (2015) 7047–7050. doi:10.1039/C5CC00128E.
  - [128] J.H. Kim, S.T. Williams, N. Cho, C.-C. Chueh, A.K.-Y. Jen, Enhanced Environmental Stability of Planar Heterojunction Perovskite Solar Cells Based on Blade-Coating, *Adv. Energy Mater.* 5 (2015) 1401229. doi:10.1002/aenm.201401229.
  - [129] W. Zhu, T. Yu, F. Li, C. Bao, H. Gao, Y. Yi, J. Yang, G. Fu, X. Zhou, Z. Zou, A facile, solvent vapor–fumigation-induced, self-repair recrystallization of  $\text{CH}_3\text{NH}_3\text{PbI}_3$  films for high-performance perovskite solar cells, *Nanoscale.* 7 (2015) 5427–5434. doi:10.1039/C5NR00225G.
  - [130] P. Luo, Z. Liu, W. Xia, C. Yuan, J. Cheng, Y. Lu, Uniform, Stable, and Efficient Planar-Heterojunction Perovskite Solar Cells by Facile Low-Pressure Chemical Vapor Deposition under Fully Open-Air Conditions, *ACS Appl. Mater. Interfaces.* 7 (2015) 2708–2714. doi:10.1021/am5077588.
  - [131] B. Li, Y. Li, C. Zheng, D. Gao, W. Huang, Advancements in the stability of perovskite solar cells: degradation mechanisms and improvement approaches, *RSC Adv.* 6 (2016) 38079–38091. doi:10.1039/C5RA27424A.
  - [132] A. Di Carlo, F. Matteocci, S. Razza, M. Mincuzzi, F. Di Giacomo, S. Casaluci, D. Gentilini, T.M. Brown, A. Reale, F. Brunetti, A. D’Epifanio, S. Licoccia, Mesoscopic perovskite solar cells and modules, in: 14th IEEE Int. Conf. Nanotechnol., IEEE, 2014: pp. 70–74. doi:10.1109/NANO.2014.6968015.
  - [133] C. Liu, J. Fan, X. Zhang, Y. Shen, L. Yang, Y. Mai, Hysteretic Behavior upon

- Light Soaking in Perovskite Solar Cells Prepared via Modified Vapor-Assisted Solution Process, *ACS Appl. Mater. Interfaces.* 7 (2015) 9066–9071. doi:10.1021/acsami.5b00375.
- [134] H.J. Snaith, A. Abate, J.M. Ball, G.E. Eperon, T. Leijtens, N.K. Noel, S.D. Stranks, J.T.-W. Wang, K. Wojciechowski, W. Zhang, Anomalous Hysteresis in Perovskite Solar Cells, *J. Phys. Chem. Lett.* 5 (2014) 1511–1515. doi:10.1021/jz500113x.
- [135] N.J. Jeon, J.H. Noh, Y.C. Kim, W.S. Yang, S. Ryu, S. Il Seok, Solvent engineering for high-performance inorganic–organic hybrid perovskite solar cells, *Nat. Mater.* 13 (2014) 897–903. doi:10.1038/nmat4014.
- [136] M. Arafat Mahmud, N. Kumar Elumalai, M. Baishakhi Upama, D. Wang, V.R. Gonçales, M. Wright, J. Justin Gooding, F. Haque, C. Xu, A. Uddin, Cesium compounds as interface modifiers for stable and efficient perovskite solar cells, *Sol. Energy Mater. Sol. Cells.* 174 (2018) 172–186. doi:10.1016/j.solmat.2017.08.032.
- [137] S. Nakamura, Y. Hashimoto, S. Igawa, M. Kajino, K. Nishi, H. Takahashi, T. Mizumoto, H. Iizuka, Childhood generalized pustular psoriasis treated by preprandial ciclosporin administration: serum cytokine pattern during the course of the disease, *Clin. Exp. Dermatol.* 34 (2009) e1023–e1024. doi:10.1111/j.1365-2230.2009.03702.x.
- [138] A.M.A. Leguy, Y. Hu, M. Campoy-Quiles, M.I. Alonso, O.J. Weber, P. Azarhoosh, M. van Schilfgaarde, M.T. Weller, T. Bein, J. Nelson, P. Docampo, P.R.F. Barnes, Reversible Hydration of CH<sub>3</sub>NH<sub>3</sub>PbI<sub>3</sub> in Films, Single Crystals, and Solar Cells, *Chem. Mater.* 27 (2015) 3397–3407. doi:10.1021/acs.chemmater.5b00660.
- [139] R. Arndt, R. Puto, Basic understanding of IEC standard testing for photovoltaic panels, [Http//Tuvamerica.Com/Services/Photovoltaics/ ....](http://Tuvamerica.Com/Services/Photovoltaics/) (2010) 1–15. <http://www.tuv-sud.us/services/photovoltaics/ArticleBasicUnderstandingPV.pdf> (accessed June 30, 2018).
- [140] J. Wohlgemuth, IEC 61215: What It Is and Isn't (Presentation), NREL (National Renewable Energy Laboratory), 2012. <https://www.nrel.gov/docs/fy12osti/54714.pdf> (accessed July 4, 2018).
- [141] H.J. Snaith, P. Hacke, Enabling reliability assessments of pre-commercial perovskite photovoltaics with lessons learned from industrial standards, *Nat. Energy.* 3 (2018) 459–465. doi:10.1038/s41560-018-0174-4.
- [142] P. Hacke, Overview of IEC TesKng for PID, 2015. [https://www.nrel.gov/pv/assets/pdfs/2015\\_pvmrw\\_113\\_hacke.pdf](https://www.nrel.gov/pv/assets/pdfs/2015_pvmrw_113_hacke.pdf) (accessed July 4, 2018).
- [143] K. Ahn, D. Kim, O. Kim, J. Nam, Analysis of transparent conductive silver nanowire films from dip coating flow, *J. Coatings Technol. Res.* 12 (2015) 855–862. doi:10.1007/s11998-015-9690-3.
- [144] J.-Y. Lee, S.T. Connor, Y. Cui, P. Peumans, Solution-Processed Metal Nanowire Mesh Transparent Electrodes, *Nano Lett.* 8 (2008) 689–692. doi:10.1021/nl073296g.

- [145] Z. Zhang, R. Lv, Y. Jia, X. Gan, H. Zhu, F. Kang, All-Carbon Electrodes for Flexible Solar Cells, *Appl. Sci.* 8 (2018) 152. doi:10.3390/app8020152.
- [146] M. Luo, Y. Liu, W. Huang, W. Qiao, Y. Zhou, Y. Ye, L.-S. Chen, Towards Flexible Transparent Electrodes Based on Carbon and Metallic Materials, *Micromachines*. 8 (2017) 12. doi:10.3390/mi8010012.
- [147] I.K. Popoola, M.A. Gondal, T.F. Qahtan, Recent progress in flexible perovskite solar cells: Materials, mechanical tolerance and stability, *Renew. Sustain. Energy Rev.* 82 (2018) 3127–3151. doi:10.1016/j.rser.2017.10.028.
- [148] M. Kaltenbrunner, G. Adam, E.D. Głowacki, M. Drack, R. Schwödiauer, L. Leonat, D.H. Apaydin, H. Groiss, M.C. Scharber, M.S. White, N.S. Sariciftci, S. Bauer, Flexible high power-per-weight perovskite solar cells with chromium oxide-metal contacts for improved stability in air, *Nat. Mater.* 14 (2015) 1032–1039. doi:10.1038/nmat4388.
- [149] C. Roldán-Carmona, O. Malinkiewicz, A. Soriano, G. Mínguez Espallargas, A. Garcia, P. Reinecke, T. Kroyer, M.I. Dar, M.K. Nazeeruddin, H.J. Bolink, Flexible high efficiency perovskite solar cells, *Energy Environ. Sci.* 7 (2014) 994. doi:10.1039/c3ee43619e.
- [150] J. Han, S. Yuan, L. Liu, X. Qiu, H. Gong, X. Yang, C. Li, Y. Hao, B. Cao, Fully indium-free flexible Ag nanowires/ZnO:F composite transparent conductive electrodes with high haze, *J. Mater. Chem. A*. 3 (2015) 5375–5384. doi:10.1039/C4TA05728G.
- [151] D.C. Choo, T.W. Kim, Degradation mechanisms of silver nanowire electrodes under ultraviolet irradiation and heat treatment, *Sci. Rep.* 7 (2017) 1696. doi:10.1038/s41598-017-01843-9.
- [152] E.T. Hoke, D.J. Slotcavage, E.R. Dohner, A.R. Bowring, H.I. Karunadasa, M.D. McGehee, Reversible photo-induced trap formation in mixed-halide hybrid perovskites for photovoltaics, *Chem. Sci.* 6 (2015) 613–617. doi:10.1039/C4SC03141E.
- [153] T. Leijtens, G.E. Eperon, S. Pathak, A. Abate, M.M. Lee, H.J. Snaith, Overcoming ultraviolet light instability of sensitized TiO<sub>2</sub> with meso-superstructured organometal tri-halide perovskite solar cells, *Nat. Commun.* 4 (2013) 2885. doi:10.1038/ncomms3885.
- [154] S. Ito, S. Tanaka, K. Manabe, H. Nishino, Effects of Surface Blocking Layer of Sb<sub>2</sub>S<sub>3</sub> on Nanocrystalline TiO<sub>2</sub> for CH<sub>3</sub>NH<sub>3</sub>PbI<sub>3</sub> Perovskite Solar Cells, *J. Phys. Chem. C*. 118 (2014) 16995–17000. doi:10.1021/jp500449z.
- [155] N. Chander, A.F. Khan, P.S. Chandrasekhar, E. Thouti, S.K. Swami, V. Dutta, V.K. Komarala, Reduced ultraviolet light induced degradation and enhanced light harvesting using YVO<sub>4</sub>:Eu<sup>3+</sup> down-shifting nano-phosphor layer in organometal halide perovskite solar cells, *Appl. Phys. Lett.* 105 (2014) 033904. doi:10.1063/1.4891181.
- [156] C.W. Kim, T.Y. Eom, I.S. Yang, B.S. Kim, W.I. Lee, Y.S. Kang, Y.S. Kang, Dual-Function Au@Y<sub>2</sub>O<sub>3</sub>:Eu<sup>3+</sup> Smart Film for Enhanced Power Conversion Efficiency and Long-Term Stability of Perovskite Solar Cells, *Sci. Rep.* 7 (2017) 6849. doi:10.1038/s41598-017-07218-4.

- [157] C. Law, L. Miseikis, S. Dimitrov, P. Shakya-Tuladhar, X. Li, P.R.F.F. Barnes, J. Durrant, B.C. O'Regan, Performance and Stability of Lead Perovskite/TiO<sub>2</sub>, Polymer/PCBM, and Dye Sensitized Solar Cells at Light Intensities up to 70 Suns, *Adv. Mater.* 26 (2014) 6268–6273. doi:10.1002/adma.201402612.
- [158] R.K. Misra, L. Ciammaruchi, S. Aharon, D. Mogilyansky, L. Etgar, I. Visoly-Fisher, E.A. Katz, Effect of Halide Composition on the Photochemical Stability of Perovskite Photovoltaic Materials, *ChemSusChem.* 9 (2016) 2572–2577. doi:10.1002/cssc.201600679.
- [159] W.L. Leong, Z.-E. Ooi, D. Sabba, C. Yi, S.M. Zakeeruddin, M. Graetzel, J.M. Gordon, E.A. Katz, N. Mathews, Identifying Fundamental Limitations in Halide Perovskite Solar Cells, *Adv. Mater.* 28 (2016) 2439–2445. doi:10.1002/adma.201505480.
- [160] R.K. Misra, S. Aharon, B. Li, D. Mogilyansky, I. Visoly-Fisher, L. Etgar, E.A. Katz, Temperature- and Component-Dependent Degradation of Perovskite Photovoltaic Materials under Concentrated Sunlight, *J. Phys. Chem. Lett.* 6 (2015) 326–330. doi:10.1021/jz502642b.
- [161] M. Antoniadou, E. Siranidi, N. Vaenas, a. G. Kontos, E. Stathatos, P. Falaras, Photovoltaic Performance and Stability of CH<sub>3</sub>NH<sub>3</sub>PbI<sub>3</sub>-<sub>x</sub>Cl<sub>x</sub> Perovskites, *J. Surfaces Interfaces Mater.* 2 (2014) 323–327. doi:10.1166/jsim.2014.1060.
- [162] J. Schoonman, Organic–inorganic lead halide perovskite solar cell materials: A possible stability problem, *Chem. Phys. Lett.* 619 (2015) 193–195. doi:10.1016/j.cplett.2014.11.063.
- [163] S.K. Pathak, A. Abate, P. Ruckdeschel, B. Roose, K.C. Gödel, Y. Vaynzof, A. Santhala, S.-I. Watanabe, D.J. Hollman, N. Noel, A. Sepe, U. Wiesner, R. Friend, H.J. Snaith, U. Steiner, Performance and Stability Enhancement of Dye-Sensitized and Perovskite Solar Cells by Al Doping of TiO<sub>2</sub>, *Adv. Funct. Mater.* 24 (2014) 6046–6055. doi:10.1002/adfm.201401658.
- [164] A. Babayigit, D. Duy Thanh, A. Ethirajan, J. Manca, M. Muller, H.-G. Boyen, B. Conings, Assessing the toxicity of Pb- and Sn-based perovskite solar cells in model organism *Danio rerio*, *Sci. Rep.* 6 (2016) 18721. doi:10.1038/srep18721.
- [165] M.H. Kumar, S. Dharani, W.L. Leong, P.P. Boix, R.R. Prabhakar, T. Baikie, C. Shi, H. Ding, R. Ramesh, M. Asta, M. Graetzel, S.G. Mhaisalkar, N. Mathews, Lead-Free Halide Perovskite Solar Cells with High Photocurrents Realized Through Vacancy Modulation, *Adv. Mater.* 26 (2014) 7122–7127. doi:10.1002/adma.201401991.
- [166] N.K. Noel, S.D. Stranks, A. Abate, C. Wehrenfennig, S. Guarnera, A.-A. Haghhighirad, A. Sadhanala, G.E. Eperon, S.K. Pathak, M.B. Johnston, A. Petrozza, L.M. Herz, H.J. Snaith, Lead-free organic–inorganic tin halide perovskites for photovoltaic applications, *Energy Environ. Sci.* 7 (2014) 3061–3068. doi:10.1039/C4EE01076K.
- [167] T.M. Koh, T. Krishnamoorthy, N. Yantara, C. Shi, W.L. Leong, P.P. Boix, A.C. Grimsdale, S.G. Mhaisalkar, N. Mathews, Formamidinium tin-based perovskite

- with low E g for photovoltaic applications, *J. Mater. Chem. A*. 3 (2015) 14996–15000. doi:10.1039/C5TA00190K.
- [168] S.J. Lee, S.S. Shin, Y.C. Kim, D. Kim, T.K. Ahn, J.H. Noh, J. Seo, S. Il Seok, Fabrication of Efficient Formamidinium Tin Iodide Perovskite Solar Cells through SnF<sub>2</sub> –Pyrazine Complex, *J. Am. Chem. Soc.* 138 (2016) 3974–3977. doi:10.1021/jacs.6b00142.
- [169] B. Lee, C.C. Stoumpos, N. Zhou, F. Hao, C. Malliakas, C.-Y. Yeh, T.J. Marks, M.G. Kanatzidis, R.P.H. Chang, Air-Stable Molecular Semiconducting Iodosalts for Solar Cell Applications: Cs<sub>2</sub>SnI<sub>6</sub> as a Hole Conductor, *J. Am. Chem. Soc.* 136 (2014) 15379–15385. doi:10.1021/ja508464w.
- [170] B. Saparov, J. Sun, W. Meng, Z. Xiao, H.-S. Duan, O. Gunawan, D. Shin, I.G. Hill, Y. Yan, D.B. Mitzi, Thin-Film Deposition and Characterization of a Sn-Deficient Perovskite Derivative Cs<sub>2</sub>SnI<sub>6</sub>, *Chem. Mater.* 28 (2016) 2315–2322. doi:10.1021/acs.chemmater.6b00433.
- [171] M.-G. Ju, M. Chen, Y. Zhou, H.F. Garces, J. Dai, L. Ma, N.P. Padture, X.C. Zeng, Earth-Abundant Nontoxic Titanium(IV)-based Vacancy-Ordered Double Perovskite Halides with Tunable 1.0 to 1.8 eV Bandgaps for Photovoltaic Applications, *ACS Energy Lett.* 3 (2018) 297–304. doi:10.1021/acsenergylett.7b01167.
- [172] X. Qiu, B. Cao, S. Yuan, X. Chen, Z. Qiu, Y. Jiang, Q. Ye, H. Wang, H. Zeng, J. Liu, M.G. Kanatzidis, From unstable CsSnI<sub>3</sub> to air-stable Cs<sub>2</sub>SnI<sub>6</sub>: A lead-free perovskite solar cell light absorber with bandgap of 1.48 eV and high absorption coefficient, *Sol. Energy Mater. Sol. Cells.* 159 (2017) 227–234. doi:10.1016/j.solmat.2016.09.022.
- [173] J. Qian, B. Xu, W. Tian, A comprehensive theoretical study of halide perovskites ABX<sub>3</sub>, *Org. Electron.* 37 (2016) 61–73. doi:10.1016/j.orgel.2016.05.046.
- [174] C.C. Stoumpos, L. Frazer, D.J. Clark, Y.S. Kim, S.H. Rhim, A.J. Freeman, J.B. Ketterson, J.I. Jang, M.G. Kanatzidis, Hybrid Germanium Iodide Perovskite Semiconductors: Active Lone Pairs, Structural Distortions, Direct and Indirect Energy Gaps, and Strong Nonlinear Optical Properties, *J. Am. Chem. Soc.* 137 (2015) 6804–6819. doi:10.1021/jacs.5b01025.
- [175] M. Lyu, J.-H. Yun, M. Cai, Y. Jiao, P. V. Bernhardt, M. Zhang, Q. Wang, A. Du, H. Wang, G. Liu, L. Wang, Organic–inorganic bismuth (III)-based material: A lead-free, air-stable and solution-processable light-absorber beyond organolead perovskites, *Nano Res.* 9 (2016) 692–702. doi:10.1007/s12274-015-0948-y.
- [176] C. Lan, J. Luo, S. Zhao, C. Zhang, W. Liu, S. Hayase, T. Ma, Effect of lead-free (CH<sub>3</sub>NH<sub>3</sub>)<sub>3</sub>Bi<sub>2</sub>I<sub>9</sub> perovskite addition on spectrum absorption and enhanced photovoltaic performance of bismuth triiodide solar cells, *J. Alloys Compd.* 701 (2017) 834–840. doi:10.1016/j.jallcom.2017.01.169.
- [177] B.E. Hayden, S. Yakovlev, Structural, dielectric and ferroelectric properties of (Bi<sub>x</sub>Na<sub>1-x</sub>)TiO<sub>3</sub>–BaTiO<sub>3</sub> system studied by high throughput screening, *Thin Solid Films.* 603 (2016) 108–114. doi:10.1016/j.tsf.2016.01.033.
- [178] A.H. Slavney, T. Hu, A.M. Lindenberg, H.I. Karunadasa, A Bismuth-Halide Double Perovskite with Long Carrier Recombination Lifetime for Photovoltaic

- Applications, J. Am. Chem. Soc. 138 (2016) 2138–2141.  
doi:10.1021/jacs.5b13294.
- [179] D. Cortecchia, H.A. Dewi, J. Yin, A. Bruno, S. Chen, T. Baikie, P.P. Boix, M. Grätzel, S. Mhaisalkar, C. Soci, N. Mathews, Lead-Free MA<sub>2</sub>CuCl<sub>x</sub>Br<sub>4-x</sub> Hybrid Perovskites, Inorg. Chem. 55 (2016) 1044–1052.  
doi:10.1021/acs.inorgchem.5b01896.
- [180] M. Leng, Y. Yang, K. Zeng, Z. Chen, Z. Tan, S. Li, J. Li, B. Xu, D. Li, M.P. Hautzinger, Y. Fu, T. Zhai, L. Xu, G. Niu, S. Jin, J. Tang, All-Inorganic Bismuth-Based Perovskite Quantum Dots with Bright Blue Photoluminescence and Excellent Stability, Adv. Funct. Mater. 28 (2018) 1704446.  
doi:10.1002/adfm.201704446.
- [181] N.C. Miller, M. Bernechea, Research Update: Bismuth based materials for photovoltaics, APL Mater. 6 (2018). doi:10.1063/1.5026541.
- [182] Q. Zhang, F. Hao, J. Li, Y. Zhou, Y. Wei, H. Lin, Perovskite solar cells: must lead be replaced – and can it be done?, Sci. Technol. Adv. Mater. 19 (2018) 425–442.  
doi:10.1080/14686996.2018.1460176.
- [183] J.L. Bernal-Agustín, R. Dufo-López, Economical and environmental analysis of grid connected photovoltaic systems in Spain, Renew. Energy. 31 (2006) 1107–1128. doi:10.1016/j.renene.2005.06.004.
- [184] S. Mageshwari, S.A. Daniel, N.A. Gounden, Feasibility studies of rooftop photovoltaic (PV) systems for domestic consumers in rural India, Int. J. Energy Stat. 05 (2017) 1750005. doi:10.1142/S2335680417500053.
- [185] J. Hirvonen, G. Kayo, S. Cao, A. Hasan, K. Sirén, Renewable energy production support schemes for residential-scale solar photovoltaic systems in Nordic conditions, Energy Policy. 79 (2015) 72–86. doi:10.1016/j.enpol.2015.01.014.
- [186] M. Gu, Y. Liu, J. Yang, L. Peng, C. Zhao, Z. Yang, J. Yang, W. Fang, J. Fang, Z. Zhao, Estimation of environmental effect of PVNB installed along a metro line in China, Renew. Energy. 45 (2012) 237–244. doi:10.1016/j.renene.2012.02.021.
- [187] S.S. Korsavi, Z.S. Zomorodian, M. Tahsidoost, Energy and economic performance of rooftop PV panels in the hot and dry climate of Iran, J. Clean. Prod. 174 (2018) 1204–1214. doi:10.1016/j.jclepro.2017.11.026.
- [188] E.F. Fernández, F. Almonacid, J.A. Ruiz-Arias, A. Soria-Moya, Analysis of the spectral variations on the performance of high concentrator photovoltaic modules operating under different real climate conditions, Sol. Energy Mater. Sol. Cells. 127 (2014) 179–187. doi:10.1016/j.solmat.2014.04.026.
- [189] P.M. Rodrigo, E.F. Fernández, F.M. Almonacid, P.J. Pérez-Higueras, Quantification of the spectral coupling of atmosphere and photovoltaic system performance: Indexes, methods and impact on energy harvesting, Sol. Energy Mater. Sol. Cells. 163 (2017) 73–90. doi:10.1016/j.solmat.2017.01.018.
- [190] F. Brunetti, Stable Next-Generation Photovoltaics : Unravelling Degradation Mechanisms of Organic and Perovskite Solar Cells by Complementary Characterization Techniques StableNextSol – MP1307 5th MC Meeting , 4th WG Meeting, (2016) 1–10.  
[http://stabenextsol.eu/docs/WG2\\_StableNextSol\\_perovskites\\_experiment.pdf](http://stabenextsol.eu/docs/WG2_StableNextSol_perovskites_experiment.pdf).

- [191] E. Mosconi, A. Amat, M.K. Nazeeruddin, M. Grätzel, F. De Angelis, First-Principles Modeling of Mixed Halide Organometal Perovskites for Photovoltaic Applications, *J. Phys. Chem. C.* 117 (2013) 13902–13913. doi:10.1021/jp4048659.
- [192] P. Umari, E. Mosconi, F. De Angelis, Relativistic GW calculations on CH<sub>3</sub>NH<sub>3</sub>PbI<sub>3</sub> and CH<sub>3</sub>NH<sub>3</sub>SnI<sub>3</sub> Perovskites for Solar Cell Applications, *Sci. Rep.* 4 (2015) 4467. doi:10.1038/srep04467.
- [193] E. Mosconi, E. Ronca, F. De Angelis, First-Principles Investigation of the TiO<sub>2</sub>/Organohalide Perovskites Interface: The Role of Interfacial Chlorine, *J. Phys. Chem. Lett.* 5 (2014) 2619–2625. doi:10.1021/jz501127k.
- [194] F. De Angelis, Modeling Materials and Processes in Hybrid/Organic Photovoltaics: From Dye-Sensitized to Perovskite Solar Cells, *Acc. Chem. Res.* 47 (2014) 3349–3360. doi:10.1021/ar500089n.
- [195] F. Aryasetiawan, O. Gunnarsson, The GW method, *Reports Prog. Phys.* 61 (1998) 237–312. doi:10.1088/0034-4885/61/3/002.
- [196] S. Tombe, G. Adam, H. Heilbrunner, D.H. Apaydin, C. Ulbricht, N.S. Sariciftci, C.J. Arendse, E. Iwuoha, M.C. Scharber, Optical and electronic properties of mixed halide (X = I, Cl, Br) methylammonium lead perovskite solar cells, *J. Mater. Chem. C.* 5 (2017) 1714–1723. doi:10.1039/C6TC04830G.
- [197] S. Colella, E. Mosconi, P. Fedeli, A. Listorti, F. Gazza, F. Orlandi, P. Ferro, T. Besagni, A. Rizzo, G. Calestani, G. Gigli, F. De Angelis, R. Mosca, MAPbI<sub>3-x</sub>Cl<sub>x</sub> Mixed Halide Perovskite for Hybrid Solar Cells: The Role of Chloride as Dopant on the Transport and Structural Properties, *Chem. Mater.* 25 (2013) 4613–4618. doi:10.1021/cm402919x.
- [198] C. Kwak, D.W. Jung, D.-H. Yeon, J.S. Kim, H.J. Park, S.-J. Ahn, S. Seo, S.M. Lee, Stabilization of high-cobalt-content perovskites for use as cathodes in solid oxide fuel cells, *RSC Adv.* 3 (2013) 10669. doi:10.1039/c3ra41145a.
- [199] A. Demont, M.S. Dyer, R. Sayers, M.F. Thomas, M. Tsiamtsouri, H.N. Niu, G.R. Darling, A. Daoud-Aladine, J.B. Claridge, M.J. Rosseinsky, Stabilization of a Complex Perovskite Superstructure under Ambient Conditions: Influence of Cation Composition and Ordering, and Evaluation as an SOFC Cathode, *Chem. Mater.* 22 (2010) 6598–6615. doi:10.1021/cm102475n.
- [200] E.F. Fernandez, S. Senthilarasu, A.J. Garcia-Loureiro, F. Almonacid, T.K. Mallick, Spectral coupling of atmosphere and the performance of perovskite solar cells, in: 2015 10th Spanish Conf. Electron Devices, IEEE, Spain, Aranjuez, 2015: pp. 1–4. doi:10.1109/CDE.2015.7087478.
- [201] A. Agresti, S. Pescetelli, A. Quatela, S. Mastroianni, T.M. Brown, A. Reale, C.A. Bignozzi, S. Caramori, A. Di Carlo, Micro-Raman analysis of reverse bias stressed dye-sensitized solar cells, *RSC Adv.* 4 (2014) 12366. doi:10.1039/c3ra47797e.
- [202] S. Mastroianni, A. Lembo, T.M. Brown, A. Reale, A. Di Carlo, Electrochemistry in Reverse Biased Dye Solar Cells and Dye/Electrolyte Degradation Mechanisms, *ChemPhysChem.* 13 (2012) 2964–2975. doi:10.1002/cphc.201200229.
- [203] D. Perganti, A.G. Kontos, T. Stergiopoulos, V. Likodimos, J. Farnell, D. Milliken, H. Desilvestro, P. Falaras, Thermal Stressing of Dye Sensitized Solar Cells Employing Robust Redox Electrolytes, *Electrochim. Acta.* 179 (2015) 241–249.

doi:10.1016/j.electacta.2015.03.206.

- [204] M. Jørgensen, K. Norrman, F.C. Krebs, Stability/degradation of polymer solar cells, *Sol. Energy Mater. Sol. Cells.* 92 (2008) 686–714.  
doi:10.1016/j.solmat.2008.01.005.
- [205] R. Roesch, T. Faber, E. von Hauff, T.M. Brown, M. Lira-Cantu, H. Hoppe, Procedures and Practices for Evaluating Thin-Film Solar Cell Stability, *Adv. Energy Mater.* 5 (2015) 1501407. doi:10.1002/aenm.201501407.
- [206] R. Cheacharoen, W.R. Mateker, Q. Zhang, B. Kan, D. Sarkisian, X. Liu, J.A. Love, X. Wan, Y. Chen, T.-Q. Nguyen, G.C. Bazan, M.D. McGehee, Assessing the stability of high performance solution processed small molecule solar cells, *Sol. Energy Mater. Sol. Cells.* 161 (2017) 368–376.  
doi:10.1016/j.solmat.2016.12.021.
- [207] A. Guerrero, G. Garcia-Belmonte, Recent Advances to Understand Morphology Stability of Organic Photovoltaics, *Nano-Micro Lett.* 9 (2017) 10.  
doi:10.1007/s40820-016-0107-3.
- [208] A. Fakharuddin, R. Jose, T.M. Brown, F. Fabregat-Santiago, J. Bisquert, A perspective on the production of dye-sensitized solar modules, *Energy Environ. Sci.* 7 (2014) 3952–3981. doi:10.1039/C4EE01724B.
- [209] T. Lund, P.T. Nguyen, H.M. Tran, P. Pechy, S.M. Zakeeruddin, M. Grätzel, Thermal stability of the DSC ruthenium dye C106 in robust electrolytes, *Sol. Energy.* 110 (2014) 96–104. doi:10.1016/j.solener.2014.09.007.
- [210] J. Gao, M. Bhagavathi Achari, L. Kloof, Long-term stability for cobalt-based dye-sensitized solar cells obtained by electrolyte optimization, *Chem. Commun.* 50 (2014) 6249–6251. doi:10.1039/C4CC00698D.
- [211] A. Kaltzoglou, D. Perganti, M. Antoniadou, A.G. Kontos, P. Falaras, Stress Tests on Dye-sensitized Solar Cells with the Cs<sub>2</sub>SnI<sub>6</sub> Defect Perovskite as Hole-transporting Material, *Energy Procedia.* 102 (2016) 49–55.  
doi:10.1016/j.egypro.2016.11.317.
- [212] A. Kaltzoglou, M. Antoniadou, A.G. Kontos, C.C. Stoumpos, D. Perganti, E. Siranidi, V. Raptis, K. Trohidou, V. Psycharis, M.G. Kanatzidis, P. Falaras, Optical-Vibrational Properties of the Cs<sub>2</sub>SnX<sub>6</sub> (X = Cl, Br, I) Defect Perovskites and Hole-Transport Efficiency in Dye-Sensitized Solar Cells, *J. Phys. Chem. C.* 120 (2016) 11777–11785. doi:10.1021/acs.jpcc.6b02175.
- [213] A. Kaltzoglou, M. Antoniadou, D. Perganti, E. Siranidi, V. Raptis, K. Trohidou, V. Psycharis, A.G. Kontos, P. Falaras, Mixed-halide Cs<sub>2</sub>SnI<sub>3</sub>Br<sub>3</sub> perovskite as low resistance hole-transporting material in dye-sensitized solar cells, *Electrochim. Acta.* 184 (2015) 466–474. doi:10.1016/j.electacta.2015.10.030.
- [214] C. Carron, An EPFL startup makes residential solar panels twice as efficient, NEWS MEDIACOM. (2016) 1. <https://actu.epfl.ch/news/an-epfl-startup-makes-residential-solar-panels-twice-as-efficient/> (accessed June 15, 2017).
- [215] S. Honsberg, Christiana; Bowden, PV Education, (n.d.).  
<https://www.pveducation.org/pvcdrom/appendices/standard-solar-spectra> (accessed June 27, 2018).